Addis Ababa University
Addis Ababa Institute of Technology
School of Mechanical & Industrial Engineering

Numerical Investigation on Charging-Discharging of a PCM Using PV and Thermal Oil for Injera Baking Application.

A Thesis Submitted to the School of Graduate Studies of Addis Ababa Institute of Technology, Addis Ababa University in partial fulfillment for the Degree of Master of Science in Mechanical Engineering (*Thermal Engineering Stream*)

By: Meseret Alemu

Advisor: Dr. Ing. Abdulkadir A.

Co-Advisor: Gashaw G. (PhD Candidate)

Addis Ababa, Ethiopia
June, 2023

Addis Ababa University
Addis Ababa Institute of Technology
School of Graduate Studies
School of Mechanical and Industrial Engineering

"Numerical Investigation on Charging-Discharging of a PCM Using PV and Thermal Oil for Injera Baking Application"

By: Meseret Alemu

Approved by the Board of Examiners:

Dr. Abdulkadir Aman Advisor Name	_____ Signature	_____ Date
Dr. Wondwossen Bogale Internal Examiner	_____ Signature	_____ Date
Dr. Yilma Tadesse External Examiner	_____ Signature	_____ Date
Dr. Araya Abera School Dean	_____ Signature	_____ Date
Dr. Sosina Mengistu Associate Director for PG Program	_____ Signature	_____ Date

Declaration

I hereby declare that the work which is being presented in this thesis entitled "Numerical Investigation on charging-discharging of a PCM using PV and thermal oil for Injera baking application" is original work of my own, has not been presented for a degree of any other university and all the resource of materials used for this thesis have been duly acknowledged.

Meseret Alemu Date

This is to certify that the above declaration made by the candidate is correct to the best of my Knowledge.

Dr. Abdulkadir Aman (Advisor) Date

ACKNOWLEDGEMENTS

First of all, I would like to thank almighty GOD for giving an encourage, and strength through my journey.

I would like to express my appreciation to my advisor Dr. Abdulkadir Aman and my co-advisor Mr. Gashaw Getent (PhD Candidate) for their assistance by giving important comments that helped me to reach here and encouraging me during the progress of this thesis work. A special thanks to all of my instructors who gave me the theoretical base during the course work.

Last but not least, I would like to thank my family for their encouragement and, support.

ABSTRACT

Millions of Ethiopians rely on bio-mass, charcoal, and animal dung to supply their energy demands. All of this energy is used to bake injera, more than 50%. This traditional biomass-based baking has an impact on women's and children's health, energy, and ability to attend school. Due to its abundant and readily accessible renewable energy source, solar energy had been considered to be a good alternative for cooking. However, because of its intermittent nature, there is a mismatch between the load and the solar energy that is available for the baking purpose, so a thermal storage system that provides the necessary energy has been integrated.

This study investigates the thermal characteristic of the charging and discharge processes and main heat transfer processes in the injera baking system with PV which was integrated with the thermal storage system.

This study was conducted, beginning with reviewing related papers, system design, data collection, and data analysis, in addition, performed mathematical and numerical models and numerical simulation was conducted using a finite-difference computational model for the thermal storages that was PCM and thermal oil. The thermal oil was used to store energy and to transfer heat, furthermore, the developed computational models are analyzed using MATLAB programming software.

From the numerical simulation result by using solar radiation data of Addis Ababa showed that the thermal storage has the capacity to store about 33 MJ during charging using constant heat flux which was from the PV. The amount of energy discharged from the PCM was 13.1 MJ and from the thermia oil was 3.50 MJ by using natural convection heat transfer and the discharging and overall efficiency of the system were about 50.2% and 46.67% respectively. Also, the baking pan surface temperature stayed between $220^{o}c$ and $146.4^{o}c$ for about three hours. This result was compared with different papers and it can be concluded that the numerically investigated solar-powered Injera baking integrated with thermal storage showed a promising result.

Keywords: PCM, Thermal Energy Storage System, PV, Thermal Oil

TABLE OF CONTENTS

LIST OF FIGURES vii

LIST OF TABLES viii

LIST OF ACRONYMS AND ABBREVIATIONS ix

CHAPTER 1: INTRODUCTION 1

1.1. Background of the study 1

1.2. Problem Statement 2

1.3. Objectives 4

1.3.1. General Objectives 4

1.3.2. Specific Objectives 4

1.4. Scope and limitation of the study 4

1.5. Significance of study 4

CHAPTER 2: LITERATURE REVIEW 5

2.1. Introduction 5

2.2. Solar cooker 5

2.2.1. Types of Solar Cookers 5

2.3. Injera Baking Technologies 6

2.3.1. Baking Pan 6

2.4. Type of Injera baking technologies 6

2.4.1. Three-Stone Open-Fire Stove 7

2.4.2. Improved Biomass Injera Baking Stoves 7

2.4.3. Biogas Injera Baking Stove 12

2.4.4. Electric Injera Baking Stoves 12

2.5. Review of Related Works 13

2.6. Solar Thermal Energy Storage Concepts 23
2.7. Types of Thermal Energy Storage 23
2.7.1. Sensible Heat Storage 23
2.7.2. Latent Heat Storage 24
2.7.3. Thermochemical Energy Storage 25
2.8. Phase Change Material (PCM) for Thermal Storage System 26
2.8.1. Organic PCM 27
2.8.2. Inorganic Phase Change Materials 27
2.8.3. Eutectics PCM 28
2.9. Selection principles and required thermo-physical properties of PCM 28
2.10. A Phase Change Material Used for Cooking 30
2.11. Encapsulation of Phase Change Materials Concept 37
2.12. Heat Transfer Fluids 44
2.12.1. Heat-Transfer Oils 44
2.13. Photovoltaic Conversion 44
2.13.1. Types of PV 45
2.14. Modes of Heat Transfer 46
2.14.1. Conduction Heat Transfer Mechanism 46
2.14.2. Convection Heat Transfer Mechanism 47
2.14.3. Radiation Heat Transfer Mechanism 48
2.15. Thermal Insulation System 48
2.15.1. Types of Insulation Materials 49
2.16. Ash Insulation 50
2.17. Conclusion from the Literature Review 50

CHAPTER 3: MATERIALS AND METHODS 51
3.1. Methods 51
3.2. Solar-powered Injera Baking System with Thermal Storage 52
3.2.1. Description of the System 52
3.2.2. Heat Demand of Injera Baking 54
3.2.3. Baking Energy 54
3.3. Selection for Phase Change Material 57
3.3.1. Quantifying the Amount of PCM 58
3.3.2. Estimation of Volume of Storage Medium (PCM) 60
3.3.3. Encapsulation of Phase Change Material 60
3.3.4. Volume sizing for thermal storage system 61
3.3.5. Energy stored in the thermal oil 62
3.4. Estimation of available solar radiation potential 63
3.4.1. Solar Radiation Data 63
3.5. Basic Sun- Earth Angles 64
3.5.1. Declination 65
3.5.2. Sunset hour angle 66
3.5.3. Hour angle 66
3.5.4. Zenith angle 66
3.5.5. Solar altitude angle 66
3.5.6. Solar azimuth angle 66
3.5.7. Tilt angle 67
3.5.8. Incidence angle 67
3.6. Design and Sizing of Solar Photovoltaic Systems 67

3.6.1. Estimating the PV system land requirements 68
3.6.2. Sizing the PV Capacity 68
3.6.3. Sizing of the Inverter 70
3.7. Heating Element 71
3.8. Selection of material for the system 71
3.8.1. Design of Baking Pan 71
3.8.2. Design of Baking Pan Cover 72
3.8.3. Materials for Storage Tank 72
3.8.4. Selection of Heat-Transfer Oils 72
3.8.5. Shell Thermia Oil B Heat Transfer Oil 72
3.9. Insulation 73
CHAPTER 4: PERFORMANCE ANALYSIS OF THERMAL ENERGY STORAGE FOR INJERA BAKING 74
4.1. Modeling the Baking Process Heat Transfer Mechanism of Mitad 74
4.2. Mathematical Model 75
4.2.1. Enthalpy Method 75
4.3. Mathematical Modeling for the Heat Transfer Fluid 78
4.4. Mathematical Modeling for the PCM 78
4.5. Governing Equation for Melting fraction in the latent heat section 79
4.6. Heat Transfer Equations for Liquid PCM 80
4.7. Mathematical Modeling for Baking Pan 81
4.8. Computational Model 81
4.9. Heat Transfer Coefficients Correlations 84
4.1. Initial and Boundary Conditions 87

4.1.1. During Charging Condition 87
4.1.2. During Discharging Condition 89
4.2. Verification of Computational Model 92
4.10. Grid Independence Test 93
CHAPTER 5: RESULT AND DISCUSSION 94
5.1. Simulation of PCM Thermal Storage 94
5.1.1. Charging Conditions 94
5.1.2. Discharging Conditions of Thermal Storage 98
5.2. Comparisons with Other Research 100
CHAPTER 6: CONCLUSIONS AND RECOMMENDATIONS 103
6.1. Conclusions 103
6.2. Recommendations 104
Reference 105
Appendix 118

LIST OF FIGURES

Figure 2-1: Types of solar cookers 6
Figure 2-2: The average fuel consumption for different Injera baking stoves 12
Figure 2-3: Heat storage as sensible heat leads to a temperature increase when heat is stored 24
Figure 2-4: Heat storage as latent heat with respect of temperature 25
Figure 2-5: Classification of latent heat storage material 27
Figure 3-1: Methodology flow chart 51
Figure 3-2: Overall system layout with section view 53
Figure 3-3: The basic solar angles 65
Figure 4-1: Thermal circuit diagram and heat loss in PV-integrated, Injera baking system ... 74
Figure 4-2: Schematic drawing shows the oil-PCM storage during charging conditions 88
Figure 4-3: Schematic drawing shows the oil-PCM storage during discharging conditions ... 89
Figure 4-4: Flow chart 91
Figure 4-5: Validation of temperature of PCM and thermal oil computational model by experimental results on charging. 92
Figure 4-6: Grid independence test 93
Figure 5-1: Temperature variation of PCM during charging for 4.7 hours 95
Figure 5-2: Comparison of the temperature of oil and PCM during charging 96
Figure 5-3: Melt fraction of PCM versus time during charging 97
Figure 5-4: Temperature of PCM, thermia oil, and baking pan during discharging 99
Figure 5-5: Solidification of PCM versus time during discharging 100
Figure 5-6: The average surface temperature of the baking pan or Mitad of solar Injera baking stoves 101
Figure 5-7: Efficiency comparisons 102

LIST OF TABLES

Table 2-1: Summary of improved and traditional biomass Injera baking stoves 8
Table 2-2: Fuel consumption of open-fire stoves 11
Table 2-3: Fuel consumption of Mirt stove 11
Table 2-4: Summary of literature related to Solar Injera baking system with and without storage system research outputs..... 17
Table 2-5: Thermo-physical properties of selected eutectic compounds..... 30
Table 2-6: Summary of literature related to PCM and numerical investigation of charging-discharging of it with heat transfer fluid. 33
Table 2-7: Types of encapsulation techniques..... 37
Table 2-8: Literatures related to effect of PCM arrangement on the heat transfer rate 40
Table 3-1: Thermo-physical properties of Injera and baking pan..... 54
Table 3-2: Useful baking energy for different numbers of Injera..... 55
Table 3-3: Total baking energy for different numbers of Injera 56
Table 3-4: The properties of phase change materials used in the TES of solar cookers..... 57
Table 3-5: Thermo-physical property of the NaNO3 - KNO3 eutectic salt (60: 40 mol %) ... 58
Table 3-6: Baking energy and amount of PCM needed for different numbers of Injera..... 60
Table 3-7: Monthly average global radiation data for Addis Ababa from (2014-2016)..... 64
Table 3-8: The size of the PV system in Wp for the peak load at STC for a different number of injera with specifications from Hi-Tech (Solar HI-Tech, 2015).. 71
Table 3-9: variation of thermal properties with the temperature of thermal oils..... 72

LIST OF ACRONYMS AND ABBREVIATIONS

NOMENCLATURE

m	Mass of the storage materials
A	Area
h	Convective heat transfer coefficient
C	Specific heat capacity
T	Temperature
g	Gravitational Acceleration
δ	Characteristic length
Nu	Nusselt number
Pr	Prandtl number
K	Thermal conductivity
V	Volume
P	Perimeter
D	Diameter
L	Height of the storage
Q	Amount of energy
U	Overall heat transfer coefficient
X	Molten fraction

GREEK SYMBOLS

ϵ	Emissivity of baking pan
ν	Kinematic viscosity
θ	Angle of incidence
∅	Latitude
Δ	Change
β	Slope
γ	Surface azimuth angle
δ	Declination

ε	Porosity (void fraction)
ω	Hour angle
η	Efficiency
σ	Stefan Boltzmann constant
λ	Latent heat of fusion

SUBSCRIPTS

pan	Pan
pcm	Phase change material
f	Working fluid
o	Oil
eff	Effective
st	Storage
v	Volumetric
pcm, s	Solid PCM
pcm, l	Liquid PCM

ABBREVIATIONS

HTF	Heat Transfer Fluid
PV	Photovoltaics
LHTES	Latent Heat Thermal Energy Storage
PCM	Phase Change Material
TES	Thermal Energy Storage

CHAPTER 1: INTRODUCTION

1.1. Background of the study

Energy is necessary for all societal development and economic prosperity. About 79% of the citizens of Ethiopia live in rural regions (Shigute et al., 2020) and use conventional biomass energy sources for heating and cooking in huge amounts. Due to the country's restricted access to modern electricity, the energy sector in Ethiopia faces some issues (Mondal et al., 2018). Technical, human capacity, financial, economic, underdeveloped rural energy markets and infrastructures, information, and political hurdles are the main obstacles to the harvesting and growth of renewable energy (Tiruye et al., 2021).

Access to modern energy sources is crucial for economic growth, improving livelihoods, and advancing the country's development agenda by enhancing educational opportunities, lowering pollution, and assuring ecologically friendly (Reddy, 2015).

Cooking still consumes the most energy in Ethiopia, where biomass is the primary energy source. Based on the most current country's energy status report, the residential sector utilized 90% of all energy in 2014, biomass accounted for 89% of the final energy supply (SNV, 2018) and Injera baking consumes more than half of this energy. The national dish of Ethiopia, injera is a flatbread with a distinctive flavor; It is a circular pancake with a sour and pleasant texture, a thickness of 2-4 mm, and a diameter of about 58 cm to be properly prepared, injera requires an oven temperature of 180–220 °C (Kahsay, et al., 2014).

Injera is a meal that has been made from several grains, including teff, millet, sorghum, maize, wheat, and rice, or mixtures of those grains, and it has gone through a fermentation process by adding leftover dough from an earlier baking process as a starter for a few days. Traditionally, injera was cooked either on an electric stove or on a three-stone stove using a ceramic pan called a Mitad (Adem & Ambie, 2017).

Solar energy is a sporadic kind of sun energy that works well for cooking. Solar thermal technologies, such as parabolic trough, tower, and dish systems for high temperature, flat plate collectors, evacuated tube collectors, and box solar collectors for low-temperature applications, are used to capture solar energy. Lowering the usage of conventional cooking methods for high-temperature cook stoves can play a significant role in improving public health and reducing environmental pollution. It is a plenty renewable resource that is easily accessible in sufficient quantities, making it the most encouraging, healthy, and environmentally friendly source. Due to sporadic characteristics of the sun's energy, TES is needed to retain energy for a certain period and provides this energy for later usage. The limitation of solar energy can be overcome by using a thermal energy storage system, and an integrated solar-storage design facilitates the direct or indirect storage of thermal energy using heat transfer fluid (Kedida et al., 2019). The imbalance within the timing of energy availability and consumer demand is fixed via energy storage.

Solar energy can be stored as electrical, chemical, mechanical, and thermal energy. For usage later, when there is no solar irradiation, the thermal energy which is not needed by the process in the day's peak hour can be stored. This heat is then used for several purposes, including food preparation, desalination, room heating, and more.

In this study, the numerical analysis will be investigated on the charging-discharging of the PCM using thermal oil as heat transfer fluid heated by PV integrated with an electrical heater for the Injera baking application.

1.2. Problem Statement

Nearly 90 percent of emerging countries and about half of the global population still utilize biomass fuel for their domestic energy needs, including lighting, heating, and cooking. Due to the significant usage of biomass fuel and the construction of traditional stoves, baking Injera is the main activity in Ethiopia that contributes to indoor air pollution (Embiale et al., 2021).

Ethiopians consume injera two to four times per day, however, the majority of Ethiopians still bake injera using an outdated, unhealthy, and ineffective open-fire stove called a three-stone fire (Adem & Ambie, 2017).

In addition, the household sector used 90% of the total energy in 2014 (SNV, 2018). Injera baking requires over 50 % of the primary energy consumption and as a result, deforestation, pollution, and poor kitchen environment are caused. The health, energy, school time, and hardship difficulties of mothers and children were all impacted by this traditional biomass-based cooking. (Kahsay, et al., 2014).

Therefore, it is important to give considerable consideration to alternative energy sources like solar, thermal gasification, and biogas. In this study, solar energy is used to reduce such energy consumption because it is a plentiful renewable resource. Although it is a natural source of energy, the demand and the energy available are incompatible because of its intermittent nature. As a result, a thermal storage system that provides the necessary energy must be developed. Numerous researchers have created solar Injera cookers using solar concentrators, parabolic troughs, and other methods and it's very important to use and test other methods of solar energy harnessing method to bake Injera which is photovoltaic systems.

In this study, the numerical analysis will investigate on charging-discharging of the thermal storage system in this case a PCM using thermal oil heated by PV integrated with an electrical heater for Injera baking application. Since the numerical model can investigate and provide predictions of the charging and discharging of thermal storage properties since it decides the input, output, and stored energy for the needed application.

Many researchers have designed solar Injera cookers, the working fluid used mostly are steam and thermal oil. In this study thermal oil is used as a working fluid and sensible energy storage, Since steam's latent heat is employed for process heating, it has a lower potential for heat transfer than thermal oil at the same temperature range, further, for high-temperature applications, thermal oil system requires, low pressure with less corrosion, more operating

flexibility, and better control (Bade & Bandyopadhyay, 2015) due to these reasons, the thermal oil is preferred over steam.

1.3. Objectives

1.3.1. General Objectives

The main objective of this research work is to numerically investigate the charging and discharging of a PCM using solar PV and thermal oil for Injera baking applications.

1.3.2. Specific Objectives

- Design Injera baking stove.
- Investigate and select the type of PCM for the Injera baking application.
- Develop the mathematical and numerical models of the equations governing the different processes.
- Conduct simulation using MATLAB software.

1.4. Scope and limitation of the study

This study aims at a numerical investigation of the main heat transfer processes in the system of thermal energy storage integrated Injera baking application. This work is also a simulation and investigation of a thermal storage system that satisfies the heat demand of Injera baking. However, the entire system simulation and experimental study are not the focus of this study.

1.5. Significance of study

The usage of solar power for baking Injera is significant to their way of life because the majority of Ethiopian people reside in rural locations where there is no access to an electrical power source. This work advances the use of the solar system in Injera baking. It additionally helps in the development of a comparable system that will work best for the baking system. This study's finding leads to the development of a cleaner baking method that will safeguard for both the surroundings and the well-being of people.

CHAPTER 2: LITERATURE REVIEW

2.1. Introduction

Solar energy is a renewable resource of energy that is not depleted by its usage and the main purposes of using this energy are to create electricity and directly capture and use heat, also to accomplish these objectives there are three types of conversion are used those are solar thermal, solar photovoltaic, and solar thermos-photovoltaic conversions. A solar cooker is a device that converts solar energy into thermal energy and uses that energy to cook food. It is also among the easiest, most practical, and most appealing ways of thermal applications of solar energy. It is the safest, cleanest, most environmentally friendly, and most practical method of cooking food without using fuel or heating the kitchen, and saving a large amount of conventional fuels (Wollele & Hassen, 2019; Kajumba et al., 2020). A short literature survey of some of the selected papers is presented here.

2.2. Solar cooker

Cooking is one of the most crucial aspects of every person and an essential household task in every community in the world. It is typically done over open fires that are fueled by firewood in the majority of rural parts of developing nations. The creation of alternate, suitable, and economical cooking techniques for usage in underdeveloped nations is urgently needed (Thirugnanam et al., 2020).

2.2.1. Types of Solar Cookers

The following are the main categories into which solar cookers can be divided (Bonsa, 2020):

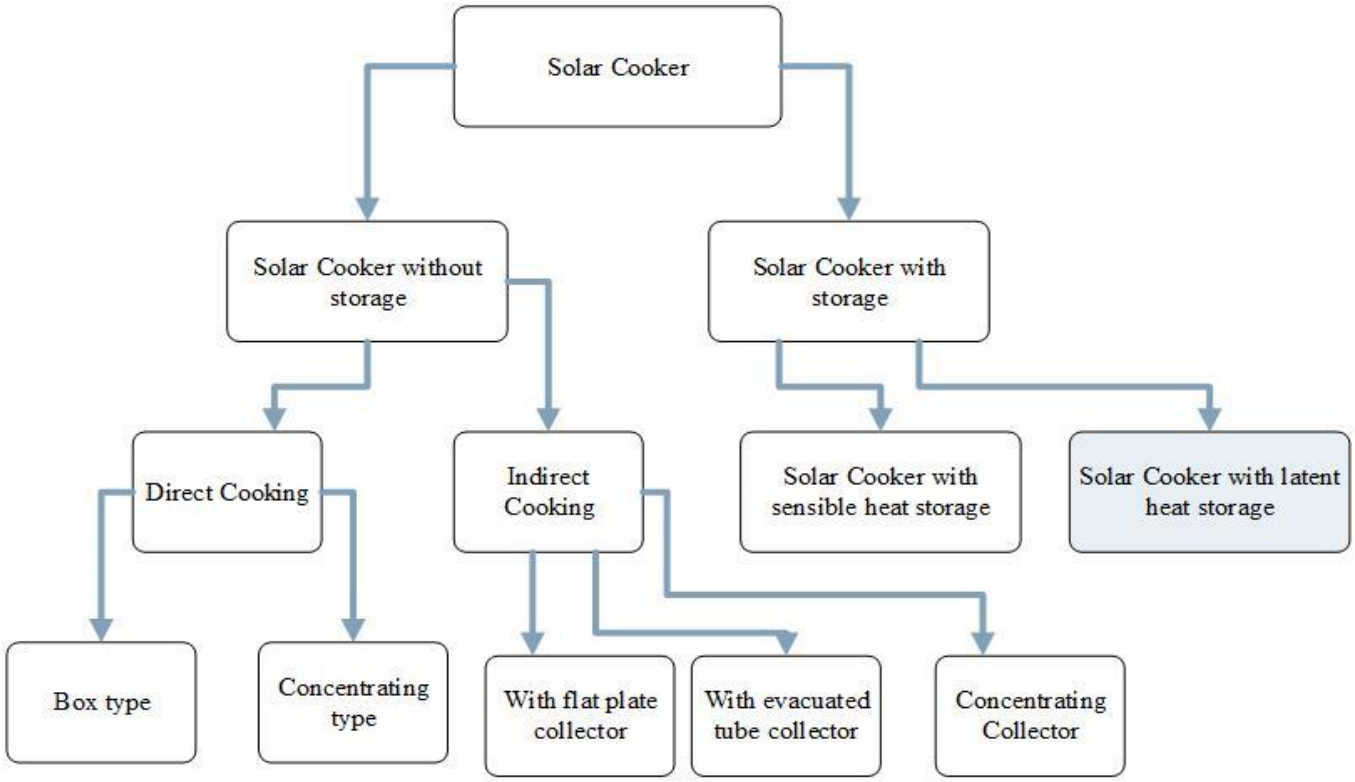

Figure 2-1: Types of solar cookers

2.3. Injera Baking Technologies

2.3.1. Baking Pan

A baking pan, also known as a Mitad in the local language, is a round disk with a smooth top surface that is used for baking injera. Mitad is constructed from clay traditionally, and baking requires a surface temperature of 180 to 200°C. Conventional baking pans typically have a diameter of 58 to 60 cm and it has a very low energy efficiency of between 52 and 55 percent. Injera baked at a lower temperature of 147 to 150°C with poorer quality, according to a newly developed ceramic pan (Adem & Ambie, 2017).

2.4. Type of Injera baking technologies

Injera is currently baked in Ethiopia using a variety of baking methods (Hassen et al., 2011; Tadesse, 2020).

2.4.1. Three-Stone Open-Fire Stove

This is a time-honored and conventional technique for baking injera. The baking pan, which has an average 60 cm diameter and 20 cm thickness, is supported or carried by three equal-sized stones arranged in a triangle. After that, firewood was placed for burning in the gaps between the stands. Injera is being baked on the pan as it is being burned below. Three-stone open fire stoves have the drawbacks of consuming a lot of firewood and generating a lot of emissions of carbon dioxide and contamination of air (Adem & Ambie, 2017). Open-fire injera baking stove is the most common in our nation.

An open-fire stove uses 931 g of wood per kilogram of injera and the measured interior air pollution was 80 ppm for CO and 1.10 mg/m3 of particulate matter (FELEKE, 2007).

2.4.2. Improved Biomass Injera Baking Stoves

efforts to develop effective biomass Injera baking started in 1980s by governmental and non-governmental institutions developed a number of improved stoves such as Burayou mud, Ambo mud, Tigrian, Sodo, Mirt, Gonziye, and Awramba stoves. Thickness and mitad competence in seasoning, fuel consumption, and ease of operation were standard performance metrics that are used for evaluating various kinds of stoves (Adem & Ambie, 2017).

Numerous experiments were carried out and comparison with baking over an open flame, Mirt saved between 30 and 49% of the fuel (Anteneh and Walelign, 2011). When compared to open three-point stoves, cooking with Mirt stoves reduced wood consumption in a rural family with five members by 48%, while Gonzie stoves lowered wood consumption by 33.85 to 54.14% depending on the availability of sand on the clay soils (Fekadu Kedir et al., 2019, Hiwote Teshome, 2011).

Table 2-1: Summary of improved and traditional biomass Injera baking stoves

	Type of stove	Injera baked per session	Method of test	Performance							Reference
				Fuel consumption (g/kg of Injera)	Total baking time (min)	% Reduction in specific fuel consumption compared to open-fire	% Reduction in time to boil compared with open-fire Injera baking stove	CO concentration (ppm)	PM concentration (mg/m3)	Thermal efficiency	
1	Mirt stove	28	CCT and UCB particle monitor and HOBO CO data logger. (8 hours Average)	524	129	45	7	7.2	0.88	-40%	(FELEKE, 2007)
	Three stone	27		1030.7	121.4			80.1	1.10 mg/m3	5% to 10%	
2	Mirt stove (slim)		CCT and Indoor air pollution (8 hours Average)	511	129	50	7				(Hiwote Teshome, 2011)
	Mirt stove (classic)			508	127	51	5	6.09	0.68		
	Three stone			1031	121			78.9	0.98		
3	Mirt with integrated chimney	25-30	controlled cooking test/CCT	596	102	42	15	-	-	-	(Antenah and Waleligh, 2011)
	Three stone			1031	121						

	Type of stove	Injera baked per session	Method of test	Performance							Reference
				Specific fuel consumption (g/kg of Injera)	Total baking time (min)	% Reduction in specific fuel consumption compared to open-fire Injera baking stove	% Reduction in time to boil compared with open-fire Injera baking stove	CO concentration (ppm)	PM concentration (mg/m3)	Thermal efficiency	
4	Mirt stove	27	Controlled Cooking Test	460		30					(Workeneh Gashie, 2005)
	Three stone	28		630							
5	Improved Mirt stove normal Mirt stoves					50		90%	50% 30%	20-30% over traditional stoves	(Asres, 2012)
6	Gonzie stove	25-30	Controlled Cooking Test (CCT)	617	106	41	7	-	-	-	(Gulilat, 2014)
	Three stone			1038	114						
7	Mirt stoves Gonzie stoves (depending on the presence of sand on the clay soils)					48, 33.85 - 54.14		53.85 to 74.14% per household			(Fekadu Kedir et al., 2019)
8	Mirt Stove					50				22%	(EnDev/GIZ, 2015)

	Type of stove	Injera baked per session	Method of test	Performance							Reference
				Specific fuel consumption (g/kg of Injera)	Total baking time (min)	% Reduction in specific fuel consumption compared to open-fire Injera baking stove	% Reduction in time to boil compared with open-fire Injera baking stove	CO concentration (ppm)	PM concentration (mg/m3)	Thermal efficiency	
9	Mirt stove Three stone		controlled cooking test	519.8g/kg dough 393.1g/kg dough		24					(Dresen et al., 2014)
10	Awramba stove Three stone open fire			573 1025	107 120	35	5				(Adem & Ambie, 2017)
11	Sodo stove		controlled cooking test	908							(Tadesse, 2020)

Table 2-2: Fuel consumption of open-fire stoves

No	Fuel consumption (g/kg of Injera)	Number of Injera baked	Reference
1	1031	-	(Hiwote Teshome, 2011)
2	630	28	(Workeneh Gashie, 2005)
3	1038	25-30	(Gulilat, 2014)
4	1025	25-27	(Adem & Ambie, 2017)
Average	931		

Table 2-3: Fuel consumption of Mirt stove

No	Fuel consumption (g/kg of Injera)	Number of Injera baked	Reference
1	524	28	(FELEKE, 2007)
2	511	-	(Hiwote Teshome, 2011)
3	508	-	(Hiwote Teshome, 2011)
4	596	25-30	(Anteneh and Walelign, 2011)
5	460	27	(Workeneh Gashie, 2005)
Average	520		

According to current studies, the development patterns of the Injera baking stove are focused on optimizing energy losses in order to decrease the specific fuel, also increases the performance of the particular stove. The fuel consumption of some Injera baking stoves is shown in Fig. 2-2 below.

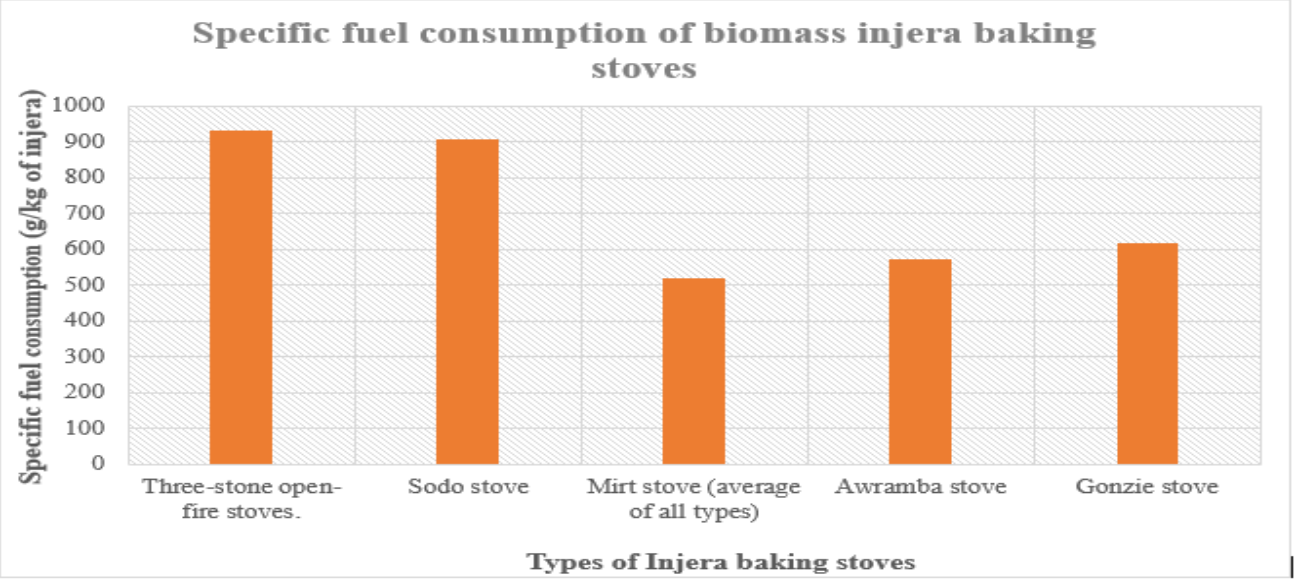

Figure 2-2: The average fuel consumption for different Injera baking stoves

2.4.3. Biogas Injera Baking Stove

Biogas is a renewable energy technology that uses garbage from municipal landfills, animal waste, and human waste to create combustible methane gas that is useful for lighting and cooking. Additionally, it is a clean and renewable source of energy, with a composition of 60–70% methane (CH4), 30–40% carbon dioxide (CO2), 1–5% hydrogen, and traces of nitrogen, hydrogen sulfide, oxygen, water vapor, and slurry and is a byproduct of the anaerobic digestion process that occurs when methanogenic bacteria operate on biodegradable materials without oxygen (Desta et al., 2020). Injera baking biogas stoves have issues with consuming a lot of gas, lose a lot of heat, and pressures that aren't evenly distributed on the perforations. This results in uneven heat distribution on Mitad (Kebede & Kiflu, 2014).

2.4.4. Electric Injera Baking Stoves

The Electric Injera baking stove was introduced to Ethiopia 40 years ago through the Ethiopian Electric Light & Power Authority, which uses 60–70% of the electricity generated by Ethiopia's hydroelectric infrastructure. The following list summarizes the main drawbacks of the current electric Mitad designs (Jones et al., 2017; Danas EE, 2015):

- It is energy inefficient. The significant quantity of electrical energy necessary to heat up to the predetermined temperature of approximately 200–250^{0}C required to bake injera is mostly blamed for the causes of energy inefficiency also heat losses due to poor insulation, and the method of manufacturing process Mitad.
- The heating element's improper adjustment, the electric wiring's insufficient size, and the excessive resistance.
- The use of poor building materials.
- Poor insulation: it is estimated that the energy lost during the baking procedure ranges from 40 – 50%.
- Lack of temperature control devices.

2.5. Review of Related Works

In this section selected existing literature about solar Injera baking systems with and without thermal storage are reviewed.

Hassen et al. (2011) a new baking system that uses solar energy as its power source is presented and experimentally tested. To heat the new ceramic pan, a steel pan with fins is placed underneath, and oil is poured into the cavity to transmit heat to the steel and fins, further heating the baking pan. The ideal baking temperature (180°–220°C) is reached after 40 minutes of oil circulation, which takes around an hour. With a 3-minute break in between each Injera, 5 were baked at 2-minute intervals and for at least four hours, radiation can be efficiently gathered. Thus, 20 Injera can be successfully baked per day utilizing the suggested solar-powered setup in around three hours and 28 minutes. However, the experimental and analytical results differ significantly from one another (300 and 350^{o}C) and no backup option is offered on days with clouds or in the absence of sunshine.

Haileselassie et al. (2014) introduce a new technology that makes it possible to bake injera with an indirect solar stove. To bake injera, a parabolic dish with a 2.54 m2 aperture area, well-insulated pipes 10mm, and a coiled stainless-steel heat exchanger was developed. According to the authors, injera can be baked at a quality-acceptable level between 135 and 160 °C. By

enlarging the collector and improving the stove's heat conductivity, the lengthy heating up, baking, and baking-interval times can be reduced. However, the simulation study didn't include its discharging behavior.

Tareke (2014) develops a finite element model for the Injera baking process for a conventional electric baking pan. According to the findings, the majority of heat losses from the pan surface for clay pans happen between two injera and during initial pan heating. By increasing the number of baking cycles, electric baking pans' thermal efficiency can be improved also the author suggested using a 2.5 kW electric baking pan with a 0.01 m thick clay plate. Moreover, lowering the thickness of the current clay pan and conducting experiments on the strength of the plate and baking capacity also replacing the power source by other renewable sources not studied.

Hassen et al. (2016) in this new form of baking system, the feasibility of baking on a glass stove is explored using solar thermal energy delivered to the kitchen via a circulating heat transfer fluid warmed by solar radiation concentrated via a parabolic trough. An experiment was carried out, and the glass baking pan's top surface temperature was 191 °C. Additionally, experiments with baking injera were carried out and it took an average of two minutes to bake a single injera and two minutes to bring the surface temperature of pan back to the baking temperature, i.e., the entire baking cycle took around four minutes. However, a storage-integrated concept could be included for indoor cooking.

Goytom (2016) conducted heat transfer analysis of the solar injera baking system. By adjusting the baking pan's thickness also the temperature of the oil in in touch with the pan, heating up of the pan was assessed. From the outcome pan thickness of 5mm and warm oil temperature of 255^{o}C, showed quick heat-up times and suitable baking periods were recorded. However, experimental investigation was not studied to validate the simulation result.

Tesfay et al. (2014) the experimental setup uses a parabolic dish solar collector linked with latent heat storage to test a solar stove for Injera baking. A self-circulating steam loop was used

to charge the heat storage, which was made of solar salt (40 percent KNO3 and 60 percent NaNO3). Depending on the level of insulation, the storage has a capacity to hold usable thermal energy for one to two days, and nineteen injera were successfully baked using the heat that had been stored during this period, with each injera taking three minutes on average to bake also the remaining heat was used to make bread. But this paper does not conduct the charging-discharging analysis on the PCM.

Haileslasie & Bayray (2019) has developed a solar cooker for injera baking that incorporates a PCM thermal storage and heat-transfer loop device. Where the system storage can hold heat for two days and has a capability of about 250^{o}C. A completely charged storage has provided enough heat to bake average household injera demands which is about 19 Injera's and with the remaining heat, additional breads were cooked. Furthermore, the receiver's ability to regulate heat loss and the tracking mechanism's durability needs to be improved.

Hailu et al. (2017) built a direct solar fryer injera baking equipment with an aluminum baking plate and parabolic solar collector. The baking pan had a 12.5 mm thickness and a 550 mm diameter. The developed system has two operational modes: alternate heating and baking modes, and continuous heating and baking cycles. The experimental findings indicate that the initial heating-up times for both operating modes were in the 30 to 45-minute range and that these initial heating-up times were equivalent to the traditional baking procedure. n the initial heat-up phase, the plate in the continuous type model has reached an average temperature of 120 to 130 °C and in the alternating type model, temperatures range from 160 to 180 °C. Also in the continuous type model's average baking time was 5 minutes, while the subsequent additional heat-up time was only 2 minutes. It offers a 563W baking power with a system thermal efficiency that includes a 37% collector efficiency. The application is, however, limited when there is insufficient solar radiation, such as on cloudy days or under the shadows of the sun. In these situations, an alternative approach needs to be researched.

Getenet (2011) develop finite element formulations and mathematical models for baking pans and injera. Two different baking pan types (clay and ceramic) with varying thicknesses were

investigated. Experiments were conducted using conventional clay baking pans. With a 2.5KW power supply, baking pans made of 10mm thickness clay and 8mm thickness ceramic performed somewhat more effectively. The efficiency of several clay baking pans for 10 baking cycles ranged from 53-66% and for ceramic baking pans was between 66–72%. Furthermore, an experimental study on improved clay baking pans with better thermal properties and energy auditing during the Injera baking process to precisely identify losses could also be studied.

Melkamu (2013) designed a solar thermal powered injera baking system integrated with thermal storage which enables cooking to be done indoors and both in the day as well as at night. The system consists of the cooking (pan) assembly, reflector, concentrator (Scheffler), and thermal storage system. The baking pan surface reached 313^0C while charging and 233^0C after cooling, allowing one baking session to produce enough injera for a family of average size. Furthermore, to develop an efficient method of heat storage, both practical and computer optimization studies are not included. The summary of reviewed journals on the development of a solar Injera baking stove is shown in Table 2-4.

Table 2-4: Summary of literature related to Solar Injera baking system with and without storage system research outputs.

Title	*Type of PCM used*	*Type of solar collector*	*Method*	*Key finding*						*Reference*
				Qualitative	*Quantitative*					
					Surface temp of pan (^{0}C)	*Time to bake*	*Idle Time (min)*	*Charging time*	*Discharging time*	*Storage temp*	
Solar powered heat storage for Injera baking in Ethiopia.	60% NaNO3 -40% KNO3	Parabolic dish	experimentally and simulation	For more than a day, a useful heat was kept.	135-160	-	-	4.5 hrs.	-	216-222	Kahsay, et al.(2014)
Performance investigation of solar powered Injera baking oven for indoor cooking.	-	Parabolic Trough	experimental investigation	A new kind of ceramic baking pan is produced and used to prepare injera.	180– 220	3:28 Per 20 Injera.	57	-	-	-	Hassen et al.(2011)

Title	*Type of PCM used*	*Type of solar collector*	*Method*	*Key finding*						*Reference*
				Qualitative	*Quantitative*					
					Thermal performance (%)	*Time to bake*	*Idel time*	*Charging time*	*Discharging time*	*Working fluid temp* ,^{0}C
Heat transfer analysis during the process of Injera baking by finite element method.	-	-	Modeling and simulation	A baking pan's heat-up and idle times are reduced when its thickness is reduced.	53–66 for clay pan and 66–72 for ceramic baking pan.	-	-	-	-	300	Getenet, (2011)
Numerical and experimental analysis of solar Injera baking with a PCM Heat storage.	40% KNO3 and 60% NaNO3	Parabolic dish collector.	Numerical and experimental Analysis	Introduces indirect charging, simultaneous charging and discharge, and heat storage discharging.	23	4hrs	-	7 hrs.	4hrs	250	Haileslasie&Bayray (2019)

Title	*Type of PCM used*	*Type of Solar collector*	*Method*	*Key finding*						*Reference*
				Qualitative	*Quantitative*					
					Surface temp of pan or Mitad, ^{0}C	*Time to bake (min)*	*Idel Time (min)*	*Charging time*	*Dischargin g time*	*Storage temp,* °C
Energy storage integrated solar Stove A case of solar Injera baking in Ethiopia.	A solar salt-based latent heat storage.	Parabolic dish	Experimental investigation.	Thermal energy that can be used can be stored for one to two days.	-	3 per Injera.	-	-	1 hr.	220	Tesfay,et al.(2014)
Design and manufacture of laboratory model for solar powered Injera baking oven.	-	Parabolic trough	Design and experimental investigation.	Heat transfer oil can retain heat for 4 hrs after energy source has been turned off.	215	2	3	-	-	-	Tsegay (2011)

Title	*Type of PCM used*	*Type of Solar collector*	*Method*	*Key finding*						*Reference*
				Qualitative	*Quantitative*					
					Surface temp of pan or Mitad, ^{0}C	*Time to bake (min)*	*Idle time*	*Charging time*	*Discharging time*	*Storage temp,* ^{0}C
Finite difference modelling of solar thermal powered Injera baking oven.	-	Parabolic trough	Simulation of transient heat transfer analysis.	According to the baking pan simulation results, system efficiency can be raised by reducing pan thickness.	180-220	-	-	-	-	-	Goytom (2016)
Integration of Scheffler concentrator and thermal storage device for indoor Injera baking.	Hitec heat transfer salt	Scheffler concentrator	Simulation	The pan's maximum temperature may be reached in about an hour, and it can retain heat for up to 10 hours.	233	3	-	-	-	142	Melkamu (2013)

Title	*Type of PCM used*	*Type of Solar collector*	*Method*	*Key finding*						*Reference*
				Qualitative	*Quantitative*					
					Surface temp of pan or Mitad ,^{0}C	*Time to bake, (min)*	*Idle Time (min)*	*Charging time*	*Discharging time*	*Storage temp*	
Design and development of solar thermal Injera baking: steam based direct baking.	-	Parabolic dish	Design and experimental investigation.	It proves indoor solar baking is feasible	135–160	2.5	-	-	-	-	Haileselassie et al. (2014)
Heat transfer analysis of electric Injera baking pan by finite element method.	-	-	Simulation	By increasing the number of baking cycles, the thermal efficiency can be improved.	-	-	-	-	-	-	Tareke (2014)

Title	*Type of PCM used*	*Type of Solar collector*	*Method*	*Key finding*						*Reference*
				Qualitative	*Quantitative*					
					Surface temp of pan or Mitad , ^{0}C	*Time to bake per Injer(* min*)*	*Idel Time (*min*)*	*Charging time*	*Discharging time*	*Heating up time (min)*
Design and manufacturing of thermal energy based Injera baking glass pan.	–	Parabolic trough	Design and experimental investigation.	After the power source is turned off, the active heat transfer fluid has the capacity to sustain the temperature for up to four hours.	191	2	2	_	_	45	Hassen et al. (2016)
A direct solar fryer for Injera baking application.	-	Parabolic dish	Design and experimental investigation	The fryer worked well and allowed for the free use of solar energy.	120 -130	5	2	-	-	30 - 45	Hailu et al.(2017)

2.6. Solar Thermal Energy Storage Concepts

Thermal energy can be stored as a change in a material's internal energy as sensible heat, latent heat or thermochemical, or a mix of these. Sensible heat storage results from material temperature changes, whereas latent heat storage results from phase changes, whether they are solid-liquid, liquid-gas, or solid-solid and thermochemical storage is created when a chemical reaction that involves a high amount of energy is employed to store energy and the reverse reaction occurs, heat that was separately stored during the reaction should be easily accessible (Sharma et al., 2009).

Different methods for thermal energy storage are employed based on the type of change that takes place on the storage medium (Khordehgah, 2020. Bauer et al., 2020) :

2.7. Types of Thermal Energy Storage

Thermal energy storage (TES) materials and systems can be categorized in a number of different ways. Storage materials can exist in a variety of physical states, such as solids, liquids, gases, or through a phase change, and the three most frequent TES kinds are distinguished (Bauer et al., 2020).

2.7.1. Sensible Heat Storage

Sensible heat storage materials have the ability to store thermal energy without the storage medium going through a phase change, which results in a rise or decrease in the temperature of the storage material. The amount of energy stored is roughly proportional to the temperature difference between the materials. Two categories of sensible heat storage are: Solid storage media and liquid storage media, respectively (Ahmed et al., 2017) and it can be expressed as (Kumar & Shukla, 2015) :

$$Q = \int_{Tf}^{Tin} mCpdT \qquad 2.1$$

$$Q = mCp(Tf - Tin) \qquad 2.2$$

Where: m - the mass (kg),

Cp - the specific heat capacity (kJ/ kg. K) and

dT - the rise in temperature during the charging process.

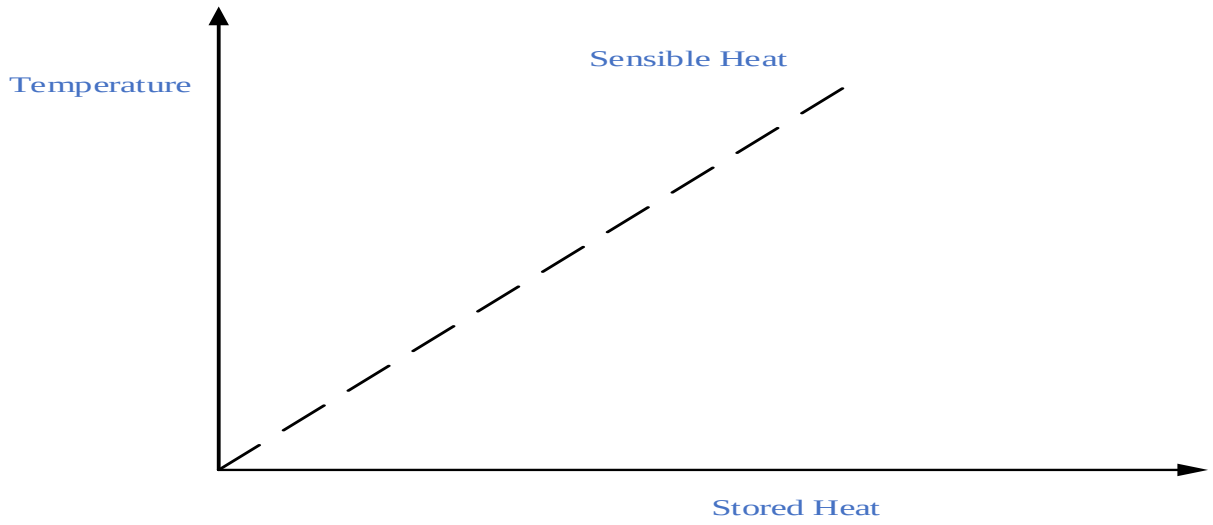

Figure 2-3: Heat storage as sensible heat leads to a temperature increase when heat is stored

2.7.2. Latent Heat Storage

Materials for the storage of latent heat are also known as phase change materials (PCM) due to the fact that they may transition from a solid to a liquid state and vice versa. The phase change is always accompanied by heat absorption during the melting of the solid and a heat release during the solidification of the liquid and occurs at the melting temperature Tm. The ability to store energy within a constrained temperature range near the phase transition temperature is the key benefit of latent heat storage techniques (Bauer et al., 2012) and the stored heat in a PCM can be calculated as follows (Kumar & Shukla, 2015):

$$Q = \int_{Ti}^{Tm} mCpdT + m\,\Delta Hm + \int_{Tm}^{Tf} mCpdT \qquad 2.3$$

$$Q = m\,[Cps\,(Tm - TL) + \Delta Hm + Cpl\,(TH - Tm) \qquad 2.4$$

Where: m - mass of heat storage medium, T_m- the melting point, C_{ps} and C_{pl} are the specific heat of the PCM in solid and liquid state respectively, and ΔHm is the phase change enthalpy.

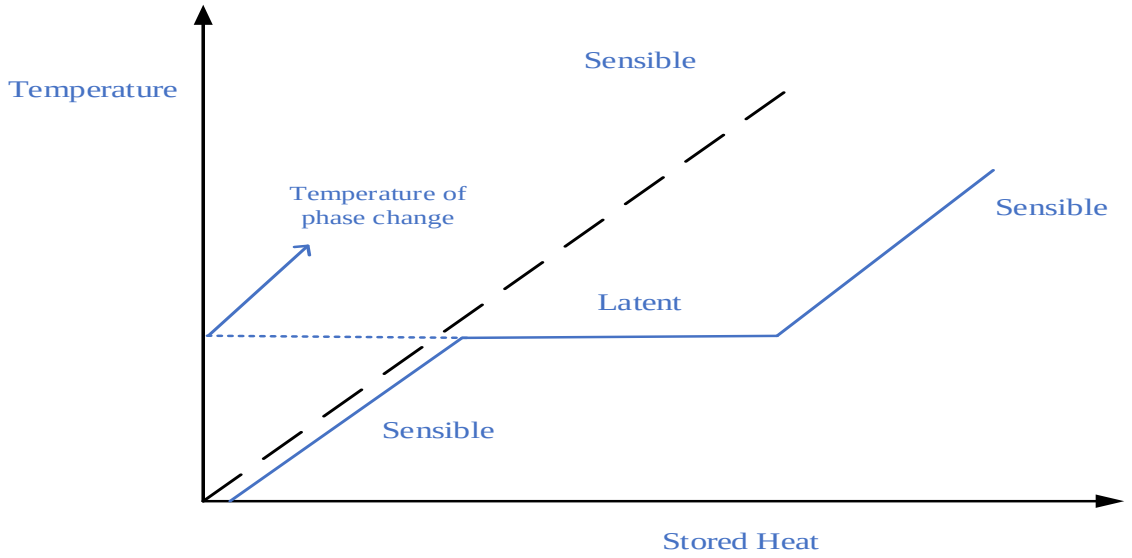

Figure 2-4: Heat storage as latent heat with respect of temperature

2.7.3. Thermochemical Energy Storage

This storage technique involves chemical reactions and Chemical reactions can be driven by thermal energy (reversible thermal decomposition reactions), and the byproducts can be kept indefinitely at room temperature without losing capacity (DOST & Department, 1996). The following is the operating theory (Prim, 2013):

$$A + HEAT = B + C \qquad 2.5$$

First, due to heat absorption (endothermic reaction) during the charging phase, chemical A is changed into two new compounds, B and C. The two new chemicals must therefore be kept at room temperature in separate vessels. Second, during the discharging phase, chemical B and chemical C engage in an exothermic reaction that creates the original chemical A and releases the heat that has been stored. The heat stored in this situation is influenced by the quantity of storage material, the endothermic heat of the reaction, and the degree of conversion (Sharma et al., 2009).

$$Q = \alpha r m \Delta hr \quad 2.6$$

Where, $a\,r =$ is the extent of the conversion reaction,

m =mass of storage material and

Δhr =change of endothermic heat of reaction.

Amongst the above thermal heat storage techniques, due to its capacity to offer high energy storage density and its ability to store heat at consistent temperatures corresponding to the phase transition temperature of phase change material (PCM), latent heat thermal energy storage is particularly attractive also in the latent heat storage materials, there is a lower temperature difference between holding and releasing heat (Alva et al., 2017).

2.8. Phase Change Material (PCM) for Thermal Storage System

Phase-change materials, often known as latent heat storage materials, during the melting process, absorb heat energy as their "latent heat of fusion". During the heat energy absorption process, there is a phase change occurring and the temperature swing is relatively little. When melting and solidifying at particular temperatures, phase change materials (PCMs) have the capacity to store and release significant amounts of energy. Thermal energy storage plays an important role in energy resource conservation by contributing to reducing the mismatch between energy supply and demand as well as improving the efficiency and reliability of energy systems (Su & Darkwa, 2015). They should have a melting point close to the TES system's needed working temperature range, melt uniformly with little sub-cooling, and be chemically stable, inexpensive, non-toxic, and non-corrosive and latent heat is significantly higher than the sensible heat in PCMs because their compactness (Farid et al., 2004). Based on their composition, PCM can be divided into a variety of categories and subgroups and the list below provides a classification of PCMs (Rai & Kumar, 2018; Dheep & Sreekumar, 2015).

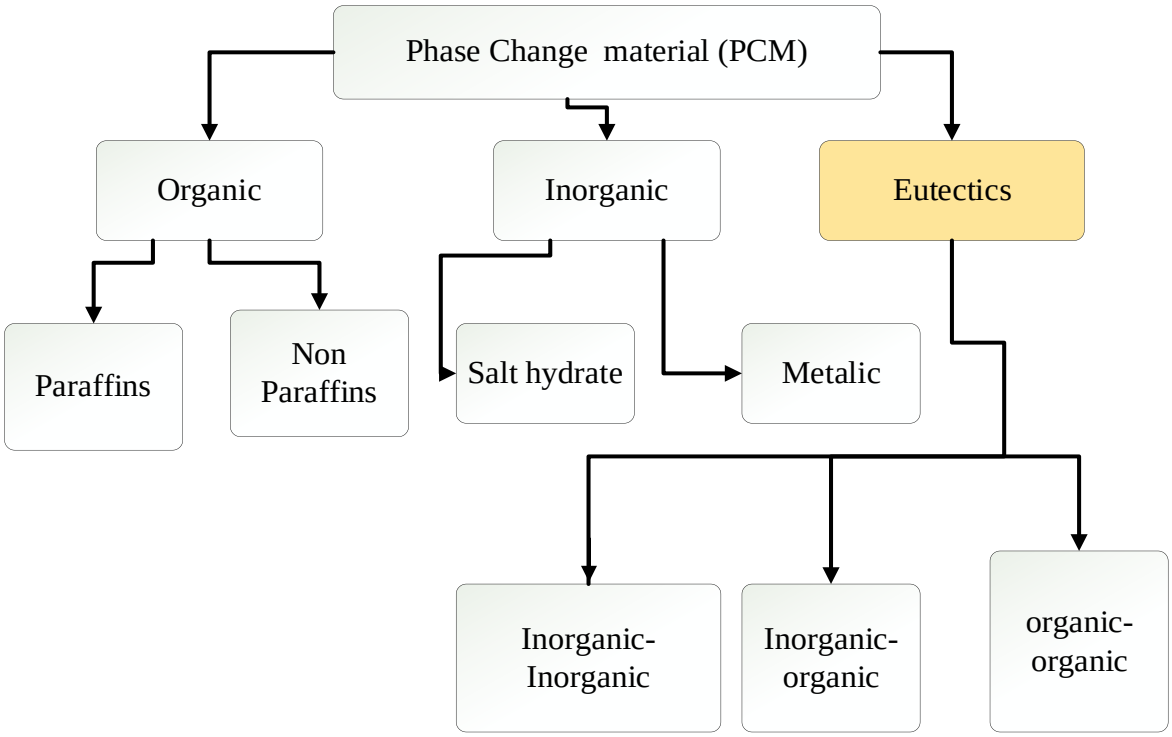

Figure 2-5: Classification of latent heat storage material

2.8.1. Organic PCM

Organic PCMs, including paraffin and non-paraffin organics, are typically made from natural fats, oils, or petrochemical compounds. The beneficial attribute of organic PCMs is that they can undergo congruent melting without phase separation. However, because of their low thermal conductivity (0.1 to 0.35 W/m.K.), which makes a large surface area is necessary for significant heat transfer rates. Additionally, their low melting points prevent them from being used in high-temperature applications (Prasad et al., 2019).

2.8.2. Inorganic Phase Change Materials

These phase transition materials do not supercool significantly, and cycling has no effect on their temperatures of fusion. In general, the volumetric latent heat storage capacity of inorganic substances is nearly twice that of organic compounds (Sharma et al., 2009) and can be further divided into metallic and salt hydrate.

Inorganic salts and water can be combined to form salt hydrates, a typical crystalline solid with the general formula AB. nH2O (Sharma et al., 2009). Compared to organic PCMs, they have benefits like high enthalpy and better thermal conductivity. There are various inorganic PCMs including salts, salt hydrates, hydroxides, metals, and metal alloys. However, they have a low heat of fusion per unit weight, which indicates that a bigger volume is needed for a given quantity of heat. (Crespo et al., 2019).

2.8.3. Eutectics PCM

Eutectic materials have a minimum melting point of two or more components, each of which melts and freezes concurrently. Eutectic materials almost never segregate during melting or freezing because they freeze into an intimate mixture of crystals, leaving little opportunity for the components to separate. They also contain salt combinations with specified melting and freezing points, usually containing two or more salts, and have great potential for thermal energy storage applications (Hasnain, 1998).

Eutectics of organic or inorganic compounds have a fixed melting or freezing point, which makes them latent heat storage materials. In terms of segregation, eutectics are typically superior to pure inorganic PCMs (Abhat, 1983).

2.9. Selection principles and required thermo-physical properties of PCM

Phase change material selection for TES systems is influenced by a variety of variables, including material properties, system storage capacity, operating temperature, HTF performance, and heat exchanger design considerations. Heat storage capacity and thermal storage/release efficiency are directly impacted by the way the chosen materials behave in various areas (Wei et al., 2018). The PCM that will be utilized to create thermal storage systems must meet certain thermophysical, requirements, including the ones listed below (Abhat, 1983; Zhong et al., 2012; Zhou et al., 2012).

Thermal properties:

- A suitable temperature for phase transitions.
- Good heat transmission and high latent heat of transition

- Higher thermal conductivity.
- Little volume changes during phase transition.

Selecting a PCM for a particular application, it is recommended that the transition temperature of the PCM and the operating temperature of the heating or cooling be matched.

Physical properties:

Favorable phase equilibrium, high density, little volume change, and low vapor pressure are all present.

Kinetic properties:

No supercooling and a high enough crystallization rate. The development of PCMs has been challenged with supercooling, especially for salt hydrates. A supercooling of more than a few degrees will obstruct the efficient removal of heat from the storage.

Chemical properties:

PCMs must have long-term chemical stability, be compatible with materials for construction, and be non-toxic, non-flammable, and non-explosive for safety.

Economics:

It's also crucial that phase change materials are accessible on a big scale and at a low cost.

The previously mentioned criteria must be met in order to use the appropriate latent heat storage system material for the required application. This PCM will be selected based on the baking temperature requirement of Injera which is around between 180-220^{0}C.

Eutectic combinations between 100 and 250^{o}C and organic and inorganic substances appear to be more promising below 100^{o}C (Pereira da Cunha & Eames, 2016). In this research work the temperature needed interval is between 180-220^{0}C and the eutectic mixture latent heat storage material should be selected. Some of the eutectic compounds where the melting temperature is

approximately the needed temperature for Injera baking application are listed in Table 5 (Pereira da Cunha & Eames, 2016;Janz, et al., 1983; Tomkins, et al., 1983).

Table 2-5: Thermo-physical properties of selected eutectic compounds

Eutectic compounds	***Mass ratio***	***Tm (^{0}C)***	***Melting enthalpy Hm (kJ/kg)***	***Cps (J/kg K)***	***Cpl (J/kg K)***	***Thermal conductivity of solid (W/m K)***	***Thermal conductivity of liquid (W/m K)***	***Density of solid(Kg/m^3)***
KNO3–NaNO3	55-45	222	110	1010	1490	0.73	0.51	2028
LiBr–LiNO3	27-73	228	279	1340	1380	1.14	0.57	2603
LiOH–NaNO3–NaOH	6-67-27	230	184	1300	2000	0.78	0.67	2154
NaNO2–NaNO3	55-45	233	163	1310	2130	0.59	0.64	2210
CaCl2–LiNO3	13-87	238	317	1500	1530	1.37	0.69	2362
LiCl–LiNO3	9-91	244	342	1580	1610	1.37	0.64	2351
NaNO3–NaOH	86-14	250	160	1190	1860	0.66	0.6	2241

2.10. A Phase Change Material Used for Cooking

In this section, the selected literature about PCM used for cooking and its charging and discharging characteristics are reviewed.

Tesfay et al. (2018) developed a steam-based heat storage, charging by using a polar-mounted solar concentrator stainless steel pipeline, and water acting as the heat transfer fluid is used to carry heat from the receiver over a short distance, from the outside to the kitchen. Nitrate salt, which is a mixture of 60% NaNO3 and 40% KNO3, can store heat up to 250°C and deliver it isothermally when baking. The charging-discharging process is carried out via a conduction

approach with the aid of fins. Using aerogel insulation and a two-phase loop thermosyphon of steam to manage the long-distance heat transportation needed between the receiver (outside) and the storage (within a house), the stored heat is preserved for around one to two days. The phase shift time for PCM storage was approximately 8 hours, and the highest temperature reached there was between 130°C and 157°C. The effectiveness of the heat transfer, retention, and charging-discharging procedures is demonstrated by the experimental and numerical findings.

However, it still required quality pipe and valve parts, and the receiver's input power is small with a lengthy charging period.

Bhave and Kale (2020) conduct a phase-changing eutectic mixture known as "solar salt" which was a NaNO3 and KNO mixture. It took 110 minutes to charge and hold heat at 220^{o}C. 0.25 kg of potato chips were fried in 17 minutes, and 0.6 kg of rice was cooked in two separate batches from one charge, each taking 20 minutes. When cooking indoors, it was simple to achieve the frying temperature of 170–180^{o}C for the oil.

Gabisa & Aman (2016) investigates a phase-change material that is said to be able to store solar thermal energy for use in home cooking applications. For the purpose of conducting an experimental examination of the thermal properties, the solar energy source can be simulated using electrical heating. It is discovered that the mixture of 40% KNO3 and 60% NaNO3 by mass has demonstrated promising thermal properties. Shiro wet and potato meals were part of an experiment to see how much energy was needed to prepare them and how much PCM was needed to store that energy. The outcome shows that 2.38kWh of energy is needed to prepare the two meals for the five members of the household for lunch and dinner. It took 4 kg of PCM to store the energy. According to the experimental results for 1.4 kg of PCM, a charging time up to 300^{o}C of 50 minutes and a discharging time down to 100^{o}C of 4.5 hours are needed.

Wollele and Hassen (2019) carry out the complete system design theoretically and need 421 W of electricity to cook 1 kg of rice in 45 minutes, which is obtained from the sun's stored energy.

Compound parabolic dish concentrator and thermal energy storage (oil and rock) are features of the solar cooker. As a result of the experiment, the pot's surface temperature averaged 380 K and less energy was delivered to the pot. After being removed from the solar collector, the TES is put on the insulated tank and filled with water before the discharge process begins. After 40 minutes, the water reaches its maximum temperature of 355 K, which is nearly the boiling point. However, the energy delivered to the cooker (pot) is reduced as a result of numerous losses; further research is needed to reduce these losses and raise the temperature of the water to its boiling point.

Saxena et al. (2013) stearic acid has been discovered to be an effective latent heat storage material in research of several phase transition materials for solar cooking. The maximum temperature achieved (134°C) during the day and 64°C at night, and the cooking time of the cooker with thermal storage decreased by roughly 15 minutes in comparison to the box cooker without thermal storage. However, the energy that has been saved is only used to make some drinks hotter or warmer, not nearly enough for cooking.

Chitra et al. (2019) investigate a solar cooker experimentally using PCM ($Mg(NO3)2.6H20$) as heat storage. According to the investigation results, it takes around 10 minutes to boil 1.5 liters of water with PCM in the space between the layers of the cooking pot, and the developed system's efficiency in March was about 44%. The dish has a 52 cm diameter and a 13 cm height, respectively. About 45 cm is the focal length of the dish as measured from the solar concentrator's bottom.

Rajendra and Shinde (2018) propose acetamide heat storage material for the cooking system.. Analysis has shown that the average and medium cooling efficiency for food heating is 40.10%. Due to infield heat loss to the atmosphere, the negative regression index demonstrates that efficiency declines with an increase in radiation. A summary of the literature related to PCM for cooking and numerical investigation is shown in Table 2-6:

Table 2-6: Summary of literature related to PCM and numerical investigation of charging-discharging of it with heat transfer fluid.

Title	***Type of PCM used***	***Method***	***Key finding***				***Reference***
			Qualitative	***Quantitative***			
				Charging time	***Discharging time***	***Storage temp***	
Characterization and experimental investigation of $NaNO_3$: KNO_3 as solar thermal energy storage for potential cooking application.	NaN_3: KNO_3 mixture	Experimental investigation	When there is no load applied, the PCM remains at its phase change temperature for around 100 minutes.	1.4 kg PCM, 50 min, 300◦C	4.5 hrs. (300 - 100◦C)	300◦C, (70◦C > PCM melting point)	Gabisa & Aman (2016)
Numerical modeling and simulation of thermal energy storage for solar cooking using COMSOL Multiphysics software.	Potassium sodium nitrate salts (KNO_3−Na O_3)	Numerical Modeling and Simulation	-	60 min	-	222^{o}C	Abreha et al.(2019)

Title	*Type of PCM used*	*Method*	*Key finding*				*Reference*
			Qualitative	*Quantitative*			
				Charging time	*Discharging time*	*Storage temp*	
Steam-based Charging-Discharging of a PCM Heat Storage.	Mixture of 60%$NaNO_3$ and 40%KNO_3	Numerical and experimental	The stored heat is retained for about one-two days by using aerogel insulation	8 hours	8 hours	250ºC	(Asfafaw H Tesfay et al., 2018)
Development of a thermal storage type solar cooker for high temperature cooking using solar salt.	60%$NaNO_3$ and 40%KNO_3	Numerical and experimentally investigation	0.6 kg of rice was cooked in two separate batches from a single charge, each requiring 20 minutes, whereas 0.25 kg of potato chips were cooked in 17 minutes.	110 min	-	220 ºC	(Bhave & Kale, 2020)

Title	*Type of PCM used*	*Method*	*Key finding*				*Reference*
			Qualitative	*Quantitative*			
				Charging time	*Discharging time*	*Storage temp*	
Design and experimental investigation of solar cooker with thermal energy storage.	Oil and rock	Experimental investigation.	The maximum temperature of water reached after 40 minutes is 355 K.	8:30	110min	355 K for rock and 420 K for oil	(Wollele & Hassen, 2019)
Solar Cooking by Using PCM as a Thermal Heat Storage.	Stearic acid	Experimental investigation	When compared to a box cooker without thermal storage, the cooking time for the cooker with thermal storage was lowered by close to 15 minutes.	-	-	52ºC	(Saxena et al., 2013)

Title	*Type of PCM used*	*Method*	*Key finding*				*Reference*
			Qualitative	*Quantitative*			
				Charging time	*Discharging time*	*Storage temp*	
Solar Cooker Thermal Energy Storage System Using Acetamide.	Acetanilide	Experimental investigation.	Efficiency declines with increased radiation, as evidenced by the negative regression index.	-	-	79°C	(Rajendra Shivaji Kachare, 2018)

Once the PCM has been selected based on the temperature range of the application, the following aspects are crucial to take into account (Pereira da Cunha & Eames, 2016):

- ❖ The geometry of the PCM container and
- ❖ The thermal and geometric properties of the container necessary for a specific amount of PCM

Most latent heat storage containers can be divided into two groups which are encapsulated and compact.

2.11. Encapsulation of Phase Change Materials Concept

Encapsulation is the process of putting a suitable coating or shell material on the cover of the PCM. Since an encapsulation can increase heat transfer surfaces, reduce significant thermal resistances associated with heat conduction in PCMs for tank storage systems, and significantly speed up heat transfer times for PCMs. This is especially crucial for a storage medium with relatively low thermal conductivity. Additionally, some PCMs have unique issues such as segregation and undercooling during thermal cycling. Encapsulation can thus lessen these issues. Using heat transfer fluid (HTF), encapsulation may additionally protect the PCM from contaminants and possible corrosion. Despite all of its benefits, encapsulation should also permit the PCM's volume to fluctuate during melting-solidification cycling. In particular, for large-scale solar power generation, the use of encapsulated phase change materials to store solar energy at a high temperature (over 300^{o}C) is expected to be an innovative thermal storage method (Zhao et al., 2013). Based on the size, encapsulated PCM can be classified as follows (Kant et al., 2017; Khordehgah, 2020).

1) Macro (1 mm to >1cm),
2) Micro ($1\mu m$–1mm) and
3) Nano (<$1\mu m$) encapsulated PCM.

Table 2-7: Types of encapsulation techniques

Encapsulation technique	**Advantage**	**Disadvantage**

Macro-encapsulation	• Environmental compatibility of enriched materials. • PCM handling is simple • A lower-cost production method. • The mechanical strength of PCM increased due to the shell's usage.	• Low heat transfer thermal conductivity • The huge capsule size causes a temperature difference at the PCM core and border.
Micro-encapsulation	• Maintains appropriate volume control throughout the phase change. Enhanced chemical strength. • Significant improvement in thermal reliability. Act as barrier and prevent leakage of PCM	• It may depend on the material's strength. • Direct-to-super cooling properties. • Expensive method of encapsulation.
Nano-encapsulation	• Exterior coating for targeted drug delivery.	• Higher production costs.

There are several studies concerning the encapsulation of PCM within metal capsules:

Zheng et al.(2013) have researched using cylindrical steel capsules filled with sodium nitrate and a eutectic of sodium chloride and magnesium chloride for high-temperature thermal energy storage.

The maximum rate of heat transfer was reportedly achieved by spherical shapes. It reduced for other geometries in the following order: cylinder, plate, and tube (Dzhonova-atan et al., 2016)

also Zhang et al. (2014) have encapsulated NaNO3/KNO3-PCM using a multi-tubular exchanger packed with PCM inside of stainless steel (AISI 321) cylinders.

Commercially available options for the low- and medium-temperature market currently exist. Examples include polymer-made flat plates and cylinders from PCM products or sphere-shaped nodules from Cristopia (Höhlein et al., 2018) but they are not available in Ethiopia. Therefore, in this research work manufacturing the selected and simulated type of PCM arrangement is recommended. Literature related to a different type of PCM arrangement is reviewed in Table 2-8 as follows.

Table 2-8: Literatures related to effect of PCM arrangement on the heat transfer rate

Title	PCM used	Method	Type of arrangement	Key finding				Schematic Diagram	Reference
				Qualitative	Quantitative				
					Charging time	*Discharging time*	*Storage temp*		
Numerical investigation of PCM-based thermal energy storage system.	Sodium nitrate	Numerical investigation	Spherical capsules	When the capsule size is reduced or the HTR flow rate is increased, the heat transfer rate rises and subsequently the charging/discharging time reduces.	20mm radii capsule size, 2 hours, 529.95 K accomplished	20mm radii capsule size: 2.22 hours	Between 578.95 to 579.95 K	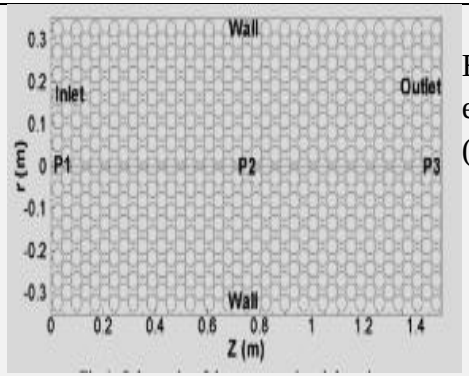	Bellan et al. (2015)
Effects of PCM arrangement and natural convection on charging and discharging performance of shell-and-tube LHS unit.	LiF/CaF_2	Numerical analysis	Shell-and-tube	With PCM placed in tube side, PCM melting time is decreased by 25.4% and latent heat storage rate is increased by 36.6%.	–	–	48^{o}C	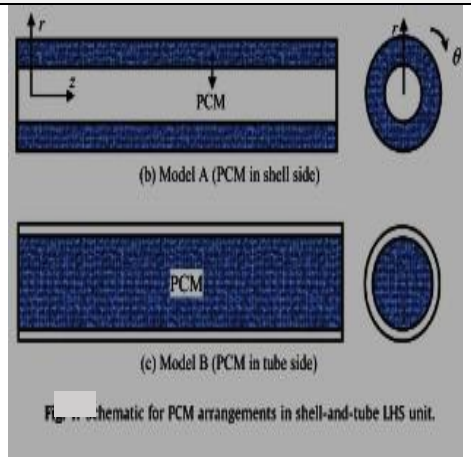	Tao et al. (2017)

Title	PCM used	Method	Type of arrangement	Key finding				Schematic Diagram	Reference
				Qualitative	Quantitative				
					charging time	*discharging time*	*Storage temp*		
Performance comparison of latent heat storage systems comprising plate fins with different shell and tube configurations.	NaNO3	Numerical investigation	Comprising plate fins with different shell and tube configuration.	In comparison to counter-flow shell and tube arrangements, the vertical arrangement of plate fins has a higher heat transfer rate.	_	_	306.8 °C	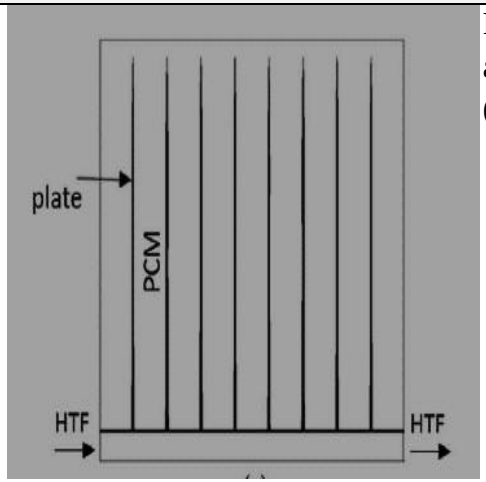	Riahi et al. (2018)
Heat transfer analysis of encapsulated phase change material for thermal energy storage.	NaNO3	Numerical investigation	Cylindrical shaped capsule	The diameters of the capsules and the types of heat transfer fluid have an impact on the heat transfer process inside the capsule.	99 min after the melting has started.	5 h	308 °C	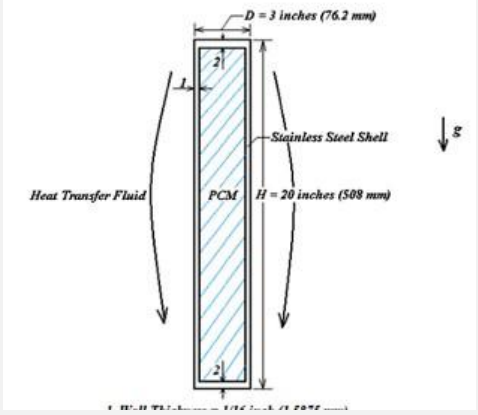	Zhao et al. (2013)

Title	PCM used	Method	Type of arrangement	Key finding				Schematic Diagram	Reference
				Qualitative	Quantitative				
					charging time	*discharging time*	*Storage temp*		
Numerical and Experimental study on the performance of a new two-layered high-temperature packed-bed thermal energy storage system with changed-diameter macro-encapsulation capsule.	Molten salt	Numerical and experimental	Packed bed with spherical capsules	The maximum TES charging rate of the older system can be increased by 12.4%, and the TES rate density of the two-layered PBTES can be improved by 13%.	Diameter 40mm takes 93.2 minutes to charge, while 15mm takes 42.6 minutes.	-	350 - 450 °C	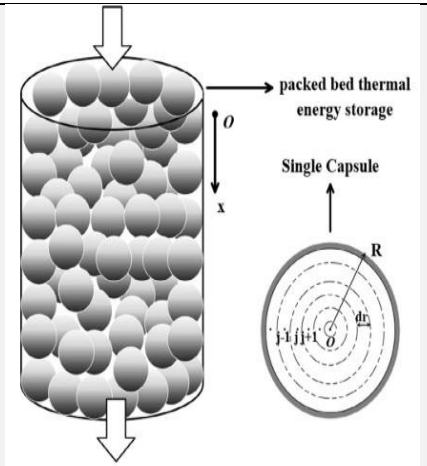	Liet al. (2018)
Numerical investigation of packed bed storage unit filled with PCM encapsulated spherical containers – A comparison between various mathematical models.	Paraffin	Numerical and experimental	Packed bed with spherical capsules	The internal conductive resistance of the PCM under consideration is more compatible with the outcomes of the experiment.	–	200 minutes of airflow at 0.5 kg/s and 550 minutes at 0.015 kg/s	55.5-66.5 ^{o}C	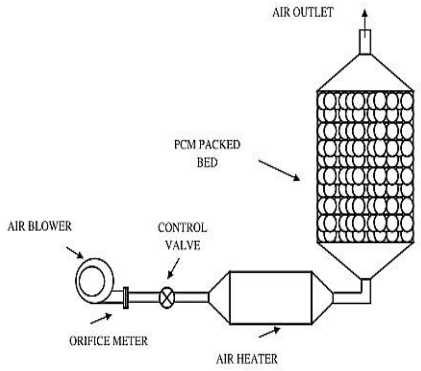	Karthikeyan & Velraj, (2012)

Title	PCM used	Method	Type of arrangement	Key finding			Schematic Diagram	Reference
				Qualitative	Quantitative			
					Discharging time	*Storage temp*		
Dynamic discharging characteristics simulation on solar heat storage system with spherical capsules using paraffin as heat storage material.	Paraffin	Numerical investigation	spherical capsules	Less time is required for complete solidification, which results in a faster rate of heat release, the higher the HTF flow rate.	The rate of heat release is 14 Kw for the first 40 minutes, then drops to 0 Kw for the next 240–300 minutes.	70^{o}C	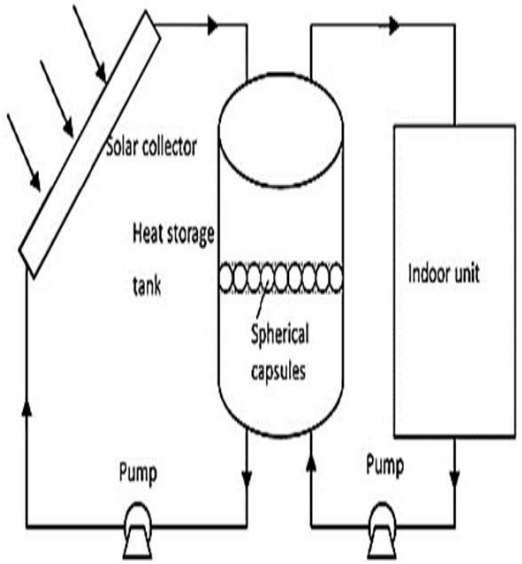	Wu et al., (2011)

2.12. Heat Transfer Fluids

Energy is transferred from the source to the end-user devices via heat transfer fluids, which can be air, water, or heat transfer oil.

2.12.1. Heat-Transfer Oils

When utilized in a closed system application, heat transfer oil is a non-corrosive heat transfer fluid that is engineered to deliver quick and effective heat transmission. For high-temperature home applications, thermal oils have the benefit of serving as both a heat transfer and a heat storage medium. These applications include producing steam and preparing meals (Mawire et al., 2014). Chemical, oil and gas, industrial, food processing, and other industries use thermal oils extensively as heat transfer fluids. The following advantages are also provided by heat transfer oil (Bade & Bandyopadhyay, 2015):

- High thermal efficiency for quick and efficient heat transmission.
- Low vapor pressure at high temperatures and a high boiling point to prevent pressure buildup.
- Not polluting during degradation and not corrosive to system components.
- Excellent compatibility with all common seal types, building materials, and coatings in heat transfer systems.
- Proven smooth operation; Virtually odorless; basically non-toxic; long service life.

2.13. Photovoltaic Conversion

Photovoltaic (PV) systems are solar electric systems that utilize the electric energy produced by the photovoltaic converter, which can range in size from a single photovoltaic cell to a massive photovoltaic array (Khamisani, n.d.).

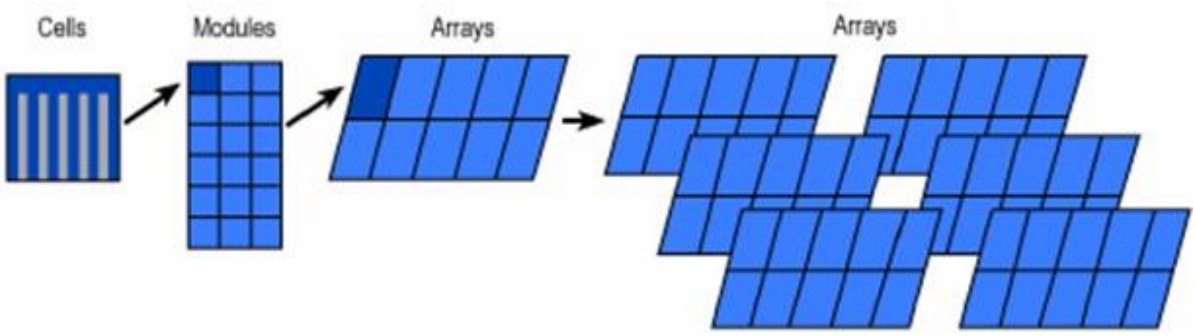

A PV system is designed in three basic steps, on average.

i. Estimating the load and the load profile
ii. Analyzing the amount of solar radiation that is available; and
iii. Designing the PV system, including the size of the PV panels, the choice of other parts, and the electrical system diagram.

2.13.1. Types of PV

The different types of PV are discussed (Bhatia, n.d.Jardas, 2012).

a. Monocrystalline PV

A single, highly pure crystal ingot with a typical size of 12.5 to 15 cm yields a monocrystalline cell. The most electrically efficient cells are those that need less surface area to produce a similar amount of power than other cell kinds. Their disadvantages include increased prices, the need for ventilation to enhance performance, and a recognizable geometric pattern. The efficiencies of commercial modules range from 14 to 19%.

b. Polycrystalline PV

By casting an ingot with a cuboid shape, polycrystalline silicon cells are created. Despite being less effective than monocrystalline, these are more affordable per square inch. In terms of cost (because to the reduction of losses) and efficiency (due to the grain boundaries), polycrystalline silicon differs from monocrystalline. Despite the little variation, larger cells (21 × 21 cm) are required to achieve the same levels of efficiency. Commercial modules typically have efficiencies of 12–15%.

c. Thin-Film PV

A thin semiconductor layer of PV material is printed or coated onto a substrate made of glass, metal, or plastic foil to create thin film photovoltaics. Thin film PV technology is more practical for use in a home solar system because the production process is quicker and less expensive and the payback period is shorter. Due to their non-single crystal structure, thin film PV cells have poor cell conversion efficiency, necessitating bigger cell sizes. These cells are less efficient than crystalline silicon ones with just a 6–7% efficiency rate, but in current times, a bigger surface area is needed for output.

2.14. Modes of Heat Transfer

A temperature differential causes the transfer of energy as heat to take place at the molecular level. Convection through fluids, radiation through empty space, and conduction through solids and fluids are all ways that heat can be conveyed. Heat transfer takes place when an object is at a different temperature. When two bodies have a temperature difference, heat is always exchanged between them. The three fundamental types of heat transfer processes are as follows (Energy, 1992):

2.14.1. Conduction Heat Transfer Mechanism

Conduction involves the transfer of heat by the interaction between nearby material molecules. The driving "force" in heat transfer by conduction is temperature difference and the resistance to heat transfer. The kind and dimensions of the heat transfer medium determine the resistance to heat transfer (Ferrell & Stahel, 1966, Vollmer & Möllmann, 2010).

Fourier's law of conduction is the most typical method of correlation in conduction heat transfer. The law is most frequently employed in its rectangular or cylindrical equation form, both of which are shown below (Energy, 1992).

Rectangular

$$\dot{Q} = -\mathrm{KA}\frac{\Delta \mathrm{T}}{\Delta x} \qquad 2.7$$

Cylinderical $$\dot{Q} = -\mathrm{KA}\frac{\Delta \mathrm{T}}{\Delta \mathrm{r}}$$ 2.8

If the temperature gradient term is expressed as a differential, the following can be written in a more general form:

$$\dot{Q} = -\mathrm{KA}\frac{\delta T}{\delta x}$$ 2.9

Where:

$\dot{Q}$= rate of heat transfer (W)

A = cross-sectional area of heat transfer (m^2)

Δx = thickness (m)

Δr = thickness of cylindrical wall (m)

ΔT = temperature difference (°C)

K = thermal conductivity (W/m -°C)

2.14.2. Convection Heat Transfer Mechanism

By moving and mixing "macroscopic" sections of a fluid (i.e., a fluid flowing across a solid boundary), convection involves the transmission of heat. If the motion and mixing are brought on by density changes brought on by fluid temperature differences, the phrase "natural convection" is employed. If this motion and mixing are brought about by an external force, such as a pump, the phrase "forced convection" is used (Energy, 1992,Vollmer & Möllmann, 2010).

Heat is transferred by convection between a surface at one temperature and a fluid at another. As a result, a constant proportionality known as the "convection heat transfer coefficient" (abbreviated h) is defined. Therefore, the convection heat transfer rate is given by:

$$\dot{Q} = hA\Delta \mathrm{T}$$ 2.10

Where:

$\dot{Q}$ = rate of heat transfer (W)

h = convective heat transfer coefficient (W/m2^{o}C)

A = surface area for heat transfer (m^2)

ΔT = temperature difference (°C)

2.14.3. Radiation Heat Transfer Mechanism

When thermal energy is transformed by the movement of electron and proton charges within a material, radiation is the transfer of energy through the emission or absorption of electromagnetic waves (Harding, 2012)**.** The Stefan-Boltzmann law states that the rate at which energy is emitted from ideal radiators is proportional to the fourth power of the absolute temperature. Additionally, the relationship between the net rate of energy exchange between ideal radiators A and B is (Kaviany, 1991);

$$\dot{Q} = \sigma A(T_A^{\,4} - T_B^{\,4}) \qquad 2.11$$

Where:

σ – Stefan-Boltzmann constant=5.67*10^{-12}w/cm^2.k^4

T_A -Temperature of body A (^{o}C)

T_B - Temperature of body B (^{o}C)

A non-black surface's net radiation to its surroundings is calculated as follows:

$$\dot{Q} = \varepsilon\sigma A(T_s^{\,4} - T_\infty^{\,4}) \qquad 2.12$$

Where: Ts – Body surface temperature (^{o}C)

T_∞- Surrounding temperature (^{o}C)

ε – Emissivity of the surface and has a value between 0 and 1, with a perfect emitter having a value of 1 and a perfect reflector having a value of 0.

2.15. Thermal Insulation System

A material or mixture of materials that, when applied, slows the transfer of heat and can be customized for any size, shape, or surface is referred to as thermal insulation. Insulation is the result of the process of thermally isolating the system using insulating materials to significantly

lower the rate of heat transfer between the system and the surrounding body or environment. In general, the proper material choice, thickness, and placement of the thermal insulation enable optimal interior thermal comfort conditions and sufficient energy savings (Deshmukh et al., 2017,AAAMSA, 2001).

2.15.1. Types of Insulation Materials

There are three types of insulation materials in general (Deshmukh et al., 2017;Ying-Zhang et al., 2013):

a. Fibrous Insulation

It is made up of fibers with a small diameter that precisely split the air volume. The fibers may be linked together or not, and they may be parallel or perpendicular to the surface being insulated. Fibers made of alumina-silica, rock wool, slag wool, and silica are also used. Glass fiber and mineral wool are the insulations of this sort that are most frequently utilized. The limited structural integrity of items made of glass fiber and mineral wool is often provided by organic binders that join the fibers together (Ying-Zhang et al., 2013).

b. Cellular Insulation

Small individual cells are separated from one another to provide cellular insulation. Glass or foamed plastics like polyisocyanurate, elastomeric, and polystyrene (closed cell) can be used as the cellular material (Ying-Zhang et al., 2013).

c. Granular Insulation

Insulation is made of granules that may include hollow areas or cavities in them. Since gas can move between the various compartments, it is not regarded as a real cellular material. This kind can be made as a loose or pourable substance, or it can be coupled with fibers and a binder, or it can go through a chemical reaction to create hard insulation (Ying-Zhang et al., 2013).

2.16. Ash Insulation

Ash is a byproduct of burning firewood, particularly while preparing food; Ash from burning wood can used for insulation systems in particular since it has low thermal conductivity (Melkamu, 2013).

2.17. Conclusion from the Literature Review

From the literature review, there is no doubt that the cooking industry benefits greatly from solar energy. Food preparation with a solar cooker has been successfully performed by utilizing solar energy. The literature review revealed that several researchers employed a variety of methods to capture solar energy, with parabolic, concentrating, and flat plate collectors being the most common. Additionally, the advancement of utilizing thermal energy storage systems for cooking applications has been seen, but it still needs refinement. Eutectic mixtures look more promising from 100-250^{o}C according to the abovementioned studies, and in this project work the temperature needed interval is between 180 and 220^{o}C and the eutectic mixture latent heat storage material should be chosen. Additionally, 60% NaNO3 and 40% KNO3 by mass were found to have extremely encouraging thermal properties for potential usage in household cooking.

It is clear from the studies analyzed that the latent heat storage material's geometry and arrangement, as well as the temperature of the heat transfer fluid, have a significant impact on the rate of heat transfer and the time of charging and discharging.

Additionally, a survey of the literature indicates that much effort has been put into developing solar injera baking with storage using concentrating solar power technology .This work studied that the charging-discharging characteristics of a PCM and thermal oil storage using electrical energy produced by a photovoltaic system for Injera baking applications.

CHAPTER 3: MATERIALS AND METHODS

3.1. Methods

The methodology followed in order to attain the objectives of the research is shown in Figure 3-1, to this end, literature reviews of journals and books that are related to this research work were conducted.

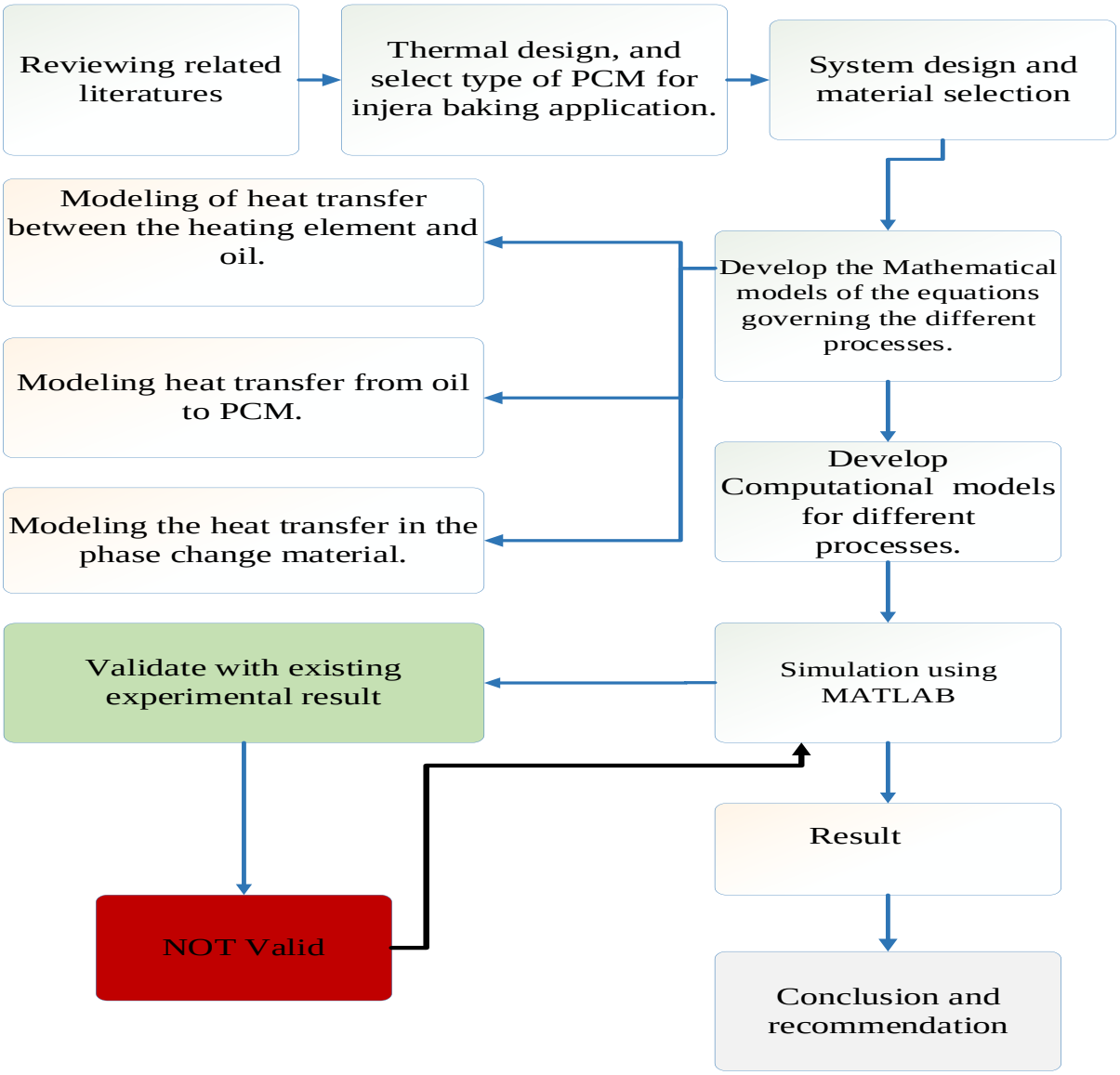

Figure 3-1: Methodology flow chart

3.2. Solar-powered Injera Baking System with Thermal Storage

3.2.1. Description of the System

Figure 3.2 shows the conceptual diagram of the suggested solar-powered injera baking system with thermal energy storage. The system consists of PV, inverter, electrical heating elements, PCM, thermal oil, heat storage tank, injera baking pan/Mitad and a portable stand.

The PV is used to collect solar energy and change it to electrical energy which is then supplied to the thermal energy storage which contains PCM which is capsuled in a cylindrical tube and thermal oil. An electric heating element is inserted at the bottom of the storage tank to increase the convective force inside the storage which produces an increase in the temperature of the fluid and PCM. Thus, the oil–PCM TES system is charged from the PV and the reverse discharging cycle is then the oil in the storage tank to the baking pan.

The heat transfer fluid in the system is the non-circulated fluid which is working as both to store sensible energy and transfer heat to the PCM inside the storage furthermore to the baking pan consists of a ceramic pan with an aluminum cover, during discharging.

During the charging process, the electric heating element inserted into the thermal storage transfer its heat energy to the oil then the oil gets heat and simultaneously transfers heat to the PCM. During the discharging process, initially, the baking pan is sealed with the storage and reaches its desired temperature for baking during charging therefore, there is no need for heating time for baking, during start baking the hot oil from the top of the storage tank starts to transfer heat to the pan since it is in contact with the baking pan underneath in which it transfers energy through natural convection at the same time the PCM is discharging its heat to the oil again through natural convection heat transfer processes. The heat extracted from the storage is until the temperature of the baking Mitad/pan is desired to bake Injera. The thermal design and sizing of the solar baking device are based on the Injera baking energy requirement.

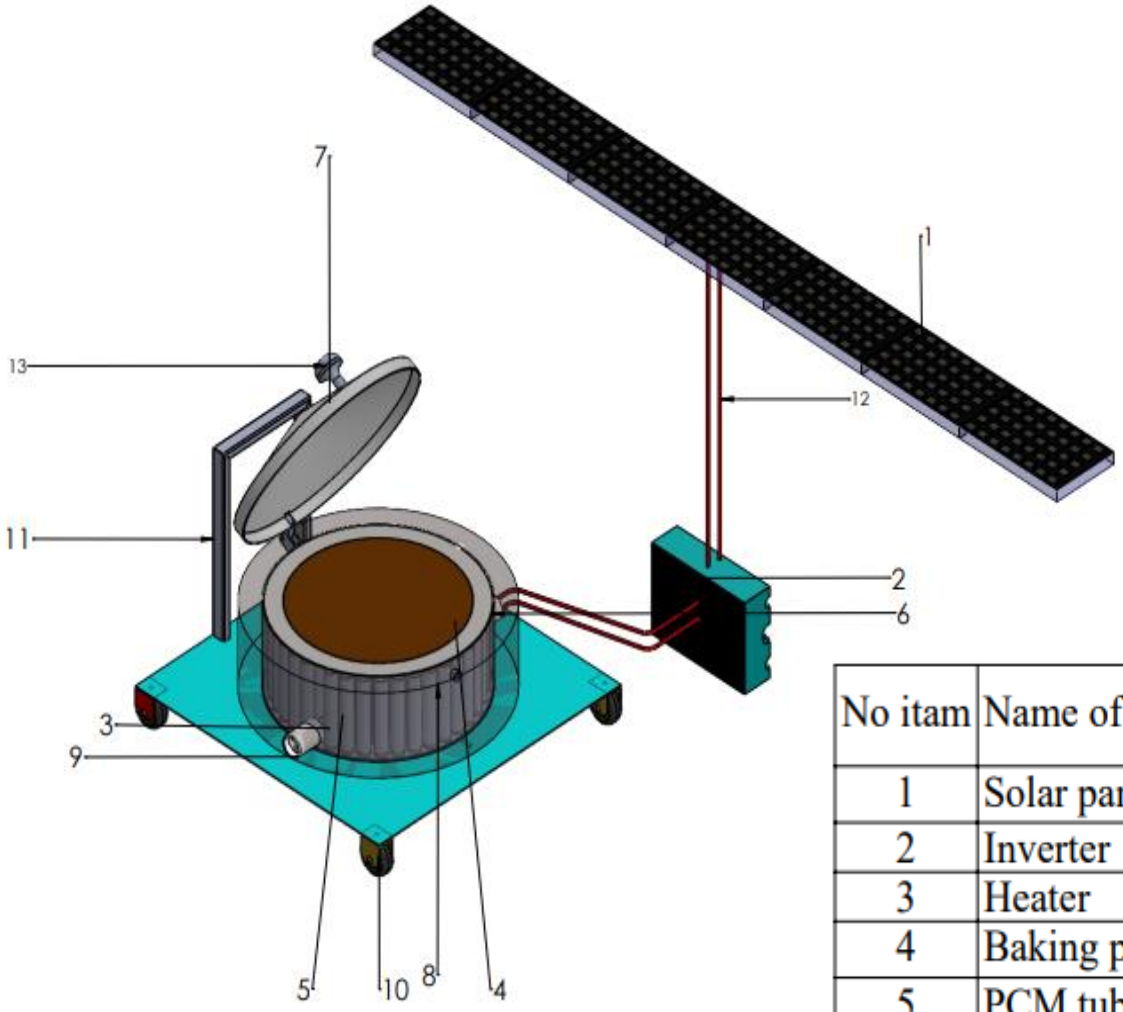

No itam	Name of part	QTY.
1	Solar panel	1
2	Inverter	1
3	Heater	2
4	Baking pan	1
5	PCM tube	115
6	Tanker	1
7	pan cover	1
8	Insulation	1
9	Heater socket	2
10	Tyer	4
11	Handel	1
12	Wire	2
13	pan cover handel	1

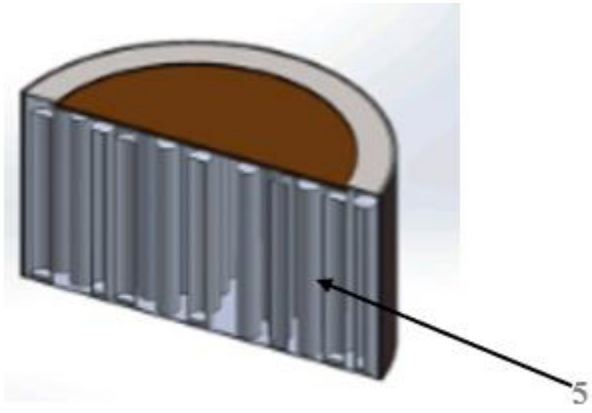

Figure 3-2: Overall system layout with section view

3.2.2. Heat Demand of Injera Baking

It is assumed that the energy used to cook injera is the energy needed to bring the batter from ambient temperature to that of the boiling point of water, that is referred to as sensible heat, in addition, the heat required to cause the water to evaporate, which is known as latent heat. In order to bake injera, a significant amount of energy must be expended, including, to bring the batter at a specific temperature and remove the water which will be wasted when baking. Both thermo-physical characteristics of Injera and the baking pan are mentioned in table 3-1 and taken into consideration in the present investigation based on the experimental and numerical inquiry conducted before on both baking pan and Injera (Tsige, 2015, Bonsa, 2020, Jones et al., 2017, Kahsay, et al., 2014, Adem & Ambie, 2017).

Table 3-1: Thermo-physical properties of Injera and baking pan

Properties	Value
Mass percentage of teff in the dough	27.4%
Mass of batter	0.4315 kg.
Mass of Injera	0.3455 kg.
The dough's water mass fraction (moisture content)	72.6%
The ceramic pan's density	2400 kg/m3
Ceramic pan's diameter	0.58 m
The ceramic pan's thickness	0.008 m
Thermal conductivity of the ceramic pan	0.8 W/m. K
Specific heat of the ceramic pan	960 kg. K

3.2.3. Baking Energy

The difference between the original weight of the batter and the finished baked injera can be used to calculate the quantity of evaporated water (Hassen et al.2011). Based on the following assumptions, the amount of thermal energy used to bake injera is determined (Getenet, 2011).

- Every single Injera loses the same amount of moisture and has the same average mass.

- In order to determine the amount of energy needed, injera batter has the same heat capacity as water.
- The weight of moisture lost during baking is equivalent to the weight difference between the baked Injera and the original batter.
- Baking begins at a temperature of 23 °C. and
- Water evaporates at a temperature of 92°C at Addis Ababa (Adem et al., 2019), which have been considered for calculating baking energy.

This baking energy [kJ] can be calculated mathematically Eq 3.1 (M. H. Hailu et al., 2017, Adem et al., 2019) :

$$Q_{baking} = m_{ba} * C_p * (T_b - T_{ba}) + (m_{ba} - m_{injera})\, h_{fg} \qquad 3.1$$

$$= 319.02 \text{ kJ}$$

Where: m_{ba} -mass of the batter

T_b -Boiling temperature of water

T_{ba}- Ambient temperature

Cp- Heat capacity of water (4.187kJ/kg. K)

m_{injera}- Mass of Injera

h_{fg}-Latent heat of vaporization of water (2260kJ/kg)

Table 3-2: Useful baking energy for different numbers of Injera

Number of injera	The total useful energy (KJ)
40	12760.87
60	**19141.3**
80	25521.73

100	31902.16
120	38282.6
150	47853.24

It is estimated that it takes 2 to 3 minutes to prepare one injera, with 3 minutes being the average. One Injera's power or heat transfer rate can be computed as follows:

$$P_{baking} = \frac{Q_{baking}}{\Delta t} \quad 3.2$$

From equation 3.2 the net power required for baking one Injera is 1.772KW**.**

During injera baking there are losses in the storage tank, in electric heater and during the baking process, on the baking pan, on the pan cover, so considering the losses and assuming a safety factor of 1.6 (Bonsa, 2020,Tsegay & Ababa, 2011) the overall energy demand needed to bake Injera for a term can be calculated as follows:

Table 3-3: Total baking energy for different numbers of Injera

Number of injera	The total useful energy (KJ)	The total energy demand (KJ)
40	12760.87	20417.28
60	**19141.3**	**30626.07**
80	25521.73	40834.765
100	31902.16	51043.456
120	38282.6	61252.15
150	47853.24	76565.184

From this, we can find the power needed to bake one Injera as:

$$P_{baking} = \frac{E_{utilized}}{t} \quad 3.3$$

$$= 2.84\text{kw}$$

Where: $E_{utilized}$ = is the total energy needed for baking

3.3. Selection for Phase Change Material

Due to the fact that PCM stores 5–14 times more heat per unit volume than sensible heat storage materials like water, masonry, or rock. A relatively constant temperature is also maintained via PCM's heat absorption and release (Foong et al., 2011).

Table 3-4: The properties of phase change materials used in the TES of solar cookers

Material	Class	Tm [^0C]	$\Delta Hfus$ [J/g]	CP [$J/g.K$]	ρ [$kg/m3$]	k [W/mK]
Magnesium nitrate hex hydrate	Inorganic	89.0	134	0.55	1643	0.55
Stearic acid	Organic	55.1	160	2.83	965	0.18
Commercial grade acetamide	Organic	82	263	1.94	1159	0.43
Commercial grade erythritol	Organic	118	339	1.38	1480	0.73
Commercial grade acetanilide	Organic	119	222	2.00	1210	0.14
Nitrate salts (KNO3 – NaNO3)	Inorganic	220	146	4.10	2200	0.8
PCM – A164	Organic	164	290	2.42	1500	-

From the above table depending on several factors described in the previous chapter, the most popular thermal energy storage for solar cooking applications at the moment and the PCM that is most appropriate for this application *(Nkhonjera et al.,* 2017*; Lentswe et al., 2021),* is a mixture of 60% of NaNO3 (sodium nitrate) and 40% of KNO3 (potassium nitrate). Regarding melting points, solar salt (a nitrate salt mixture of 40% KNO3 and 60% NaNO3) is around 220°C, which has been found compatible with the temperature required on the surface of an injera baking pan (Hassen et al., 2011).

Sodium nitrate (NaNO3) and potassium nitrate (KNO3) are inorganic PCMs and have a melting point of 310ºC and 330ºC respectively (Pincemin et al., 2008; Zhong et al., 2012). Solar thermal power plants have successfully utilized molten salt, or so-called solar salt, as a means of transporting and storing thermal energy (Peng et al., 2010). Additionally, since the melting

temperature is in an acceptable range, the NaNO3-KNO3 binary mixture can be used to store latent heat for cooking purposes (Tesfay et al., 2014; Foong et al., 2011). The heat capacity and thermophysical data of these solar salts are listed in Table 3-5.

Table 3-5: Thermo-physical property of the NaNO3 - KNO3 eutectic salt (60: 40 mol %)

Parameter	**Values**
Thermal conductivity	0.8 W/m k
Density $>220^0$c	1700 Kg/m3
Density $<220^0$c	1800Kg/m3
Enthalpy of fusion	108.67KJ/Kg
Phase transition Enthalpy	31.91KJ/Kg

3.3.1. Quantifying the Amount of PCM

PCM has a heat of fusion of 108.67 KJ/Kg and a melting point of 220°C. The overall energy needed for baking injera is used to calculate the amount of PCM. For the needed amount of energy, the demanded mass of PCM can be calculated as follow. The thermal capacity of the system using a PCM medium or the heat stored in a PCM is given as follows (Kumar & Shukla, 2015; Sharma et al., 2009):

$$Q = \int_{Ti}^{Tm} mCpdT \; + ma_m \Delta H_m + \int_{Tm}^{Tf} mCpdT \qquad 3.4$$

$$Q \; = \; m\,[Cps\;(Tm - Ti) \; + \; a_m \Delta Hm \; + \; Cpl\;(Tf \; - Tm) \qquad 3.5$$

The PCM's specific heat capacity had been modified to (Foong et al., 2011):

$$Cp = \frac{KJ}{Kg} \quad \begin{cases} 0.75\{if\ T < 110℃ \\ 4.2\ \{if\ 110 \leq T \leq 120℃ \\ 1.4\{if\ 120℃ \leq T \leq 210℃ \\ 12\{if\ 210℃ \leq T \leq 220℃ \\ 1.6\{T > 220℃ \end{cases} \qquad 3.6$$

Therefore, the total energy from the PCM is calculated as follows:

$$Q = \int_{Ti}^{Ts} mCpsdT + m * am\,\Delta Hm + \int_{Ts}^{Tm} mCpldT + \int_{Tm}^{Tl} mCpldT + \int_{Tl}^{Tf} mCpldT \quad 3.7$$

$$Q=\int_{23}^{109} mCpsdT+m*1*\Delta H_m+\int_{110}^{120} mCpldT+\int_{121}^{209} mCpldT+\int_{210}^{220} mCpldT \quad 3.8$$

$Q = m_{pcm}\,[458.37KJ/kg]$,

Where Q=30.626MJ, which is the energy required for the system. By rearranging the above equation, we can get the mass of the PCM as:

$$m\_pcm = 66.815Kg$$

But the HTF used is thermal oil and has capacity to store sensible energy. Therefore, from the total energy required by the system thermal oil is expected to store some amount of energy, assume about one-fourth of the total energy is stored by thermal oil which is about 7.656MJ. The mass of the PCM required becomes:

$$m_{pcm}=50.1Kg$$

Where:

Q = the quantity of heat stored (J)

m_{pcm} = mass of PCM (Kg)

C_{ps} = specific heats in the solid phases (KJ/Kg.^{0}C)

C_{pl} = specific heats in liquid phases (KJ/Kg.^{0}C)

h = enthalpy of phase fusion (KJ/Kg)

Tm = melting temperature, (°C)

Ts = temperature of the solid (°C)

Tl = temperature of the liquid (°C)

Tin = initial temperature (°C)

a_m = melted fraction

Table 3-6: Baking energy and amount of PCM needed for different numbers of Injera

Number of injera	The total useful energy (KJ)	The total energy demand (KJ)	Amount of PCM (kg)
40	12760.86	20417.38	44.54
60	**19141.3**	**30626.07**	**66.815**
80	25521.73	40834.765	89.1
100	31902.16	51043.456	111.36
120	38282.6	61252.15	133.63
150	47853.24	76565.184	167.04

3.3.2. Estimation of Volume of Storage Medium (PCM)

Volume of PCM can be determined as:

$$V_{pcm} = \frac{\boldsymbol{m_{pcm}}}{\rho_{pcm}} \qquad 3.9$$

Where: ρ_{pcm} =1700 Kg/m^3

V_{pcm}=0.03$m3$ $= 30\ liter.$

3.3.3. Encapsulation of Phase Change Material

The PCM was zinc, and numerical simulations were used to examine the stresses in spherical and cylindrical capsules. The materials for the sphere and the cylinder were assumed to be nickel and stainless steel (316L), respectively. It has been determined that the cylinder is the most practical geometry for encapsulation (Blaney et al., 2013).

The cylindrical tube in which the PCM is enclosed ensures the best possible heat transfer between the PCM and the heat transfer medium. As a result, aluminum will serve as the material of encapsulation for a phase change substance composed of a sodium and potassium salt mixture inside the storage tank. Salt will be stored there while it is being charged and discharged. Additionally, the volume is extended during charging (PCM melting) and a 10% clearance volume was required (Asfafaw Haileselassie Tesfay, Kahsay, et al., 2014) since the

system is closed and it's better to consider 20% clearance volume during melting the total volume of PCM is calculated as follow.

$$V_{total} = V_{PCM} * 0.2 + V_{PCM} \quad (3.10)$$

$$V_{PCM-total} = 36 \text{ liter}$$

3.3.4. Volume sizing for thermal storage system

The thermal storage tank is sized by taking into account the energy given by heat-transferring fluid and the necessary storage capacity for the specified operational application. A cylindrical tube made of 6061 aluminum is filled with PCM. The capsule has an overall length of 250 mm, an outer diameter of 43 mm, and a wall thickness of 1.5 mm. Aluminum is selected because it exhibits good accessibility and applicability of the sealing idea (Höhlein et al., 2018). The size of the PCM storage can be calculated as follow.

Number of cylindrical tubes,

$$V_{pcm,total} = 0.036m^3$$

$$V_{pcm} = n * V_{tube} \quad (3.11)$$

V_{tube} for the selected data:

$$V_{tube} = \frac{\pi Di^2}{4} * L \quad (3.12)$$

Where $L = 0.25m$

$V_{tube} = 0.00031416$ m3

Number of tubes (n);

$$n = \frac{0.036m^3}{0.00031416\ m^3}$$

$n = 115$

The total volume of PCM in the tank is calculated as follows:

$$V_{tube,out} = \frac{\pi Do^2}{4} * L \quad (3.13)$$

$V_{tube,out} = 0.00036305\ \text{m}^3$

$$V_{PCM,total} = n * V_{tube,out} \quad (3.14)$$

Considering the safety factor 1.2;

$$V_{PCM,total} = 0.05m^3$$

Where;

m_{pcm} = mass of PCM (Kg)

$V_{pcm,total}$ = volume of PCM (m^3)

V_{pipe} = volume of cylindrical pipe or capsule (m^3)

ρ_{pcm} = density of PCM (Kg/m^3)

3.3.5. Energy stored in the thermal oil

As discussed above the energy stored in thermal oil is 7.665MJ and for transferring heat the temperature of fluid could greater than the PCM during charging of the system, assume the temperature reaches 250^{o}C.

The mass of the storage medium, the temperature change, and the specific heat of the thermia oil determine how much sensible heat is stored (Kumar & Shukla, 2015) :

$$Q_{oil} = m_{oil} C_{poil} (T_{oil} - T_{inff}) \quad (3.15)$$

$$7665\text{kJ} = m_{oil} * \frac{2.306\text{kJ}}{\text{kg}}.\text{k} * (227k)$$

$$m_{oil} = 15kg$$

The volume of the fluid is given as follows;

$V_{oil} = \frac{m_{oil}}{\rho_{oil}}$, Where: ρ_{oil} =787 Kg/m^3

Considering the safety factor 1.3 due to the losses;

V_{oil}=0.025$m3$ $= 25\ liter.$

Where: m_{oil} = mass oil (kg),

C_{poil} = the specific heat capacity of oil (2.306kJ/ kg. K)

T_{oil} = Average final temperature of oil (^{o}C)

T_{inff}= ambient temperature

V_{oil}=volume of oil (m^3)

ρ_{oil} =density of oil (Kg/m^3)

For a cylindrical storage tank, the inner diameter is considered as 0.62m of (to integrate with the baking pan), and the outer diameter of 0.64m with 0.26m of height.

$$V_{total,tank} = (\pi r^2 * h) \quad 3.16$$

$$V_{total,tank} = 0.08\text{m}^3$$

Where;

$V_{total,tank}$= volume of total storage tank (m^3)

Porosity (ε) and (1-ε) is the volume fraction of oil and PCM inside the storage tank and it can be calculated as follow (Tumilowicz et al., 2014):

$$\varepsilon = \frac{V_{oil}}{V_{total,tank}} \quad 3.17$$

$$\varepsilon = 0.32$$

3.4. Estimation of available solar radiation potential

Detailed data about solar radiation is the primary input in developing photovoltaic thermal systems, as an initial point in solar energy estimation for thermal system design.

3.4.1. Solar Radiation Data

The Ethiopian metrological agency collects solar data for Addis Ababa, Ethiopia, which is found at 9.033^{o} latitude and 38.747^{o} longitude. The monthly average global radiation data is

taken from the Ethiopian metrology agency (Biadgelegn, 2018) and utilized as a precondition to designing solar PV.

Table 3-7: Monthly average global radiation data for Addis Ababa from (2014-2016)

Monthly average Global radiation [W/m2]												
Month of the year												
Year	Jan	Feb	Mar	April	May	June	July	Aug	Sept	Oct	Nov	Dec.
2014	604	620	616	524	529	513	432	441	547	608	595	598
2015	613	631	628	597	556	524	465	470	611	615	632	638
2016	556	632	623	438	522	438	396	414	-	-	-	585
Aver.	591	627.7	622.3	519.7	535.7	491.7	**431**	441.7	579	611.5	613.5	607

3.5. Basic Sun- Earth Angles

Solar energy reaching the upper atmosphere is 1367 W/m2. However, atmosphere and the clouds absorb part of the sun's rays that hit the ground and reflect them back. The sun's rays when they hit the ground create certain angles.

The sun's angles govern where the sun will be at certain times and also serve to trace the sun's movement throughout the day. Throughout the same period, the solar angles changes depending on the location's latitude and longitude. Therefore, to ascertain sun's position, the solar angles must be understood. For this research work, for the design consideration, the month of lowest average monthly global radiation (July) is selected and can be made a calculation based on (Karafil et al., n.d.).

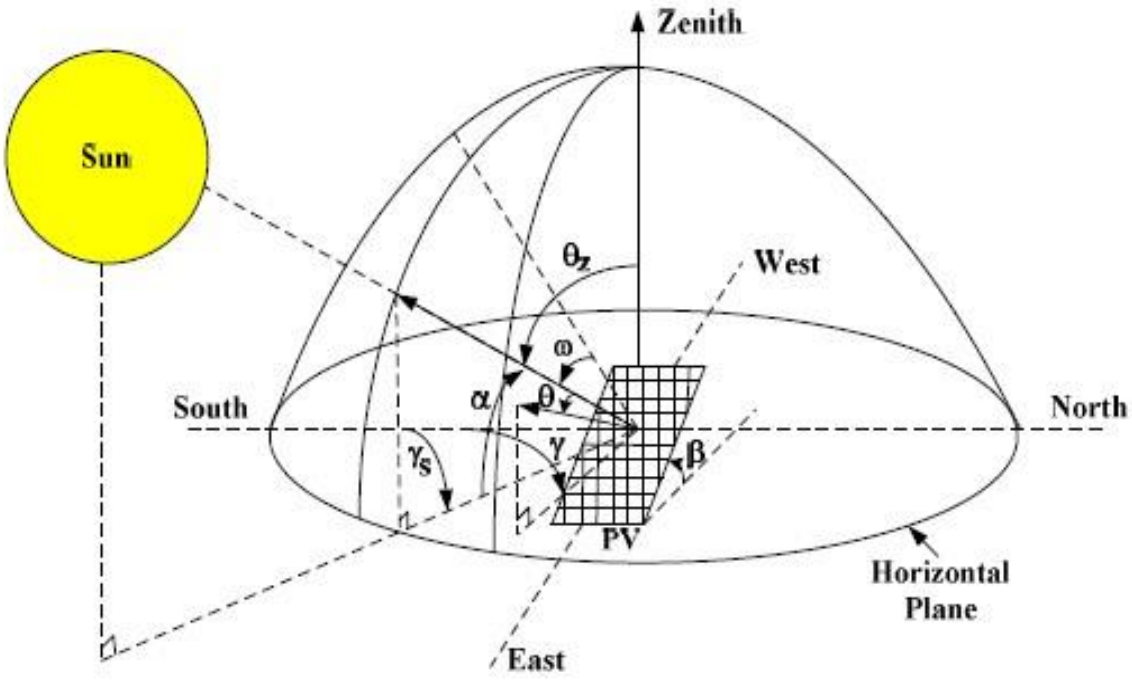

Figure 3-3: The basic solar angles

Data from site location (Addis Ababa):

- Latitude angle: the angle that the equator's center creates. he equator's north and south are positive and negative, respectively, with a range of $-90^{o} \leq Ø \leq 90^{o}$. $\emptyset = 9.033$
- The month under consideration for the design of PV system is JULY at which global radiation is minimum

3.5.1. Declination

The declination is the angular position of the sun with respect to the equatorial plane at solar noon. Cooper's equation provides its value in degrees:

$$\delta = 23.45 \sin\left(\frac{360}{365}(284 + n)\right) = 21.2\,^{\circ} \qquad 3.18$$

Where $n = 198$ (July 17th recommended average day)

3.5.2. Sunset hour angle

The solar hour angle that corresponds to sunset hour is provided by:

$$\omega_{ss} = \cos^{-1}(-\tan\emptyset \tan\delta) \quad 3.19$$

$$\omega_{ss} = 93.54°$$

3.5.3. Hour angle

The angle through which the earth would turn to put the point's meridian directly under the sun is known as the hour angle of a point on the surface of the earth. According to the following relationship between the hour angle and solar time in hours, one may determine the hour angle at 1: 30 PM for this instance.

$$\omega = (ST - 12) \times °15 \quad 3.20$$

$$\omega = 22.5\,°$$

3.5.4. Zenith angle

It is angle formed by the rays of the sun and a line perpendicular to a horizontal plane and obtained as follows:

$$\cos\theta_z = \cos\emptyset \cos\delta \cos\omega + \sin\delta \sin\emptyset \quad 3.21$$

$$\theta_z = 24.85°$$

3.5.5. Solar altitude angle

It is formed by the horizontal plane and the line to the sun, calculated as:

$$\alpha = 90 - \theta_z \quad 3.22$$

$$\alpha = 65.155°$$

3.5.6. Solar azimuth angle

It is formed between the sun's north or south location and the direct solar radiation and can be determined using the equation below.

$$\cos\gamma_s = [\sin(\alpha)\sin(\emptyset) - \sin(\delta)/\cos(\alpha)\cos(\emptyset)] \quad 3.23$$

γ_s=122°

3.5.7. Tilt angle

The tilt angle, which ranges from 0° to 180°, is the angle formed by the panels and the horizontal plane. The tilt angle of the surface will be fixed for each day when a plane is rotated about the horizontal east-west axis with a single daily adjustment, as determined by the following equation.

$$\beta = |\emptyset - \delta| \qquad 3.24$$

3.5.8. Incidence angle

It is the angle between the normal of the surface and the radiation falling on that surface directly which is calculated from the following equation.

$$\cos\theta_i = (\cos(\emptyset - \beta)\cos\delta\cos\omega + \sin\delta\,(\sin(\emptyset - \beta))) \qquad 3.25$$

$$\theta_i = 39\,°$$

3.6. Design and Sizing of Solar Photovoltaic Systems

For this system design monocrystalline cell comes from a single crystal ingot of high purity, is selected. Because they are the most electrically efficient, these cells can produce a comparable amount of power with less space than other cell types.

They are particularly well suited to atrium roofs, partial vision glass in facades, rooftop installations in homes, commercial sun shade, or rooftop retrofits where maximum electricity generation is needed but installation space is constrained. Commercial modules efficiency range is around 14-19%.

$$E_{utilized} = 30{,}626.07KJ/day\ ,$$

$$= \frac{30{,}626.07KJhr}{hr}/day$$

$$= 8.51KWhr\ /day$$

3.6.1. Estimating the PV system land requirements

Geographic Location: Addis Ababa, Ethiopia.

Average daily energy consumption: 30626.07KJ/day=8.51kWh/day.

Irradiation (peak-sun-hours) for Addis Ababa (from Global Solar Atlas): 4.607kWh/m^2 per day.

The size of the PV system for the peak load in Wp, can be defined as follow (Bhatia, n.d.; Khamisani, n.d.);

$$A_{pv} = \frac{E_L}{\mathrm{H} * \eta_{PV}} \quad (3.26)$$

$$A_{pv} = \frac{8.51\mathrm{kWh/day}}{4.607\mathrm{kWh}/m^2\ /\mathrm{day} * 0.7}$$

$$A_{pv} = 2.64m^2$$

By considering different losses due to shading, dust and dirt, reflection, irradiation, array mismatch, cables, inverter, and thermal losses on PV the overall efficiency of PV system was assumed 0.7 (Projects & Solar, 2021).

Where; A_{pv}=total area of photovoltaic requirement (m^2)

E_L=peak daily required electrical energy (Wh/day)

H =daily global irradiation (Wh/m^2 /d).

η_{PV}=overall photovoltaic efficiency

3.6.2. Sizing the PV Capacity

To meet the demand for electricity, the necessary photovoltaic modules' power P_{PV} (W) can be estimated as follows:

$$P_{PV} = A_{PV} * H_{sc} * \eta_{PV} \quad (3.27)$$

$$P_{PV} = 1848W$$

Where; H_{sc} =standard solar irradiation $1000 W/m^2$

The total amount of modules can be calculated using the readily accessible dimension of one PV panel after estimating total area of PV panel and the total energy requirement of the system (total load), i.e., the total connected useable load to the PV panel system. The number of modules can be determined as follows:

$$N_m = \frac{P_{PV}}{P_m} \qquad 3.28$$

$N\_m = 7$, by approximated to the next integer.

Where; P_m is the power of a single module which is 300W for the selected monocrystalline cell for the system design with specifications from Hi-Tech (Solar HI-Tech, 2015).

To get the right combination of voltage and current, panels must be linked in series and parallel as necessary.

The system's overall current need is determined as follows:

$$I_{DC} = \frac{P_{pv}}{V_{DC}} \qquad 3.29$$

$$I_{DC} = 56.81\ Amp$$

Where; P_{pv} =Peak power

V_{DC} = System Dc voltage

The number of parallel modules can be obtained from the total module current and the rated current of a single module.

$$N_p = \frac{I_{DC}}{I_r} \qquad 3.30$$

$$N_p = 6.1682 \cong 7$$

Where; I_r = rated current of one module.

The number of series modules is also obtained from the direct voltage of the system and the rated voltage of one module.

$$N_s = \frac{V_{DC}}{V_r} \qquad 3.31$$

$$N_s = 1$$

Where; V_r = rated voltage of one module.

Thus, the peak power P_{PV} (W) of the photovoltaic modules becomes:

$$P_{PV} = 2100W$$

But for the selected PV module, which is a commercial module with efficiencies of about 18%, and the selected date is at STC 1000w/m^2 and 25^{o}c, but for this design, the critical month considered is July and the maximum radiation is 431 W/m^2, which is very small to achieve the needed photovoltaic modules power P_{PV} (1848W), to fulfill the requirement for electric load. Therefore, to achieve the required power, the number of modules approximately is about **14** with a dimension of 1.64m*0.99m.

To determine the whole module's actual area, A_t at the exact peak power for the total modules P_t, using following equations:

$$A_t = N_m{}' * A_m \qquad 3.32$$

$$A_t = 22.7m^2$$

Where: $N_m{}'$ is the updated quantity of modules, rounded to the closest whole number (14).

Arrange the array consisting of 14 parallel modules and 1 series module.

3.6.3. Sizing of the Inverter

The conversion of solar PV DC electricity to AC at the needed voltage is made easier by solar PV inverters. The fundamental duties of an inverter in power conditioning (Energy Program 905 Plum Street SE, Bldg 3 Olympia, 2009) are:

- ✓ Changing the DC power from the PV modules or battery bank to AC power
- ✓ Making the AC power's frequency 60 cycles per second
- ✓ Reducing voltage variations

Sizing the inverter is depending upon the actual power needed by the system which is 2100 watts. The inverter should be able to handle about 2100-W at 220-Vac. Therefore, we can select a Latronics inverter, which is suitable for the system, LS- 2324, 2300-W, 24-Vdc, 240-Vac.(Series, 2016).

3.7. Heating Element

An electric heater is a type of electrical appliance that produces heat from electricity. Every electric heater has a heating element inside that is nothing more than an electrical resistor. By use of joule heating, an electric current that flows through a resistor converts electrical energy into thermal energy. 2100W electrical heating elements corresponding to 220Vac are connected to the inverter also these elements are inserted in two sides of the storage tank. Therefore, we can select Sinus Jevi Immersion Heaters with $2100W$ of power corresponding to 220Vac.

Table 3-8: The size of the PV system in Wp for the peak load at STC for a different number of injera with specifications from Hi-Tech (Solar HI-Tech, 2015).

Number of injera	The total useful energy (KJ)	The total energy demand (KJ)	Amount of PCM (kg)	Required photovoltaic modules power P_{PV} (W)	Number of modules	Actual photovoltaic modules power P_{PV} (W)
40	12760.86	20417.38	44.54	1231.06	5	1500
60	**19141.3**	**30626.07**	**66.815**	**1848**	**7**	**2100**
80	25521.73	40834.765	89.1	2462.12	9	2700
100	31902.16	51043.456	111.36	3077.65	11	3300
120	38282.6	61252.15	133.63	3693.18	13	3900
150	47853.24	76565.184	167.04	4616.5	16	4800

3.8. Selection of material for the system

3.8.1. Design of Baking Pan

A baking pan is a flat, circular baking dish that is typically between 50 and 60 cm in diameter. It was formerly used over big clay hearths to bake injera. In this system 8mm thick and 580mm

diameter the ceramic pan is selected since compared to the clay pan or locally accessible one, it has a higher thermal conductivity.

3.8.2. Design of Baking Pan Cover

To prevent thermal loss from the system when baking and charging the storage, an insulated pan cover which is made from aluminum with a 64cm diameter is assembled.

3.8.3. Materials for Storage Tank

Stainless steel was chosen as the material for the thermal storage tank because it is resistant to corrosion and high temperatures (Xie et al., 2019, the R Core Team, 2015).

3.8.4. Selection of Heat-Transfer Oils

It is crucial to take the coefficient of expansion, viscosity, thermal capacity, freezing point, boiling point, and flash point into account when choosing a heat-transfer fluid. The table below illustrates how temperature affects the thermal characteristics of several thermal oils (Mawire et al., 2014).

Table 3-9: variation of thermal properties with the temperature of thermal oils

Thermal oil	Density(kg/m3)	Specific heat capacity (J/kg. k)	Thermal conductivity (w/m. k)
Sunflower oil	ρ_s=930.62-0.65T	$C_s = 2115.00 + 3.13T$	$k_s = 0.161 + 0.018\exp(-T/26.142)$
Shell Thermia C	ρ_s=893.00-0.67T	$C_c = 1798.00 + 3.58T$	$k_c = 0.121 + 0.0132\exp(-T/18.659)$
Shell Thermia B	ρ_s=876.00-0.65T	$C_B = 1809.00 + 3.50T$	$k_B = 0.118 + 0.018\exp(-T/168.660)$

Table 3-9 demonstrates how the thermal characteristics of various oils change with temperature. The most temperature-dependent, density and specific heat capacity is found in sunflower oil. It appears that the thermal conductivities are in the same region (Mawire et al., 2014).

3.8.5. Shell Thermia Oil B Heat Transfer Oil

The highly refined mineral oils, shell thermia oil B are chosen for their superior performance in enclosed circulating heat transfer systems as well as indirect closed fluid heat transfer systems. With application restrictions of a maximum film temperature of 340^{o}C and a maximum bulk

temperature of 320^{o}C, it can be employed in high-temperature continuous heat transfer equipment. The system's layout and operation affect how long shell thermia oil B lasts. The typical design data for shell thermia B heat transfer oil (Q, 2009) is listed in appendix table B.

3.9. Insulation

The fiberglass insulation is selected to this operating temperature with the most economical thickness of 75mm with a density of 64kg/m3 (AAAMSA, 2001) because glass fiber is good workability, non-combustible, low compression resistance, and many facings available also work on a temperature range of 455-538^{o}C (Ying-Zhang et al., 2013).

CHAPTER 4: PERFORMANCE ANALYSIS OF THERMAL ENERGY STORAGE FOR INJERA BAKING

4.1. Modeling the Baking Process Heat Transfer Mechanism of Mitad

The assumptions for the analysis of an equivalent thermal circuit diagram of a PV-integrated Injera baking system, the effect of conductive heat transfer of aluminum supporting plate on the bottom of baking pan is assumed insignificant.

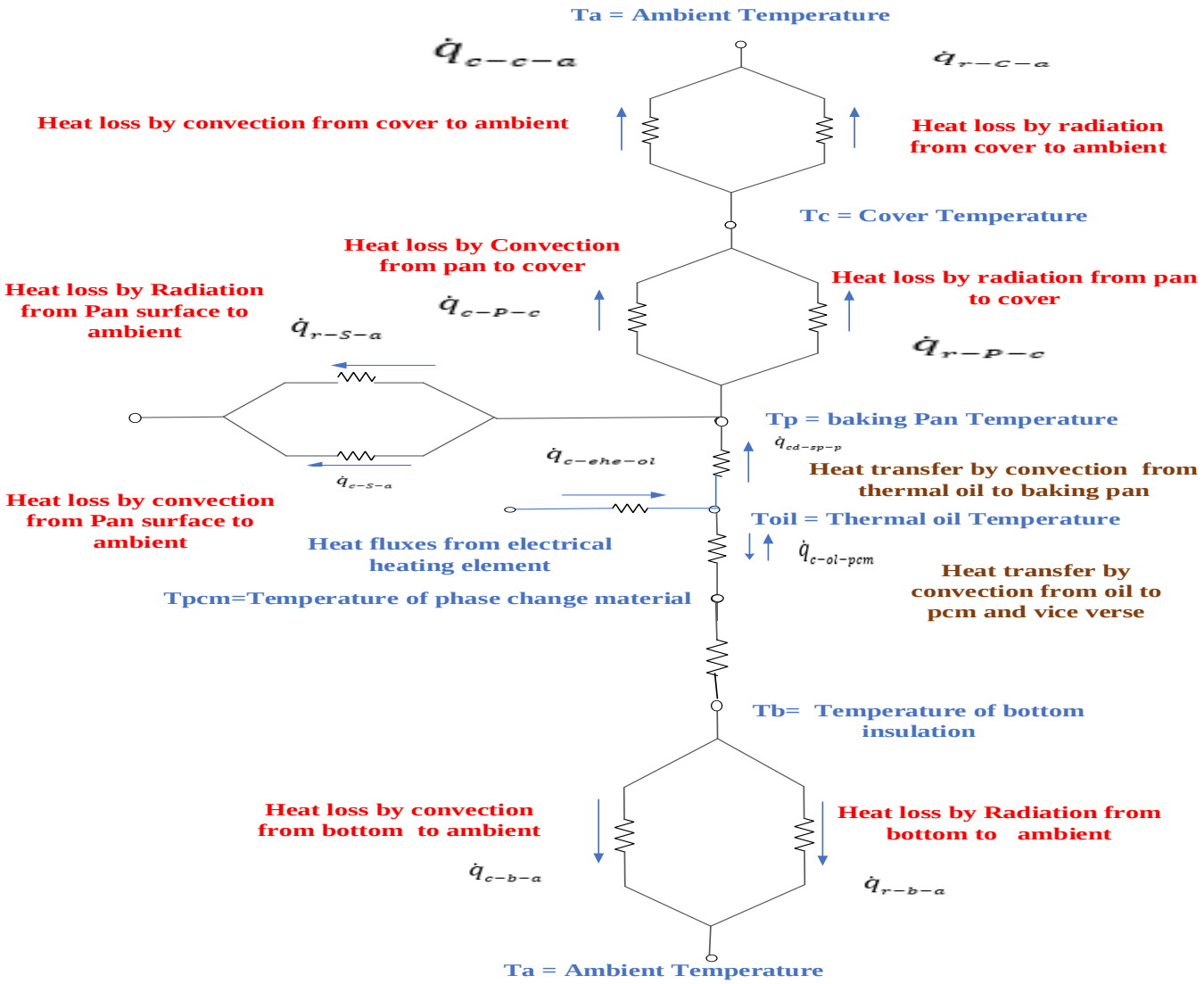

Figure 4-1: Thermal circuit diagram and heat loss in PV-integrated, Injera baking system

Depending on the heat transfer process shown on the thermal circuit the mathematical model for a different processes are discussed below.

4.2. Mathematical Model

The storage serves as a sink during the melting of the PCM when the oil temperature is equal to or higher than the melting temperature and serves as a source of heat during the solidification of the PCM when the temperature of oil is lower below the solidification temperature of the PCM.

A two-phase model that treats the system as a continuous medium rather than a medium made up of discrete particles is used to analyze the thermal behavior of a storage system. One-dimensional continuous models of heat conduction can only happen in the axial direction; two-dimensional continuous models can only happen in the axial and radial directions. It is assumed that a one-dimensional continuous model applies to the current system.

Several techniques, based on both experimental and theoretical studies, have been presented in the literature to address the phase change problem. There are five crucial techniques (Regin et al., 2008), specifically, the enthalpy method, front fixing method, flexible grid generation method, fixed grid method, and variable grid method. The mathematical model employed in the current work is based on the enthalpy formulation where the dependent variable is enthalpy.

4.2.1. Enthalpy Method

In phase change problems, non-linear heat equations are solved using the enthalpy approach. The phase change problem is solved by using the relationship between temperature and enthalpy, which is considered a temperature-dependent variable when using the enthalpy formulation method. The flow of latent heat is expressed in terms of volumetric enthalpy as a function of the temperature of the PCM. The enthalpy approach was created by (Voller, 1990) and it is among the most popular techniques for handling phase change boundaries.

For these uses, cylindrical LHTES with cylindrically encapsulated molten salt have been developed. The heat from the PV is accumulated by the LHTES. These models' basic

assumption is that the PCM capsules function as a continuous medium rather than as a media made up of discrete particles (Arkar & Medved, 2005).

Energy conservation can be described in terms of total volumetric enthalpy and temperature for a phase change process involving either melting or freezing (Saman et al., 2005):

$$\frac{\partial H}{\partial t} + \nabla(uH) = \nabla(K(\nabla T)) \qquad 4.1$$

Where:

H= total volumetric enthalpy, J/m^3

t= time, s

u= velocity

k = thermal conductivity, w/m ^{O}C

T= temperature, ^{O}C

The total volumetric enthalpy H in the equations above is equal to the summation of the sensible and latent heats of the PCM and is proportional to its temperature as follows:

$$H(T) = \int_{T_m}^{T} \rho c dT + \rho f_l \lambda \qquad 4.2$$

Where: Tm = melting temperature, ^{O}C

λ = latent heat of fusion, J/kg

In the equation above, the first component on the right side represents sensible heat, and the second term represents the latent heat of the PCM.

The present system is analyzed as a one-dimensional problem and the mathematical model for phase change of the encapsulated PCM and the heat transfer fluid is derived as follows;

$$\frac{\partial H}{\partial t} + \nabla(uH) = \nabla(K(\nabla T)) \quad 4.3$$

Since H is total volumetric enthalpy, which is total enthalpy divided by total volume, total enthalpy;

$$H\,\mathrm{t} = h * m \quad 4.4$$

$$H\,t = \rho V * h \quad 4.5$$

$$\frac{H\,t}{V} = \rho * h \quad 4.6$$

$$H = \rho * h \quad 4.7$$

Where: h = specific enthalpy and

m = mass of the particle

The above equation for one-dimensional problem analysis becomes;

$$\rho\frac{\partial h}{\partial t} + v\rho\frac{\partial h}{\partial x} = \nabla(K(\nabla T)) \quad 4.8$$

Since, $\frac{\partial h}{\partial t}$ = c$\frac{\partial T}{\partial t}$ and $\frac{\partial h}{\partial x}$= $c\frac{\partial T}{\partial x}$ where, c= specific heat

$$\rho\mathrm{c}\frac{\partial T}{\partial t} + v\rho\mathrm{c}\frac{\partial T}{\partial x} = \nabla(K(\nabla T)) \quad 4.9$$

$$\rho\mathrm{c}\left(\frac{\partial T}{\partial t} + v\frac{\partial T}{\partial x}\right) = \nabla(K(\nabla T)) \quad 4.10$$

In general, the HTF and PCM's one-dimensional energy equations can be written individually (de Gracia & Cabeza, 2017), by assuming that the heat transfer occurs only along the axial direction for both HTF and PCM also the following assumptions are considered:

- The porosity and storage configuration are both consistent.

- Because of the low temperature, radiation heat transfer in the storage medium is disregarded.
- The conduction heat transfer in the oil was neglected
- The heat transfer oil is not flowing and no energy is delivered by heat transfer fluid from the control volume.
- The influence of natural convection within the molten PCM was ignored.

4.3. Mathematical Modeling for the Heat Transfer Fluid

According to an energy balance, the change of internal energy of oil during time dt of the differential element is calculated as follows;

$$\varepsilon\rho_o c_o \frac{\partial T_o}{\partial t} = h_{op}a_p(T_P - T_o) - U_W a_W(T_o - T_{sur}) \qquad 4.11$$

Where: ρ_o=the density of oil

c_o= specific heat of the oil

T_o = temperature of the oil

a_p= the heat transfer area of the storage per unit storage volume

a_w= the heat transfer area per unit storage volume

T_P = the temperature of the PCM

ε=porosity

h_{op}= the effective convective heat transfer coefficient between the HTF and the PCM

4.4. Mathematical Modeling for the PCM

For the present system considering the above assumption, the energy balance for PCM is, the rate of change of internal energy of the PCM is determined as the sum of the heat transferred from the oil to the PCM and the heat conducted in the PCM in the axial direction. Hence, the energy equation for the solid phase is obtained as follows:

$$(1-\varepsilon)\rho_p c_p \frac{\partial T_p}{\partial t} = k_{sx}\frac{\partial^2 T_p}{\partial x^2} + h_{op}a_p(T_o - T_p) \qquad 4.12$$

Where ρ_p is the density of PCM, k_{sx} effective thermal conductivity of PCM and ε is porosity, which is the volume fraction of oil and 1-ε is the volume fraction of the PCM tube.

4.5. Governing Equation for Melting fraction in the latent heat section

The heat transfer process of a PCM during phase transformation can be modeled by using molten fraction with the time difference. A liquid PCM's quality can be predicted using the molten fraction and is given by:

$$X = \frac{m_{liq,pcm}}{m_{total}} \quad 4.13$$

Where X = melt fraction.

The energy provided to the PCM is stored in the material as latent heat once the PCM temperature reaches the fusion temperature. The rate of heat obtained from PCM, $\dot{Q}$ determines the rate of change of PCM's enthalpy.

$$\frac{dH}{dt} = \dot{Q} \quad 4.14$$

$$\frac{d(\rho_p V_p h)}{dt} = \dot{Q} \quad 4.15$$

$$\rho_p V_p \frac{dh}{dt} = \dot{Q} \quad 4.16$$

The total volumetric enthalpy H in the equations above is equal to the sum of the sensible and latent heats of the PCM and is proportional to the temperature of the PCM:

$$H(T) = \int_{T_m}^{T} \rho c dT + \rho X \lambda \quad 4.17$$

$$\rho * h = \rho c \Delta T + \rho X \lambda \quad 4.18$$

The temperature does not change during phase transition, and the temperature's first derivative is zero:

$$\rho_p V_p \lambda \frac{dX}{dt} = \dot{Q} \quad 4.19$$

Dividing both sides by the total volume and calculating the liquid fraction from:

$$(1-\varepsilon)(\rho\lambda)_{eff}\frac{dX}{dt} = h_v(T_f - T_p) \quad 4.20$$

$$\frac{dX}{dt} = \frac{h_v}{(1-\varepsilon)*(\rho\lambda)_{eff}}(T_f - T_p) \quad 4.21$$

Where: $(\rho\lambda)_{eff} = (1-\varepsilon)(\rho_p\lambda)$

4.6. Heat Transfer Equations for Liquid PCM

Convective heat transfer from the oil to the PCM determines the temperature change of the liquid PCM over time.

$$(1-\varepsilon)\rho_{efp,l}c_{efp,l}\frac{\partial T_p}{\partial t} = h_v(T_f - T_p) \quad 4.22$$

$$\frac{\partial T_p}{\partial t} = \frac{h_v}{(1-\varepsilon)\rho_{p,l}c_{p,l}}(T_f - T_p) \quad 4.23$$

Where: $Tm = \text{melting temperature, oC}$

$\lambda =$ latent heat of fusion, $\frac{J}{kg}$

$h_v =$ volumertric het transfer coefficient ($h_{op}a_{p)}$

$X =$ Liquid fraction of the PCM

$\rho_p =$ density of PCM (kg/m3)

$C_{P,PCM,l} =$ the specific heat of liquid PCM (J /kgK)

4.7. Mathematical Modeling for Baking Pan

Based on the following assumptions, the mathematical model for the baking pan is developed:

- The baking pan is initially covered and reaches its needed temperature and no initial heating-up condition.
- Heat loss due to the material which is aluminum metal with a very small thickness between the pan and the hot oil is negligible.
- Only along the thickness or in the axial direction does the temperature change.
- There is no heat generation, and the baking pan's thermal conductivity remains constant.

The heat transfer process through the baking pan is modeled by transient heat conduction, which is given as:

$$\rho_{pan} \mathrm{c}_{pan} \frac{\partial T_p}{\partial t} = k_{pan} \frac{\partial^2 T_{pan}}{\partial x^2} \qquad 4.24$$

Where ρ_{pan}, is density (kg/m^3), c_{pan}, specific heat capacity (J /kg. k.) and T is the temperature of the baking pan varying with space and time.

4.8. Computational Model

Finite difference approximation is used with the explicit technique to replace the one-dimensional transient governing equation. The second-order central differencing formula is used to discretize the spatial second derivative, while the first-order central differencing formula is used to discretize the time derivative. The domain $0 \leq x \leq L$ is discretized into segments of length ∇x, where L is the total length of the PCM.

$$\frac{\partial T_o}{\partial t} = \frac{{T_{o,i}}^{n+1} - {T_{o,i}}^{n}}{\Delta t} \qquad 4.25$$

$$\frac{\partial T_o}{\partial x} = \frac{{T_{o,i+1}}^{n} - {T_{o,i-1}}^{n}}{2\Delta x} \qquad 4.26$$

$$\frac{\partial^2 T_o}{\partial x^2} = \frac{{T_{o,i+1}}^n - 2{T_{o,i}}^n + {T_{o,i-1}}^n}{\Delta x^2} \quad 4.27$$

For thermal oil

$$\varepsilon \rho_o c_o \frac{\partial T_o}{\partial t} = h_{op} a_p (T_P - T_o) - U_W a_W (T_{sur} - T_o) \quad 4.28$$

$$\varepsilon \rho_o c_o \frac{{T_{o,i}}^{n+1} - {T_{o,i}}^n}{\Delta t} = h_{op} a_p \left({T_{p,i}}^n - {T_{o,i}}^n\right) - U_W a_W \left({T_{sur,i}}^n - {T_{o,i}}^n\right) \quad 4.29$$

$$\frac{{T_{o,i}}^{n+1} - {T_{o,i}}^n}{\Delta t} = \frac{h_{op} a_p}{\varepsilon \rho_o c_o} \left({T_{p,i}}^n - {T_{o,i}}^n\right) - \frac{U_W a_W}{\varepsilon \rho_o c_{Po}} \left({T_{sur,i}}^n - {T_{o,i}}^n\right) \quad 4.30$$

$${T_{o,i}}^{n+1} = {T_{o,i}}^n + R\left({T_{p,i}}^n - {T_{o,i}}^n\right) - F\left({T_{sur,i}}^n - {T_{o,i}}^n\right) \quad 4.31$$

Where, $F = \frac{U_W a_W \Delta t}{\varepsilon \rho_o c_{Po}}$,

$R = \frac{h_{op} a_p \Delta t}{\varepsilon \rho_o c_o}$

Similar to this, the discretization of the differential equations for heat transmission in PCM throughout the solid phase is as follows:

$$(1-\varepsilon)\rho_{efp} c_{efp} \frac{\partial T_p}{\partial t} = k_{sx} \frac{\partial^2 T_p}{\partial x^2} + h_{op} a_p (T_o - T_p) \quad 4.32$$

$$\frac{\partial T_P}{\partial t} = \frac{{T_{P,i}}^{n+1} - {T_{P,i}}^n}{\Delta t} \quad 4.33$$

$$\frac{\partial T_P}{\partial x} = \frac{{T_{P,i+1}}^n - {T_{P,i-1}}^n}{2\Delta x} \quad 4.34$$

$$\frac{\partial^2 T_p}{\partial x^2} = \frac{{T_{p,i+1}}^n - 2{T_{p,i}}^n + {T_{p,i-1}}^n}{\Delta x^2} \quad 4.35$$

$$\frac{{T_{p,i}}^{n+1} - {T_{p,i}}^n}{\Delta t} = k_{sx}\frac{{T_{p,i+1}}^n - 2{T_{p,i}}^n + {T_{p,i-1}}^n}{(1-\varepsilon)\rho_p \mathrm{c}_p \Delta x^2} + \frac{h_{op} * a_p({T_{o,i}}^n - {T_{p,i}}^n)}{(1-\varepsilon)\rho_p \mathrm{c}_p} \quad 4.36$$

$$\frac{{T_{p,i}}^{n+1} - {T_{p,i}}^n}{\Delta t} = k_{sx}\frac{{T_{p,i+1}}^n - 2{T_{p,i}}^n + {T_{p,i-1}}^n}{(1-\varepsilon)\rho_p \mathrm{c}_p \Delta x^2} + \frac{h_{op} * a_p({T_{o,i}}^n - {T_{p,i}}^n)}{(1-\varepsilon)\rho_p \mathrm{c}_p} \quad 4.37$$

$${T_{p,i}}^{n+1} = {T_{p,i}}^n + RP\left({T_{p,i+1}}^n - 2{T_{p,i}}^n + {T_{p,i-1}}^n\right) + FP({T_{o,i}}^n - {T_{p,i}}^n) \quad 4.38$$

$${T_{p,i}}^{n+1} = {T_{p,i}}^n(1 - FP - 2RP) + RP\left({T_{p,i+1}}^n + {T_{p,i-1}}^n\right) + FP{T_{o,i}}^n \quad 4.39$$

Where, $RP = \frac{k_{sx}\Delta t}{(1-\varepsilon)\rho_p c_p \Delta x^2}$

$$FP = \frac{h_{op} a_p \Delta t}{(1-\varepsilon)\rho_p c_p}$$

For the Melting Fraction

The molten fraction is calculated by discretizing the aforementioned equation as follows.

$$\frac{dX}{dt} = \frac{h_v}{(1-\varepsilon)*(1-\varepsilon)(\rho_p \lambda)}(T_o - T_p) \quad 4.40$$

$${X_{,i}}^{n+1} = {X_{,i}}^n + \frac{h_v}{(1-\varepsilon)*(1-\varepsilon)(\rho_p \lambda)}({T_{o,i}}^n - {T_{p,i}}^n) \quad 4.41$$

For the PCM during the liquid phase

By discretizing the aforementioned equation, the PCM's temperature when it is in liquid form can be determined as follow:

$$\frac{\partial T_p}{\partial t} = \frac{h_v}{(1-\varepsilon)\rho_{p,l}c_{p,l}}(T_o - T_p) \quad 4.42$$

$$\frac{{T_{P,i}}^{n+1} - {T_{P,i}}^{n}}{\Delta t} = \frac{h_v}{(1-\varepsilon)\rho_{p,l}c_{p,l}}({T_{o,i}}^{n} - {T_{p,i}}^{n}) \quad 4.43$$

For the Baking pan

$$\rho_{pan}c_{pan}\frac{{T_{pan,i}}^{n+1} - {T_{pan,i}}^{n}}{\Delta t} = k_{pan}\frac{{T_{pan,i+1}}^{n} - 2{T_{pan,i}}^{n} + {T_{pan,i-1}}^{n}}{\Delta x^2} \quad 4.44$$

$$\frac{{T_{pan,i}}^{n+1} - {T_{pan,i}}^{n}}{\Delta t} = k_{pan}\frac{{T_{pan,i+1}}^{n} - 2{T_{pan,i}}^{n} + {T_{pan,i-1}}^{n}}{\rho_{pan}c_{pan}\Delta x^2} \quad 4.45$$

$${T_{pan,i}}^{n+1} = {T_{pan,i}}^{n} + PP\left({T_{pan,i+1}}^{n} - 2{T_{pan,i}}^{n} + {T_{pan,i-1}}^{n}\right) \quad 4.46$$

Where: $PP = \frac{k_{pan}\Delta t}{\rho_{pan}c_{pan}\Delta x^2}$

Where, i and $i+1$ denote the current and front spatial nodes in the axial directions, whereas n and $n+1$ denote the current and following time step.

4.9. Heat Transfer Coefficients Correlations

Conduction and natural convection are two ways that heat is transferred inside the thermal storage tank. Although there is no forced velocity in the system, there are still convection currents in the fluid; these conditions are known as free or natural convection. This works when a body force from the gravitational field interacts with a fluid that has density gradients caused by temperature gradients.

Heat transmission by natural convection over surfaces is primarily influenced by:

- The surfaces' geometry and orientation,,
- The temperature distribution over the surfaces, and
- The fluid's thermos-physical characteristics.

The flow regimes in natural convection are governed by a dimensionless number known as the Grashof number. The following is the definition of the Grashof number;

$$Gr = \frac{Buoyancy\ forces}{Viscous\ forces} \qquad 4.47$$

$$Gr = \frac{(g\beta(T_s - T_\infty)\delta^3}{v^2} \qquad 4.48$$

Where, Gr = Grashof number

g= gravitational acceleration,

T_s= temperature of the surface,

T_∞ =temperature of fluid sufficiently far away from the surface,

δ =Characteristic length of the geometry,

v = kinematic viscosity of the fluid,

β= coefficient of thermal expansion.

The Rayleigh number for such internal (enclosure) flows is given as follows;

$$Ra = \frac{(g\beta(T_s - T_\infty)\delta^3}{v^2} Pr \qquad 4.49$$

Where, Pr =Prandtl number

The convective heat transfer coefficient for the thermal oil in the storage is determined from the following correlations given for the hot surface at the bottom. There are several

experimental correlations for the average Nusselt number given as follows (Incropera & DeWitt, 1996).

$$Nu = 0.13Ra^{0.3} \qquad for\ Ra\ \ 3.7 * 10^4 - 10^8 \qquad 4.50$$

$$Nu = 0.057Ra^{1/3} \qquad for\ Ra > 10^8 \qquad 4.51$$

The convective heat loss between the baking pan surface and the environment is determined from the following correlations given for the horizontal plate where the upper surface is hot;

$$Nu = 0.54Ra^{1/4} \qquad for\ Ra\ \ 10^4 - 10^7 \qquad 4.52$$

$$Nu = 0.15Ra^{1/3} \qquad for\ Ra\ \ 10^7 - 10^{11} \qquad 4.53$$

Where Nu is the Nusselt number, Ra is the Rayleigh number.

By using the Nusselt number correlation, one may calculate the convection heat transfer coefficient;

$$h = \frac{k}{\delta} Nu \qquad 4.54$$

$$\delta = \frac{A}{P} \qquad 4.55$$

Where k = the thermal conductivity of the fluid

δ = the characteristic length, A is surface area and P is the perimeter.

There is also the radiation heat transfer between the baking pan surface and the atmosphere and the radiation heat transfer coefficient at the surface of the baking Pan is given by;

$$hr = \left[\frac{\sigma e\left(T_s{}^4 - T_\infty{}^4\right)}{(T_s - T_\infty)}\right] \qquad 4.56$$

Where $\sigma = 5.67 * 10(-8)$, Stefan Boltzmann constant $W/(m^2.k^4)$ and $e = 0.95$ the emissivity of the baking pan surface. The properties used in the previously mentioned correlations are performed at the film temperature T_f=$(T_s - T_\infty)/2$.

Convection and radiation's combined effects are taken into account when calculating the overall heat transfer coefficient on the surface of the baking pan.

$$h_t = hc + hr \qquad 4.57$$

hc =convective heat transfer coefficient (W/m^2.K)

hr =radative heat transfer coefficient (W/m^2.K)

h_t =surface overall heat transfer coefficient (W/m^2.K)

The overall heat transfer coefficient through the wall of the storage tank is calculated from the equation given below.

$$\frac{1}{U_w A} = \frac{1}{h_i A} + \frac{X_{in}}{K_{in} A} + \frac{1}{h_o A} \qquad 4.58$$

Where, U_w=overall heat transfer coefficient throughout the wall

A=surface area of the storage tank wall

h_i=internal convective heat transfer coefficient

h_o=outer convective heat transfer coefficient

X_{in}=thickness of insulation

K_{in}=thermal conductivity of the insulation

4.1. Initial and Boundary Conditions

4.1.1. During Charging Condition

During charging conditions, the constant heat fluxes on the bottom of the storage tank are supplied to the thermia oil initially, and then through the natural convection heat transfer process, the heat is transferred to the PCM bottom continuously. Initially, also the baking pan is sealed with the thermal storage tank, and the baking pan is covered with the pan cover which was insulated with fiberglass.

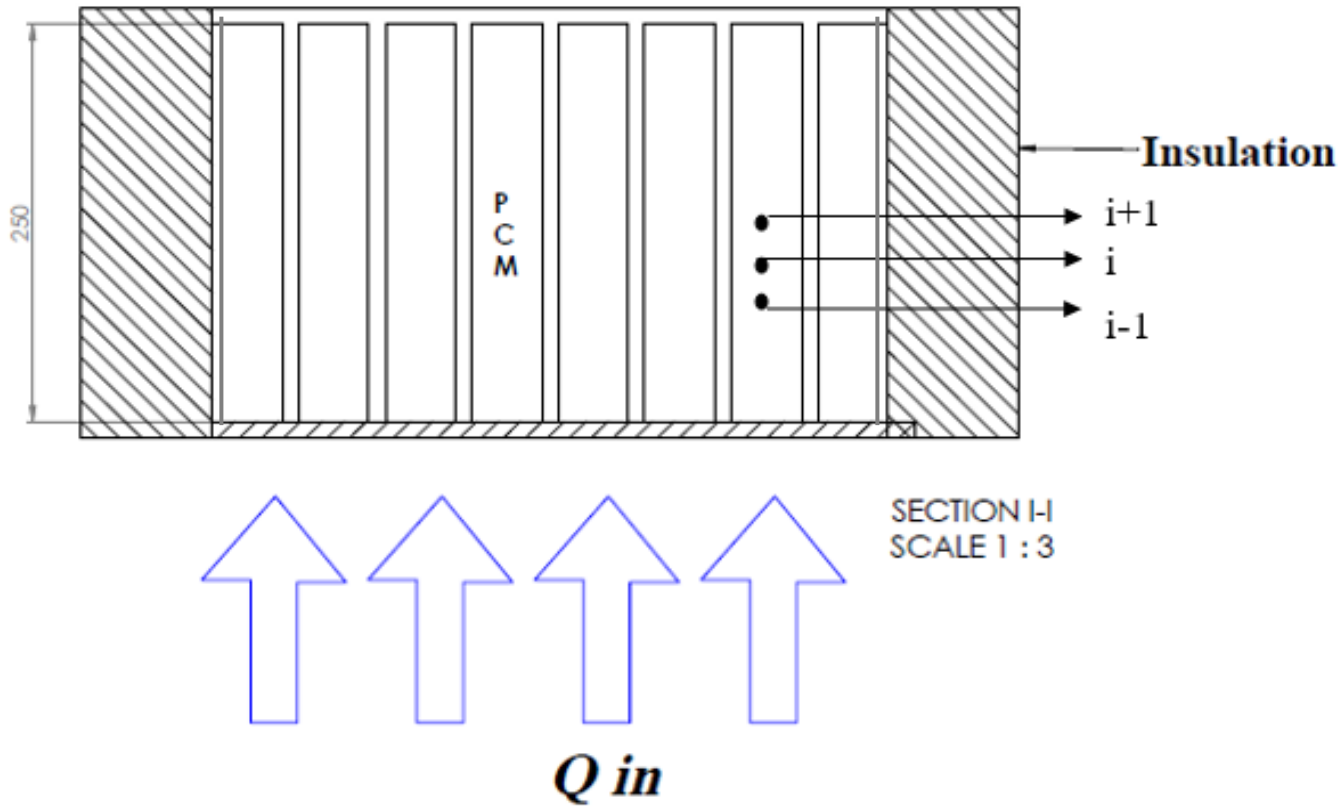

Figure 4-2: Schematic drawing shows the oil-PCM storage during charging conditions

The initial condition at *t=0*

$$Tpcm(x,0) = Toil(x,0) = Tinf$$

Where, $Tinf$ =23℃

Boundary conditions at $t > 0$

$$(q = h(Toil(0,t) - Tpcm(0,t)) \qquad 4.59$$

$$Tpcm(0,t) = Tpcm(1,t)$$

$$Tpcm(x,t) = Tpcm(x+1,t)$$

$$Toil(0,t) = Tinlet(\mathrm{t})$$

Where *q*the heat flux is supplied at the bottom of the storage tank from the electric heater and h is the effective convective heat transfer coefficient.

The maximum time for charging is 4.7 hours which is the monthly peak sun hour for Addis Ababa.

4.1.2. During Discharging Condition

In this condition the PCM and thermia oil is discharging their heat to the baking pan and the baking pan surface is left uncovered to know the maximum surface temperature on its surface throughout the discharging time.

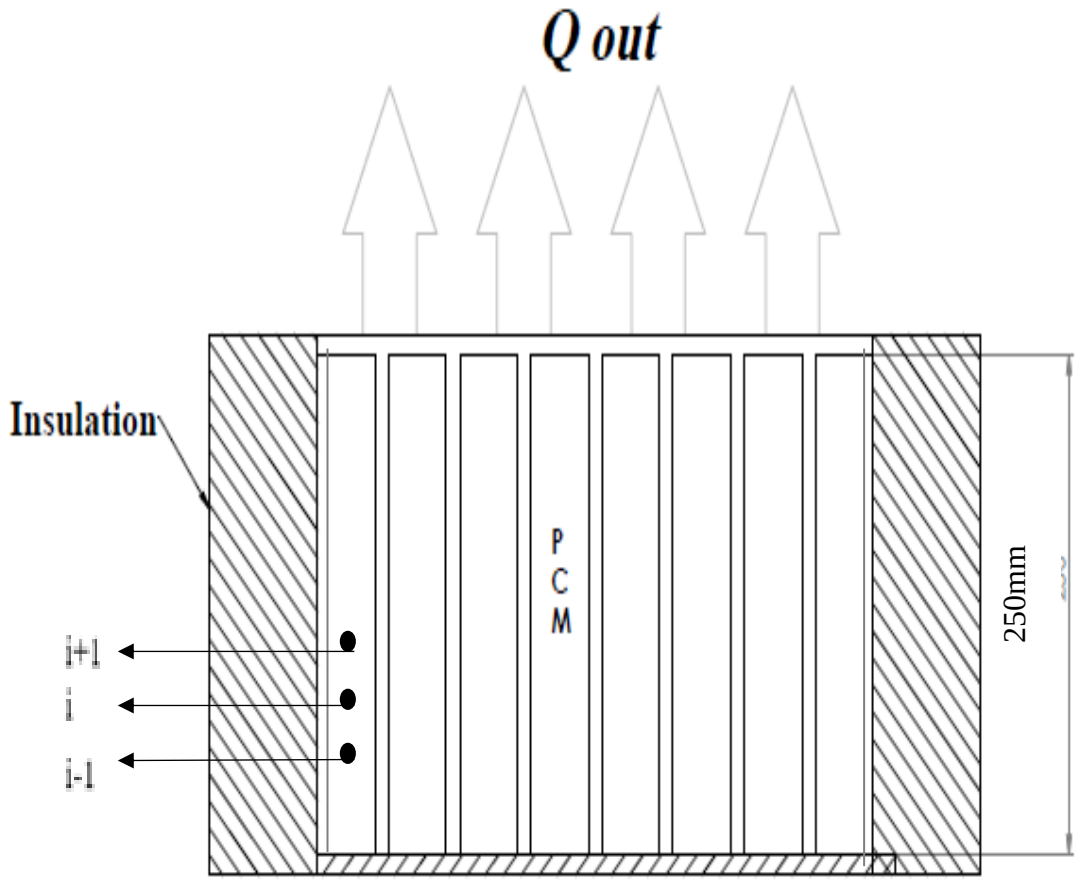

Figure 4-3: Schematic drawing shows the oil-PCM storage during discharging conditions

The initial condition at *t=0*

$$Tpan(x,0) = Tpcm(x,0) = Toil(x,0) = Tf$$

Where, Tf = the final temperature of the storage (℃) after charging for 4.7 hours.

Boundary conditions at $t > 0$

At x=0, at the bottom of the baking pan

$$-(k_{pan}\frac{\partial T_{pan}}{\partial x})_{x=0} = h_{od}(T_{od} - T_{pan,b}) \quad 4.60$$

At x=L, at the top of the baking pan

$$-(k_{pan}\frac{\partial T_{pan}}{\partial x})_{x=L} = h_t(T_{pan,t} - T_{inf}) \quad 4.61$$

Where, k_{pan}=thermal conductivity of the pan

L=thickness of the baking pan

h_{od}=convective heat transfer coefficient of the thermia oil (W/m^2.K)

h_t= the baking pan top surface and air overall heat transfer coefficient (W/m^2.K)

General steps followed on MATLAB programming software are described as follows.

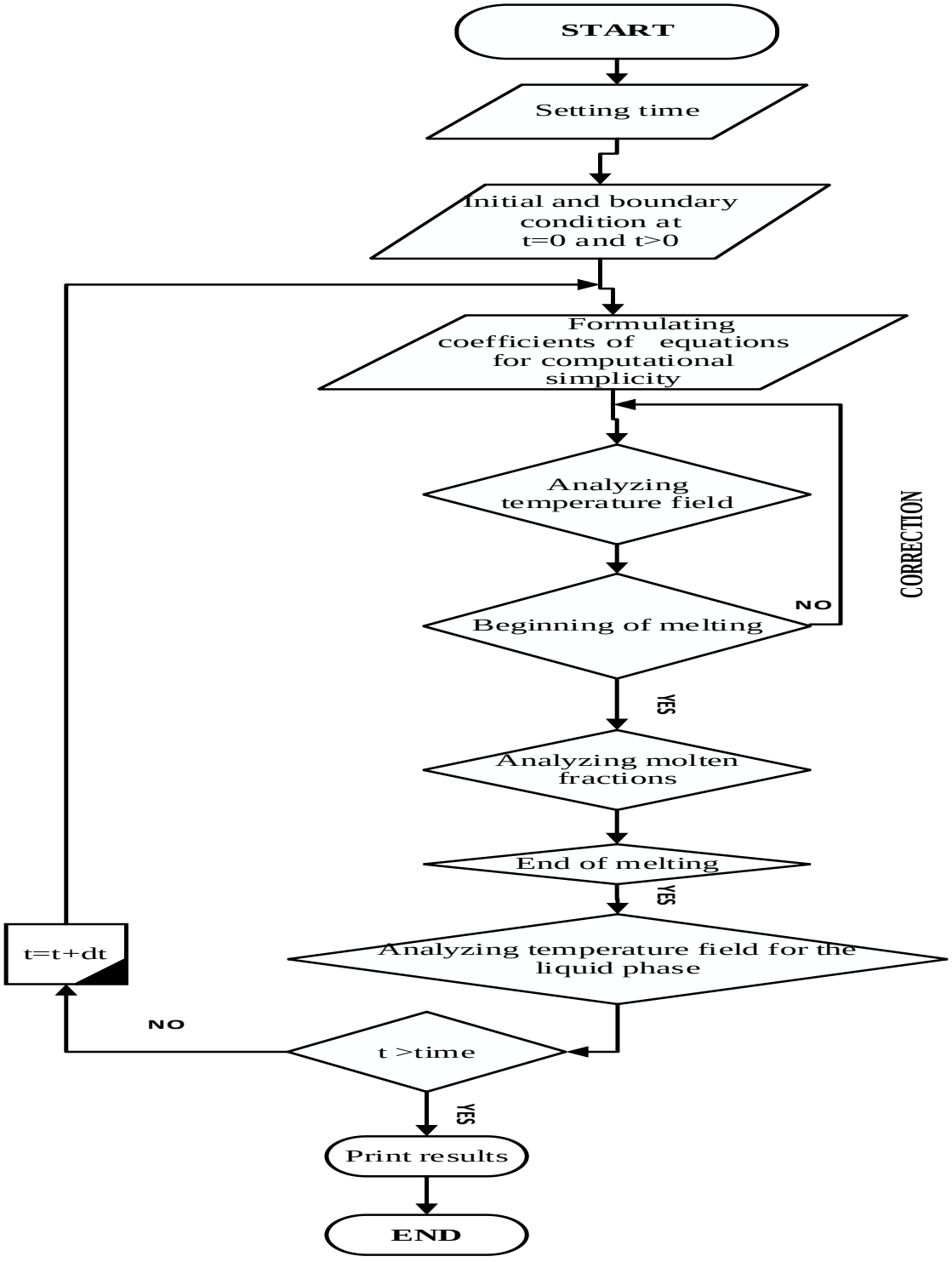

Figure 4-4: Flow chart

4.2. Verification of Computational Model

A mathematical model developed for this study and practical test results utilizing Duratherm 630 as the heat transfer fluid are used to compare the mean PCM and thermal oil temperature variance in Figure 4-5 and the PCM was a binary homogeneous mixture of $NaNO3 - KNO3$, with a molar ratio of 60:40 respectively (Geiran, 2021). The PCM has a mass of 11.66kg, for six cylindrically tubes with 1.08 liter volume each. The identical conditions for the experiment were used for the modeling. As it is shown in Figure 4-5, the correlation between the computational model and the experimental outcomes is good and from this, we can conclude that the computational model can predict the performance of the thermal storage containing PCM and thermal oil reasonably, where EXP is for the experiment and COMP is for the computational.

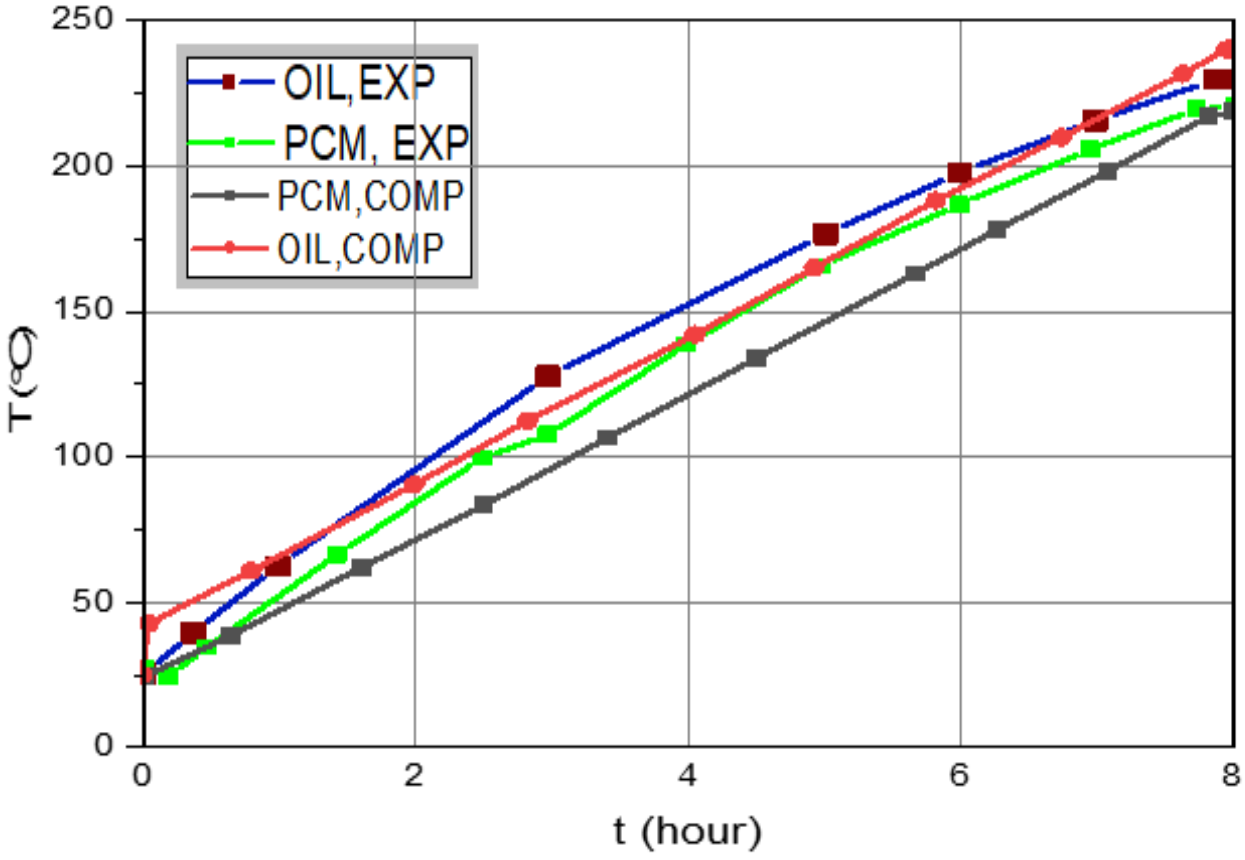

Figure 4-5: Validation of temperature of PCM and thermal oil computational model by experimental results on charging.

4.10. Grid Independence Test

Using the numerical framework created in this study, the experimental findings and simulation results were compared. There was good agreement with slight errors after charging for 8 hours. Therefore, it can be claimed that the precision of the model was adequate to simulate PV-integrated thermal storage during charging and discharging conditions. The temperature along the length of the storage is reasonably comparable with negligible errors when the grid independence is verified for various spatial nodes as shown below.

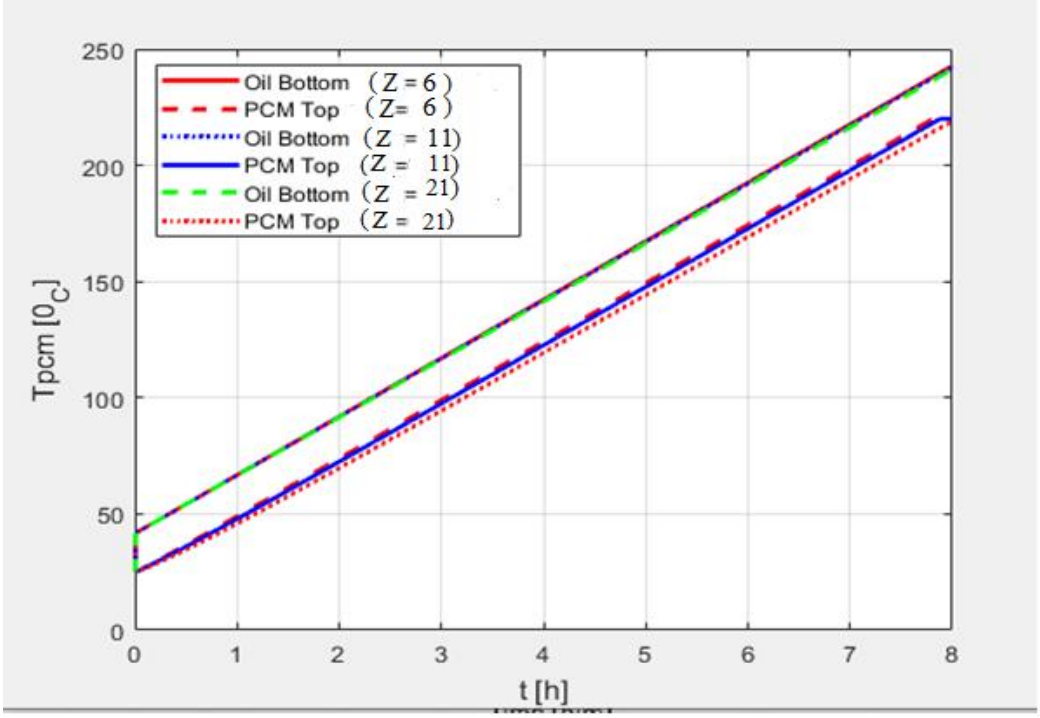

Figure 4-6: Grid independence test

Where Z, is the spatial nodes at different space steps or grid.

CHAPTER 5: RESULT AND DISCUSSION

5.1. Simulation of PCM Thermal Storage

5.1.1. Charging Conditions

During the charging process, the time dependent temperature pattern inside the thermal storage (oil-PCM), as well as the molten fraction of PCM and performance analyses, have been investigated. Figure 5-1 shows the temperature change in a PCM thermal storage which was charged using an electric heater from the PV for 4.7 hours which is the peak sun hour of the selected site which is Addis Ababa. The temperatures reached 303.6^{o}C, and 283.4^{o}C at the bottom and top of the PCM tube, respectively since constant heat fluxes are supplied at the bottom of the storage. The temperature of PCM rise up to solid PCM began to melt, which is sensible heating; after that, the temperature remained constant and the PCM began to melt, it did so when the temperature hit 220°C. The liquefied region's temperature rises when the PCM melts completely. After charging the storage for about 4.7 hours with 2100 W the energy stored in the system was 33MJ.

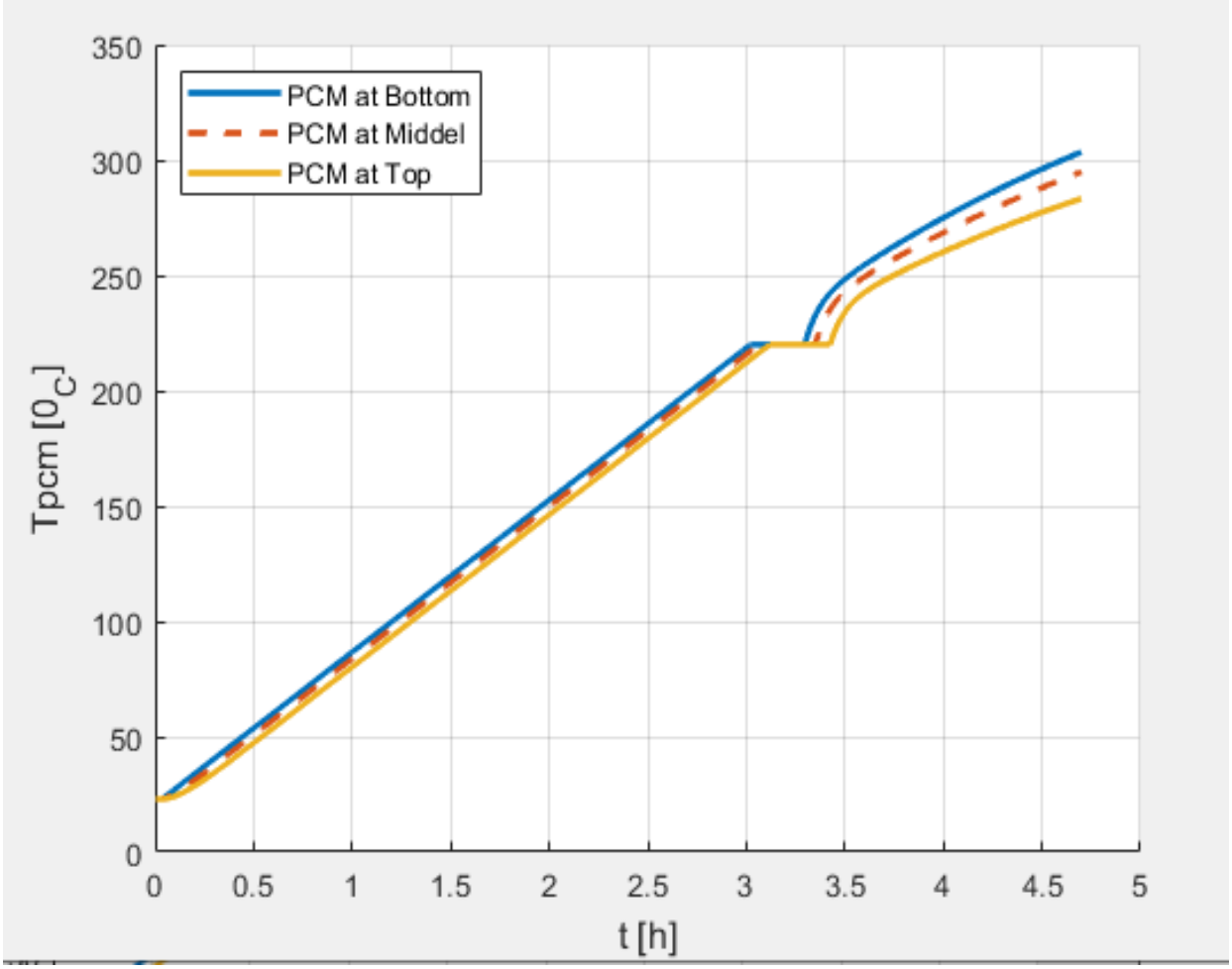

Figure 5-1: Temperature variation of PCM during charging for 4.7 hours

Figure 5-2 compares the temperature changes of the oil and PCM at the top and bottom of the thermal storage during the 4.7-hour charging period.

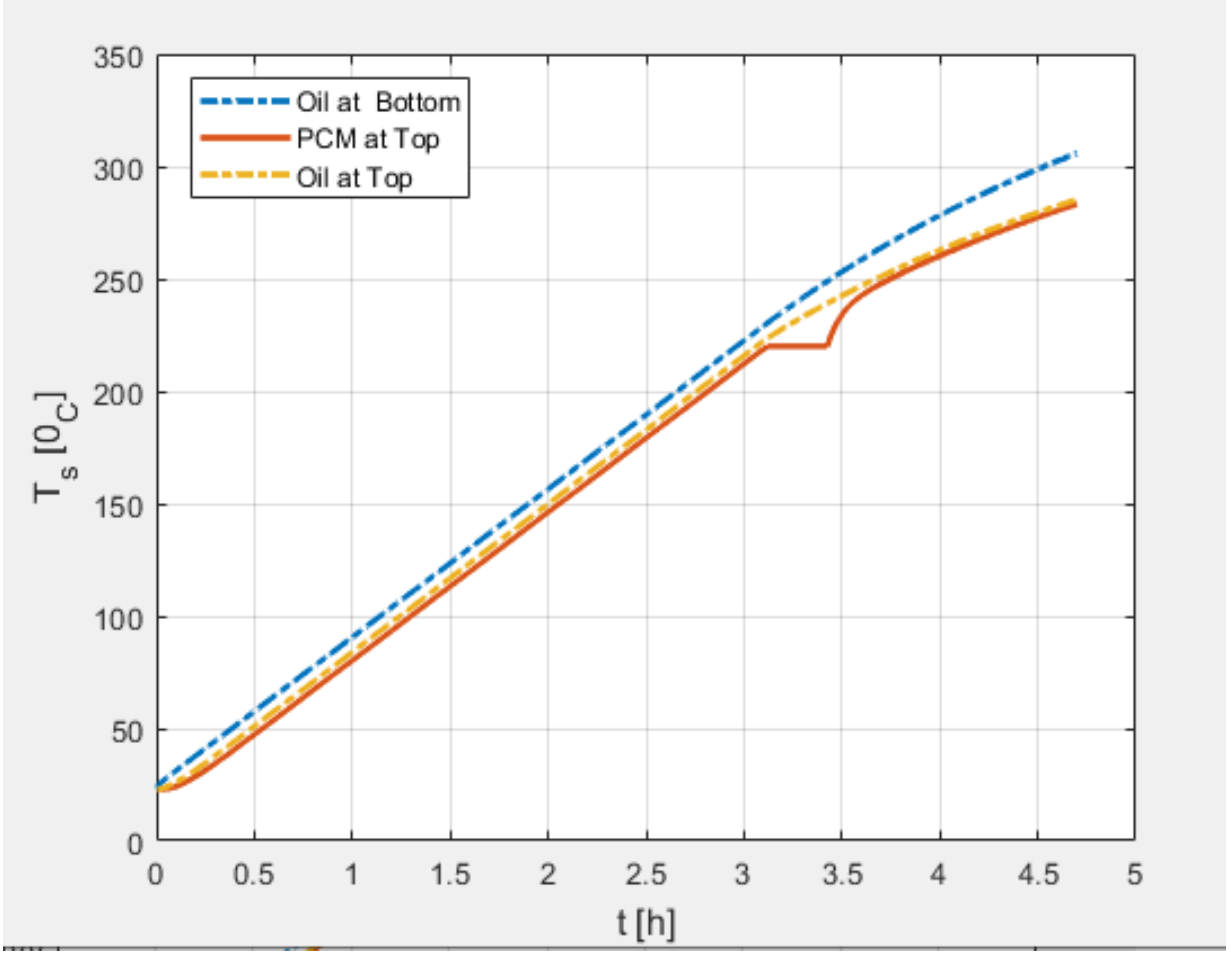

Figure 5-2: Comparison of the temperature of oil and PCM during charging

The phase change and the molten fraction variation at the top and bottom of the cylindrical tubes during the charging of the system are shown in Figure 5-3. After being charged for 3.425 hours, PCM tubes in the storage are fully melted.

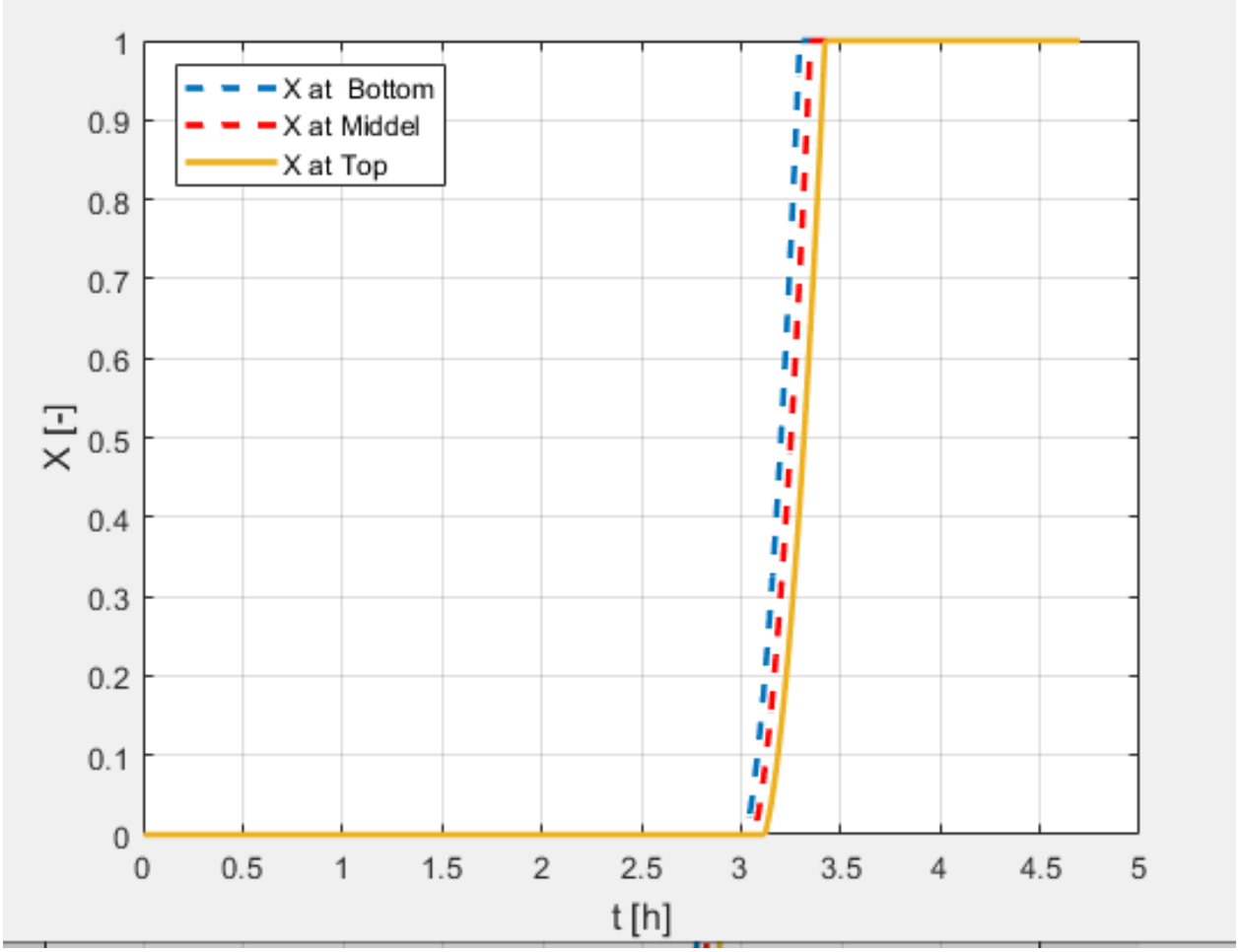

Figure 5-3: Melt fraction of PCM versus time during charging

5.1.2. Discharging Conditions of Thermal Storage

The energy stored in the thermal storage was discharged by free or natural convection to the baking ceramic pan on the top of the storage. Initially, the baking pan is sealed with storage during charging, and the surface of the baking pan is reached its desired temperature for baking Injra. The discharging analysis was conducted by assuming that the pan cover is removed and the top is directly discharging to the air for about 3 hours which is the expected time to cook the desired amount of Injera. Degradation of the thermal storage's transient temperature and baking pan surface with respect to time during discharging is shown in Figure 5-4.

Initially, the thermal storage average temperature reached about 295^{o}**C** then the temperature of the PCM decreased until the liquid PCM reaches its phase-changing temperature (220^{o}C), then the temperature becomes constant and the PCM begins to solidifying. Because the heat transfer process was natural convection boundary the PCM stayed for more time to change its phase to solid which means more latent heat is stored in the system during constant heat fluxes was supplied. The temperature continued to drop when the PCM solidified. After discharging the thermal storage for about 3 hours the temperature degraded to 194.3^{o}**C,** 191.7^{o}**C,** and 146.4^{o}**C** for the PCM top, oil top, and baking pan top respectively. The amount of energy discharged by the system was 16.6MJ and the discharging (thermal) efficiency of the system was about 50.2% also the overall efficiency of the system was 46.67%.

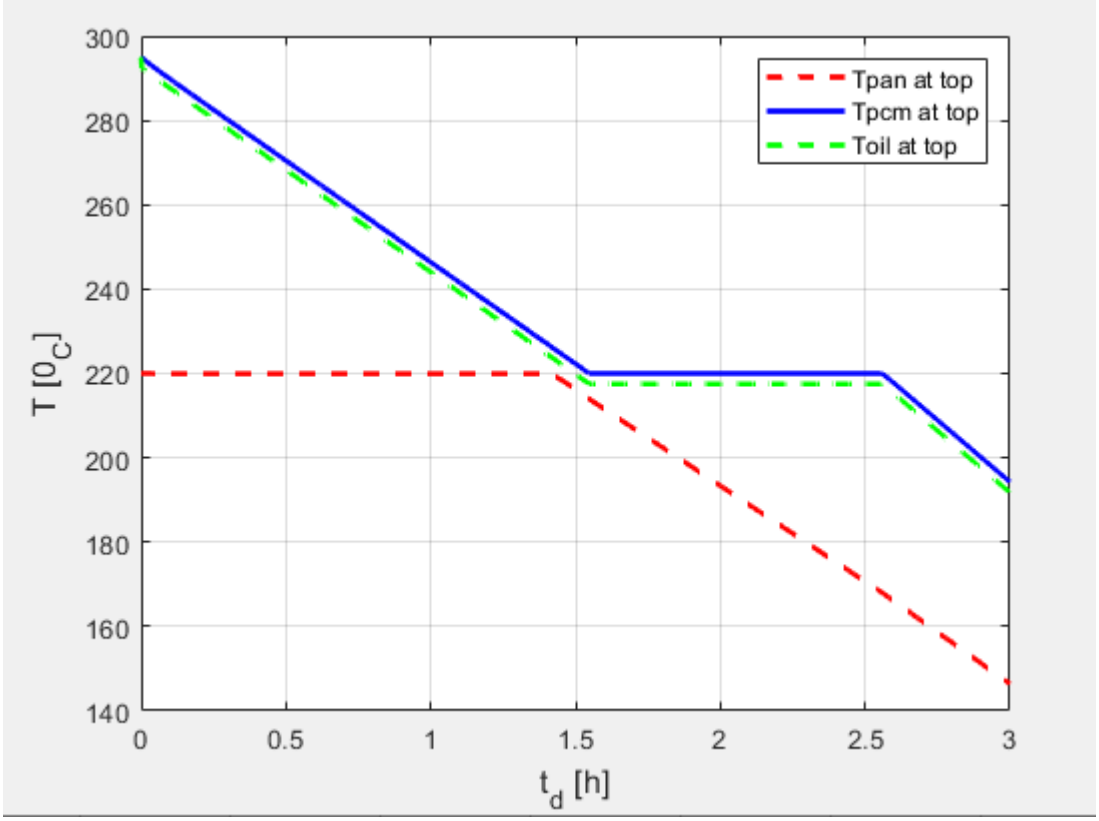

Figure 5-4: Temperature of PCM, thermia oil, and baking pan during discharging

The molten fraction (quality) change at the PCM during system discharge is another indicator of the solidification of PCM thermal storage and is shown in Figure 5-5. The PCM began to shift its phase after discharging for 1.54 hours and all the PCM in the storage are completely crystallized after being discharged for 2.56 hours.

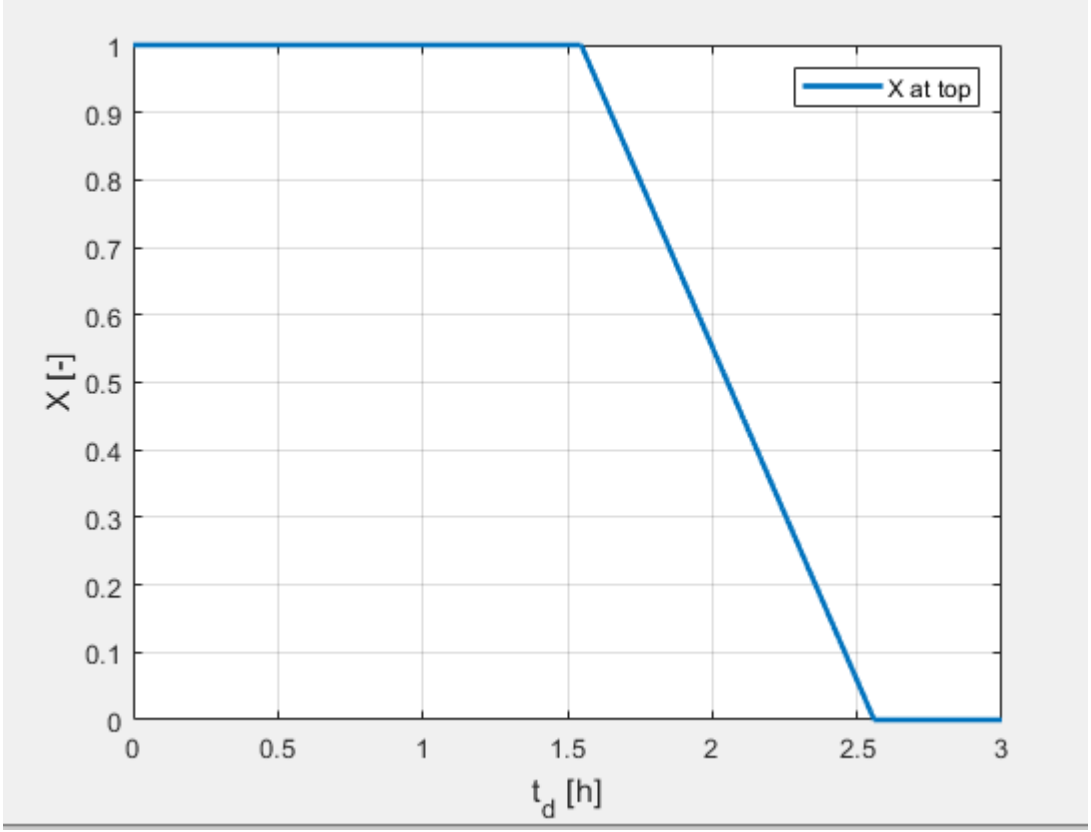

Figure 5-5: Solidification of PCM versus time during discharging

5.2. Comparisons with Other Research

This result was compared with different papers as shown below.

Solar-powered Injera baking stoves were investigated by various researchers and have tried to get a baking pan's surface temperature on average to be approximately 180-250^{o}C. However, from there outputs obtained by experimental work, they investigates that, it was possible to use a surface temperature of a cooking pan or Mitad between 120-233^{o}C as shown in the figure 5-6. Also the overall efficiency of the system was compared with different injera baking

technology and the computational result shows that the current injera baking stove has a good performance as shown figure 5-7.

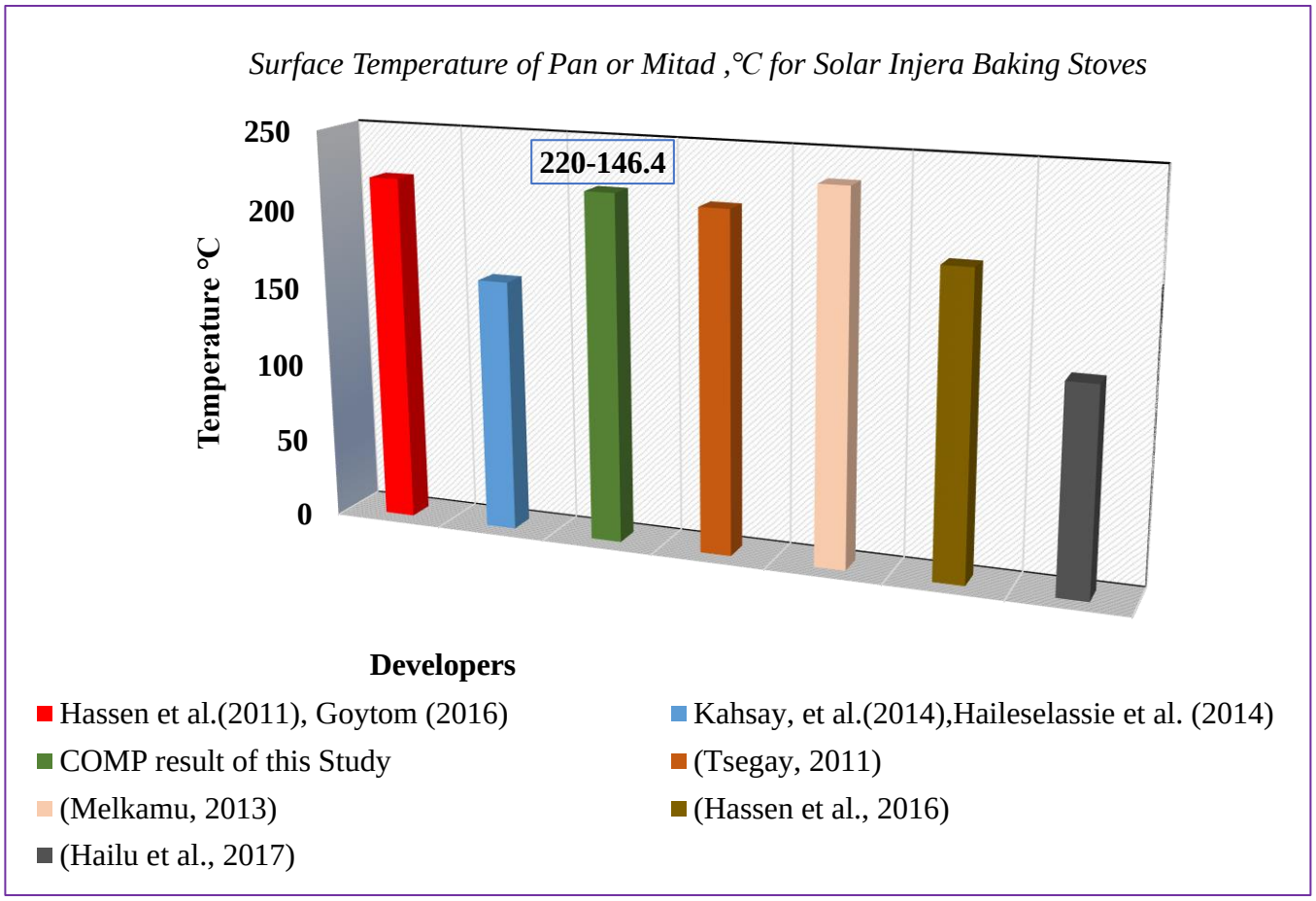

Figure 5-6: The average surface temperature of the baking pan or Mitad of solar Injera baking stoves

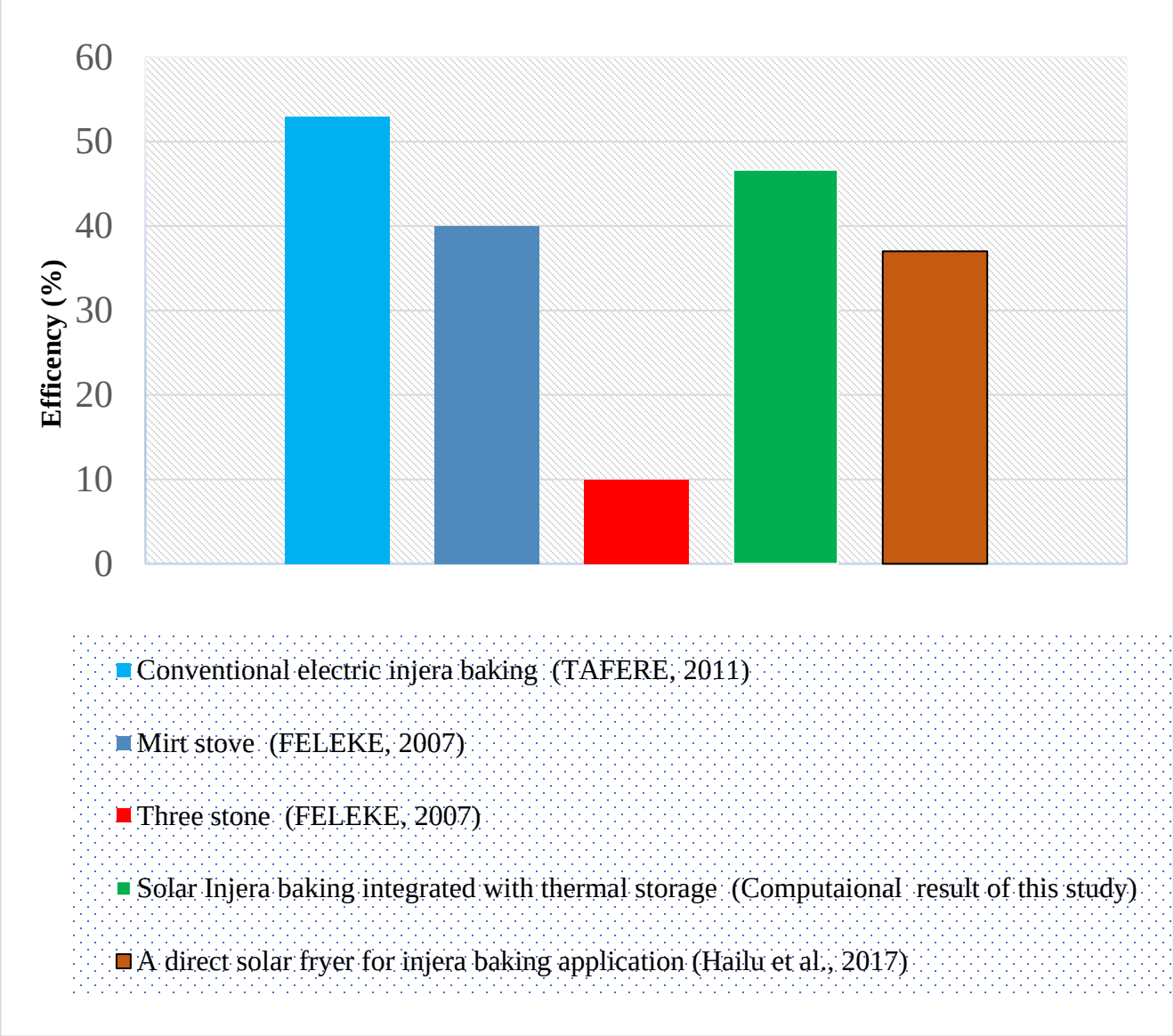

Figure 5-7: Efficiency comparisons

Finally, from the comparisons conducted above the numerically investigated solar-powered Injera baking integrated with thermal storage showed a promising result.

CHAPTER 6: CONCLUSIONS AND RECOMMENDATIONS

6.1. Conclusions

In Ethiopia, the household sector accounted for 90% of total energy consumption in 2014, while 89% of the country's ultimate energy supply comes from biomass sources (SNV, 2018). Injera baking consumes more than half energy accounted for the household. Due to its abundance as a renewable resource, solar energy is seen to be a good alternative for cooking. However, because there is an imbalance among the demand and the energy supplied, a thermal storage system that provides the necessary energy has been integrated.

For PCM and thermia oil, the simulation was performed and the storage effectiveness was examined. The total amount of energy stored in the PCM was 23.78 MJ, also 9.25 MJ was stored in the thermia oil.

The total amount of energy discharged from the PCM was 13.1 MJ and from the thermia oil was 3.50 MJ. Also, the baking pan surface temperature was between 220^{o}c and 146.4^{o}c for about three hours, and once the system is charged, it was not fully discharged for the baking application and it is at some amount of temperature and would need small hours for charging for the next day compared with the first charging hour and we can use the energy from the PV for different household purpose like, water boiling, stoves for cooking, lighting etc.

Finally, it can be concluded that the numerically investigated solar-powered injera baking integrated with thermal storage showed a promising result and to bake 60 injera traditionally about 17875.2g of fuel should consumed and it causes a very large amount of CO and particulate matter emission therefore, this study used a clean source of energy, and it can avoided the above problem regarding the air pollution and the effect of health on females and children.

6.2. Recommendations

This study provides the numerical model and performance evaluation of thermal storage that incorporates with photovoltaics which converts solar radiation to electrical energy, to charge thermal storage for injera baking applications.

PCM and thermia oil thermal storage have been modeled since the thermal oil was used for both heat transfer fluid and thermal storage. After that, the efficiencies were assessed, and it was advised that experimental work be examined in order to validate the efficiency and other outcomes.

It is also recommended that the further study on the PV control system during the fluctuation of the solar radiation, the analysis of simultaneous charging and discharging and cost analysis of the overall system should performed which is very important to know the financial feasibility of the system.

Reference

AAAMSA. (2001). *THERMAL INSULATION Incorporating the Architectural Glass Industry Incorporating the Architectural Glass Industry*. *April*.

Abhat, A. (1983). Low temperature latent heat thermal energy storage: Heat storage materials. *Solar Energy*, *30*(4), 313–332. https://doi.org/10.1016/0038-092X(83)90186-X

Abreha, B. G., Mahanta, P., & Trivedi, G. (2019). Numerical modeling and simulation of thermal energy storage for solar cooking using Comsol multiphysics software. *AIP Conference Proceedings*, *2091*(April). https://doi.org/10.1063/1.5096495

Adem, K. D., & Ambie, D. A. (2017). A review of injera baking technologies in Ethiopia: Challenges and gaps. *Energy for Sustainable Development*, *41*, 69–80. https://doi.org/10.1016/j.esd.2017.08.003

Adem, K. D., Ambie, D. A., Arnavat, M. P., & Henriksen, U. B. (2019). *First injera baking biomass gasifier stove to reduce indoor air pollution , and fuel use*. *7*(April), 227–245. https://doi.org/10.3934/energy.2019.2.227

Ahmed, S. F., Khalid, M., Rashmi, W., Chan, A., & Shahbaz, K. (2017). Recent progress in solar thermal energy storage using nanomaterials. *Renewable and Sustainable Energy Reviews*, *67*, 450–460. https://doi.org/10.1016/j.rser.2016.09.034

Alva, G., Liu, L., Huang, X., & Fang, G. (2017). Thermal energy storage materials and systems for solar energy applications. *Renewable and Sustainable Energy Reviews*, *68*(October 2016), 693–706. https://doi.org/10.1016/j.rser.2016.10.021

Anteneh and Walelign. (2011). *Stove testing results*.

Arkar, C., & Medved, S. (2005). Influence of accuracy of thermal property data of a phase change material on the result of a numerical model of a packed bed latent heat storage with spheres. *Thermochimica Acta*, *438*(1–2), 192–201. https://doi.org/10.1016/j.tca.2005.08.032

Asres, T. S. (2012). *The Current Status of Traditional Biomass Energy Utilization and Its*

Alternative Renewable Energy Technology in the Amhara Region of Ethiopia. 104.

Bade, M. H., & Bandyopadhyay, S. (2015). Energy Modelling of Thermal Oil Based Cooking System. *Energy Procedia*, *75*, 1746–1751. https://doi.org/10.1016/j.egypro.2015.07.448

Bauer, T., Aerospace, G., & Thermodynamics, E. (2020). *Chapter 1 : Fundamentals of high temperature thermal energy storage , transfer and conversion*.

Bauer, T., Steinmann, W.-D., Laing, D., & Tamme, R. (2012). Thermal Energy Storage Materials and Systems. *Annual Review of Heat Transfer*, *15*(15), 131–177. https://doi.org/10.1615/annualrevheattransfer.2012004651

Bhatia, A. (n.d.). *Design and Sizing of Solar Photovoltaic Systems*. *877*.

Bhave, A. G., & Kale, C. K. (2020). Solar Energy Materials and Solar Cells Development of a thermal storage type solar cooker for high temperature cooking using solar salt. *Solar Energy Materials and Solar Cells*, *208*(January), 110394. https://doi.org/10.1016/j.solmat.2020.110394

Biadgelegn, M. (2018). *DESIGN AND EXPERIMENTAL INVESTIGATION OF SOLAR COOKER WITH THERMAL ENERGY STORAGE* (Issue November). Addis Ababa University.

Blaney, J. J., Neti, S., Misiolek, W. Z., & Oztekin, A. (2013). Containment capsule stresses for encapsulated phase change materials. *Applied Thermal Engineering*, *50*(1), 555–561. https://doi.org/10.1016/j.applthermaleng.2012.07.014

Bonsa. (2020). *Investigating the Performance of Parabolic Trough Solar Collector with Thermal Energy Storage System for Injera Baking Applications Investigating the Performance of Parabolic Trough Solar Collector with Thermal Energy Storage System for Injera Baking Appl*.

Chitra, L., Prakash, S., Anand, M., Mathew, J., & Varghese, D. (2019). *Design and Development of Portable Solar Parabolic Cooker with Inorganic PCM Storage*. *2*, 528–531. https://doi.org/10.35940/ijitee.B1192.1292S419

Crespo, A., Barreneche, C., Ibarra, M., & Platzer, W. (2019). Latent thermal energy storage for solar process heat applications at medium-high temperatures – A review. *Solar Energy*, *192*(October 2017), 3–34. https://doi.org/10.1016/j.solener.2018.06.101

Danas EE. (2015). *Project document on Electric Injera Mitad* (Issue May). http://www.ethioenergyauthority.gov.et/attachments/article/62/Final report_ Project document Electric Injera Mitad May 10 2015.pdf

Deshmukh, G., Birwal, P., Datir, R., & Patel, S. (2017). Thermal Insulation Materials: A Tool for Energy Conservation. *Journal of Food Processing & Technology*, *08*(04), 8–11. https://doi.org/10.4172/2157-7110.1000670

Desta, G. A., Melka, Y., Sime, G., Yirga, F., Marie, M., & Haile, M. (2020). Biogas technology in fuelwood saving and carbon emission reduction in southern Ethiopia. *Heliyon*, *6*(10), e04791. https://doi.org/10.1016/j.heliyon.2020.e04791

DOST, I. D. A. S., & Department. (1996). a Perspective on Thermal Energy Storage. *Water*, *20*(November 1994), 547–557.

Dresen, E., DeVries, B., Herold, M., Verchot, L., & Müller, R. (2014). Fuelwood savings and carbon emission reductions by the use of improved cooking stoves in an afromontane forest, Ethiopia. *Land*, *3*(3), 1137–1157. https://doi.org/10.3390/land3031137

Dzhonova-atan, D. B., Georgiev, A. G., & Popov, R. K. (2016). *Numerical study of heat transfer in macro-encapsulated phase change material for thermal energy storage*. *48*, 189–194.

Embiale, A., Chandravanshi, B. S., Zewge, F., & Sahle-Demessie, E. (2021). Indoor air pollution from cook-stoves during Injera baking in Ethiopia, exposure, and health risk assessment. *Archives of Environmental and Occupational Health*, *76*(2), 103–115. https://doi.org/10.1080/19338244.2020.1787317

EnDev/GIZ. (2015). *Energising Development Ethiopia Improved Cook Stoves*. 1–2. https://energypedia.info/images/9/92/EnDev_ET_ICS_Factsheet_Oct_2015_en.pdf

Energy Program 905 Plum Street SE, Bldg 3 Olympia, W. 98504-3165. (2009). *Solar Electric System Design , Operation and Installation*. *October*.

Energy, U. S. D. of. (1992). *HEAT TRANSFER - heat_transfer_revised.pdf*. http://www.polydynamics.com/heat_transfer_revised.pdf

Farid, M. M., Khudhair, A. M., Razack, S. A. K., & Al-Hallaj, S. (2004). A review on phase change energy storage: Materials and applications. *Energy Conversion and Management*, *45*(9–10), 1597–1615. https://doi.org/10.1016/j.enconman.2003.09.015

Fekadu Kedir, M., Bekele, T., & Feleke, S. (2019). Problems of Mirt, and potentials of improved Gonzie and traditional open cook stoves in biomass consumption and end use emission in rural wooden houses of Southern Ethiopia. *Scientific African*, *3*. https://doi.org/10.1016/j.sciaf.2019.e00064

FELEKE, Y. A. (2007). *SSESSING ENVIRONMENTAL BENEFITS OF MIRT STOVE WITH PARTICULAR REFERENCE TO INDOOR AIR POLLUTION (Carbon monoxide & Suspended particulate matter) AND ENERGY CONSERVATION* (Issue June). [Msc Thesis],Addis Ababa Universtiy.

Ferrell, J. K., & Stahel, E. P. (1966). Heat transfer. *Industrial and Engineering Chemistry*, *58*(12), 42–54. https://doi.org/10.1021/ie50684a008

Foong, C. W., Nydal, O. J., & Løvseth, J. (2011). Investigation of a small scale double-reflector solar concentrating system with high temperature heat storage. *Applied Thermal Engineering*, *31*(10), 1807–1815. https://doi.org/10.1016/j.applthermaleng.2011.02.026

Gabisa, E. W., & Aman, A. (2016). *Characterization and Experimental Investigation of NaNO 3 : KNO 3 as Solar Thermal Energy Storage for Potential Cooking Application*. *2016*.

Geiran, M. S. (2021). Experiments with a latent heat storage for frying. *Master's Thesis in Mechanical Engineering, June*.

George A. Lane. (1983). Solar Heat Storage: Latent Heat Materials. In *Boca Raton*.

Getenet, G. (2011). *HEAT TRANSFER ANALYSIS DURING THE PROCESS OF INJERA* (Issue November). Addis Abeba University.

Goytom, D. (2016). *Finite Difference Modelling of Solar Thermal Powered Injera Baking Oven*. *3*(12). https://doi.org/10.17148/IARJSET.2016.31223

Gulilat, A. (2014). *Stove Testing Result A Report on Controlled Cooking Test of Gonzie Stove*.

Haileselassie, A., Bayray, M., & Jørgen, O. (2014). Design and development of solar thermal Injera baking : steam based direct baking. *Energy Procedia*, *57*, 2946–2955. https://doi.org/10.1016/j.egypro.2014.10.330

Haileslasie, A., & Bayray, M. (2019). *Numerical and experimental Analysis of Solar Injera Baking with a PCM Heat Storage Numerical and experimental Analysis of Solar Injera Baking with a PCM Heat Storage*. *January*. https://doi.org/10.4314/mejs.v11i1.1

Hailu, A. D., & Hassen, A. A. (2018). *Experimental Investigation and Loss Quantification in Injera Baking Process*. *1*(1), 1–7.

Hailu, M. H., Nydal, O. J., Kahsay, M. B., & Tesfay, A. H. (2017). A direct solar fryer for injera baking application. *ISES Solar World Congress 2017 - IEA SHC International Conference on Solar Heating and Cooling for Buildings and Industry 2017, Proceedings*, 1475–1485. https://doi.org/10.18086/swc.2017.24.02

Harding, K. G. (2012). Heat Transfer Introduction. *Research Gate*, *December*, 2–6.

Hasnain, S. M. (1998). Review on sustainable thermal energy storage technologies, part I: Heat storage materials and techniques. *Energy Conversion and Management*, *39*(11), 1127–1138.

Hassen, A. A., Amibe, D. A., & Nydal, O. J. (2011). *PERFORMANCE INVESTIGATION OF SOLAR POWERED INJERA BAKING OVEN FOR INDOOR COOKING*.

Hassen, A. A., Kebede, S. B., & Wihib, N. M. (2016). Design and manufacturing of thermal energy based Injera baking glass pan. *Energy Procedia*, *93*(March), 154–159. https://doi.org/10.1016/j.egypro.2016.07.164

Hiwote Teshome, G.-S. E. (2011). *To :*

Höhlein, S., König-Haagen, A., & Brüggemann, D. (2018). Macro-encapsulation of inorganic phase-change materials (PCM) in metal capsules. *Materials*, *11*(9). https://doi.org/10.3390/ma11091752

Incropera, F. P., & DeWitt, D. P. (1996). *Fundamentals of Heat and Mass Transfer* (p. 890). https://doi.org/10.1016/j.applthermaleng.2011.03.022

Janz, G. J., Tomkins, R. P. T., Vol, M. S., Single, A., Component, M., Systems, S., Conductance, E., Janz, G. J., & Tomklns, R. P. T. (1983). *Molten Salts : Volume 5 , Part 2 . Additional Single and Multi - Component Salt Systems . Electrical Conductance , Density , Viscosity and Surface Tension Data Published by the AIP Publishing Articles you may be interested in " Molten Salts : Volume 5 , P. 5*. https://doi.org/10.1063/1.555693

Janz, G. J., Tomkins, R. P. T., Volume, M. S., Single, P. A., Component, M., Systems, S., Conductance, E., Single, A., Component, M., & Conductance, E. (1983). *Molten Salts : Vol . 5 , Part 1 , Additional Single and Multi - Component Salt Systems . Electrical Conductance , Density , Viscosity , and Surface Tension Data Published by the AIP Publishing Articles you may be interested in Molten SCi Its : Volume 5 , . 5*(1980). https://doi.org/10.1063/1.555635

Jardas, D. (2012). *Photovoltaic systems*.

Jones, R., Diehl, J. C., Simons, L., & Verwaal, M. (2017). The development of an energy efficient electric Mitad for baking injeras in Ethiopia. *Proceedings of the 25th Conference on the Domestic Use of Energy, DUE 2017*, 75–82. https://doi.org/10.23919/DUE.2017.7931827

Kajumba, P. K., Okello, D., Nyeinga, K., & Nydal, O. J. (2020). Experimental investigation of a cooking unit integrated with thermal energy storage system. *Journal of Energy Storage*, *32*(August 2019), 101949. https://doi.org/10.1016/j.est.2020.101949

Kant, K., Shukla, A., & Sharma, A. (2017). Advancement in phase change materials for

thermal energy storage applications. *Solar Energy Materials and Solar Cells*, *172*(April), 82–92. https://doi.org/10.1016/j.solmat.2017.07.023

Karafil, A., Ozbay, H., Kesler, M., & Parmaksiz, H. (n.d.). *Calculation of Optimum Fixed Tilt Angle of PV Panels Depending on Solar Angles and Comparison of the Results with Experimental Study Conducted in Summer in Bilecik , Turkey*. 971–976.

Karthikeyan, S., & Velraj, R. (2012). Numerical investigation of packed bed storage unit filled with PCM encapsulated spherical containers - A comparison between various mathematical models. *International Journal of Thermal Sciences*, *60*, 153–160. https://doi.org/10.1016/j.ijthermalsci.2012.05.010

Kaviany, M. (1991). *Conduction Heat Transfer*. 115–151. https://doi.org/10.1007/978-1-4684-0412-8_3

Kebede, D., & Kiflu, A. (2014). Design of Biogas Stove for Injera Baking Application. *International Journal of Novel Research in Engineering and Science*, *1*(1), 6–21.

Kedida, D. K., Amibe, D. A., & Birhane, Y. T. (2019). Performance of a Pebble Bed Thermal Storage Integrated with Concentrating Parabolic Solar Collector for Cooking. *Journal of Renewable Energy*, *2019*, 1–12. https://doi.org/10.1155/2019/4238549

Khamisani, A. A. (n.d.). *Design Methodology of Off-Grid PV Solar Powered System (A Case Study of Solar Powered Bus Shelter) Author : Ayaz A . Khamisani Advisors : Dr . Peter Ping Liu , Dr . Jerry Cloward , Dr . Rendong Bai Table of content*.

Khordehgah, N. (2020). Latent Thermal Energy Storage Technologies and Applications : A Review. *International Journal of Thermofluids*, 100039. https://doi.org/10.1016/j.ijft.2020.100039

Kumar, A., & Shukla, S. K. (2015). A Review on Thermal Energy Storage Unit for Solar Thermal Power Plant Application. *Energy Procedia*, *74*, 462–469. https://doi.org/10.1016/j.egypro.2015.07.728

Lentswe, K., Mawire, A., Owusu, P., & Shobo, A. (2021). A review of parabolic solar

cookers with thermal energy storage. *Heliyon*, *7*(10), e08226. https://doi.org/10.1016/j.heliyon.2021.e08226

Li, M. J., Jin, B., Yan, J. J., Ma, Z., & Li, M. J. (2018). Numerical and Experimental study on the performance of a new two-layered high-temperature packed-bed thermal energy storage system with changed-diameter macro-encapsulation capsule. *Applied Thermal Engineering*, *142*(July), 830–845. https://doi.org/10.1016/j.applthermaleng.2018.07.026

Mawire, A., Phori, A., & Taole, S. (2014). Performance comparison of thermal energy storage oils for solar cookers during charging. *Applied Thermal Engineering*, *73*(1), 1323–1331. https://doi.org/10.1016/j.applthermaleng.2014.08.032

Melkamu. (2013). *Integration of Scheffler Concentrator and Thermal Storage Device for Indoor Injera Baking By Melkamu Yayeh* (Issue April). Addis Abeba University.

Mondal, M. A. H., Bryan, E., Ringler, C., Mekonnen, D., & Rosegrant, M. (2018). Ethiopian energy status and demand scenarios: Prospects to improve energy efficiency and mitigate GHG emissions. *Energy*, *149*(February), 161–172. https://doi.org/10.1016/j.energy.2018.02.067

Nkhonjera, L., Bello-Ochende, T., John, G., & King'ondu, C. K. (2017). A review of thermal energy storage designs, heat storage materials and cooking performance of solar cookers with heat storage. *Renewable and Sustainable Energy Reviews*, *75*(October), 157–167. https://doi.org/10.1016/j.rser.2016.10.059

Peng, Q., Ding, J., Wei, X., Yang, J., & Yang, X. (2010). The preparation and properties of multi-component molten salts. *Applied Energy*, *87*(9), 2812–2817. https://doi.org/10.1016/j.apenergy.2009.06.022

Pereira da Cunha, J., & Eames, P. (2016). Thermal energy storage for low and medium temperature applications using phase change materials - A review. *Applied Energy*, *177*, 227–238. https://doi.org/10.1016/j.apenergy.2016.05.097

Pincemin, S., Olives, R., Py, X., & Christ, M. (2008). *Highly conductive composites made of phase change materials and graphite for thermal storage*. *92*, 603–613.

https://doi.org/10.1016/j.solmat.2007.11.010

Prasad, D. M. R., Senthilkumar, R., & Lakshmanarao, G. (2019). *A critical review on thermal energy storage materials and systems for solar applications*. *7*(July), 507–526. https://doi.org/10.3934/energy.2019.4.507

Prim, E. O. (2013). *Thermal energy storage (TES) using phase change materials (PCM) for cold applications PhD Thesis Thermal energy storage (TES) using phase change materials (PCM) for cold applications Directors of the PhD thesis*.

Projects, D. S., & Solar. (2021). *Solar Website Solar Energy Website-DIY Solar Projects Solar Panel Sizing-How To Calculate Home Solar System Size Sizing Solar Panels-How many solar panels does it take to power your home?*

Q, I. 6743-12 F. (2009). *Shell Thermia Oil B High Performance Heat transfer fluid*. 2–3.

Rai, A. K., & Kumar, A. (2018). *A review on phase change materials and their applications*. *November*.

Rajendra Shivaji Kachare, N. N. S. (2018). *Solar Cooker Thermal Energy Storage System Using Acetamide*. *5*, 71–79.

Reddy, B. S. (2015). Access to modern energy services: An economic and policy framework. *Renewable and Sustainable Energy Reviews*, *47*, 198–212. https://doi.org/10.1016/j.rser.2015.03.058

Regin, A. F., Solanki, S. C., & Saini, J. S. (2008). Heat transfer characteristics of thermal energy storage system using PCM capsules: A review. *Renewable and Sustainable Energy Reviews*, *12*(9), 2438–2458. https://doi.org/10.1016/j.rser.2007.06.009

Riahi, S., Saman, W. Y., Bruno, F., Belusko, M., & Tay, N. H. S. (2018). Performance comparison of latent heat storage systems comprising plate fins with different shell and tube configurations. *Applied Energy*, *212*(December 2017), 1095–1106. https://doi.org/10.1016/j.apenergy.2017.12.109

Saman, W., Bruno, F., & Halawa, E. (2005). Thermal performance of PCM thermal storage

unit for a roof integrated solar heating system. *Solar Energy*, *78*(2), 341–349. https://doi.org/10.1016/j.solener.2004.08.017

Saxena, A., Lath, S., & Tirth, V. (2013). *Solar Cooking by Using PCM as a Thermal Heat Storage*.

Search, H., Journals, C., Contact, A., & Iopscience, M. (n.d.). *Charging and Discharging Processes of Thermal Energy Storage System Using Phase change materials*. *012040*. https://doi.org/10.1088/1757-899X/197/1/012040

Series, L. S. (2016). *Inverter Specifications*. 3–4.

Sharma, A., & Kar, S. K. (2015). Energy Sustainability Through Green Energy. *Green Energy and Technology*. https://doi.org/10.1007/978-81-322-2337-5

Sharma, A., Tyagi, V. V., Chen, C. R., & Buddhi, D. (2009). Review on thermal energy storage with phase change materials and applications. *Renewable and Sustainable Energy Reviews*, *13*(2), 318–345. https://doi.org/10.1016/j.rser.2007.10.005

Shigute, Z., Mebratie, A. D., Alemu, G., & Bedi, A. (2020). Containing the spread of COVID-19 in Ethiopia. *Journal of Global Health*, *10*(1), 1–4. https://doi.org/10.7189/JOGH.10.010369

SNV. (2018). *Review of Policies and Strategies Related to the Clean Cooking Sector in Ethiopia Final Report Strengthening the Enabling Environment for Clean Cooking Project*. *May*.

Solar HI-Tech. (2015). *300w Mono Black 60 cell*.

Su, W., & Darkwa, J. (2015). *Review of solid-liquid phase change materials and their encapsulation technologies*.

Tadesse, M. (2020). The Developmental Patterns of Injera Baking Stoves: Review on the Efficiency, and Energy Consumption in Ethiopia. *International Journal of Mechanical Engineering*, *7*(1), 7–16. https://doi.org/10.14445/23488360/ijme-v7i1p102

TAFERE, A. T. (2011). *EXPERIMENTAL INVESTIGATION ON PERFORMANCE*

CHARACTERISTICS AND EFFICIENCY OF ELECTRIC INJERA BAKING PANS („MITAD"). Addis Abeba University.

Tao, Y. B., Liu, Y. K., & He, Y. (2017). International Journal of Heat and Mass Transfer Effects of PCM arrangement and natural convection on charging and discharging performance of shell-and-tube LHS unit. *International Journal of Heat and Mass Transfer*, *115*, 99–107. https://doi.org/10.1016/j.ijheatmasstransfer.2017.07.098

Tareke, A. A. (2014). *HEAT TRANSFER ANALYSIS OF INJERA BAKING PAN BY FINITE ELEMENT METHOD*. *May*.

Tesfay, Asfafaw H, Kahsay, M. B., & Nydal, O. J. (2018). *Steam-based Charging-Discharging of a PCM Heat Storage*. *10*(1), 15–27.

Tesfay, Asfafaw Haileselassie, Kahsay, M. B., & Nydal, O. J. (2014). Solar powered heat storage for Injera baking in Ethiopia. *Energy Procedia*, *57*, 1603–1612. https://doi.org/10.1016/j.egypro.2014.10.152

Tesfay, Asfafaw Haileselassie, Nydal, O. J., & Kahsay, M. B. (2014). Energy Storage Integrated Solar Stove A case of solar Injera baking in Ethiopia. *IEEE Global Humanitarian Technology Conference (GHTC 2014)*, 659–666. https://doi.org/10.1109/GHTC.2014.6970353

the R Core Team. (2015). Changes in R. *R Journal*, *7*(2), 293–297.

Thirugnanam, C., Karthikeyan, S., & Kalaimurugan, K. (2020). Materials Today : Proceedings Study of phase change materials and its application in solar cooker. *Materials Today: Proceedings*, *xxxx*. https://doi.org/10.1016/j.matpr.2020.02.780

Tiruye, G. A., Besha, A. T., Mekonnen, Y. S., Benti, N. E., Gebreslase, G. A., & Tufa, R. A. (2021). Opportunities and challenges of renewable energy production in ethiopia. *Sustainability (Switzerland)*, *13*(18), 1–25. https://doi.org/10.3390/su131810381

Tsegay, M. M. (2011). *DESIGN AND MANUFACTURE OF LABORATORY MODEL FOR SOLAR POWERED INJERA BAKING OVEN*. Addis Abeba university.

Tsegay, M. M., & Ababa, A. (2011). *Design and Manufacture of Laboratory Model for Solar powered Injera baking Oven*. 1–87.

Tsige, G. A. (2015). *PERFORMANCE ANALYSIS AND RELIABLITY TESTING OF A CERAMIC BAKE WARE FOR AN ELECTRIC INJERA BAKING STOVE: Vol. II* (Issue April). Addis Abeba University.

Tumilowicz, E., Chan, C. L., Li, P., & Xu, B. (2014). An enthalpy formulation for thermocline with encapsulated PCM thermal storage and benchmark solution using the method of characteristics. *International Journal of Heat and Mass Transfer*, *79*, 362–377. https://doi.org/10.1016/j.ijheatmasstransfer.2014.08.017

Voller, V. R. (1990). Numerical Heat Transfer , Part B : Fundamentals : An International Journal of Computation and Methodology FAST IMPLICIT FINITE-DIFFERENCE METHOD FOR THE ANALYSIS OF PHASE CHANGE PROBLEMS. *Numerical Heat Transfer*, *17*(September 2012), 155–169.

Vollmer, M., & Möllmann, K.-P. (2010). Some Basic Concepts of Heat Transfer. In *Infrared Thermal Imaging*. https://doi.org/10.1002/9783527630868.ch4

Wei, G., Wang, G., Xu, C., Ju, X., Xing, L., Du, X., & Yang, Y. (2018). Selection principles and thermophysical properties of high temperature phase change materials for thermal energy storage: A review. *Renewable and Sustainable Energy Reviews*, *81*(May), 1771–1786. https://doi.org/10.1016/j.rser.2017.05.271

Wollele, M. B., & Hassen, A. A. (2019). *Design and experimental investigation of solar cooker with thermal energy storage*. *7*(August), 957–970. https://doi.org/10.3934/energy.2019.6.957

Workeneh Gashie. (2005). Faculty of Science Environmental Science Program Factors Controlling Households Energy Use : Implication for the Conservation of the Environment. In *[Msc Thesis] Addis Abeba Universtiy* (Issue June). Addis Abeba Universtiy.

Wu, S., Fang, G., & Liu, X. (2011). Dynamic discharging characteristics simulation on solar

heat storage system with spherical capsules using paraffin as heat storage material. *Renewable Energy*, *36*(4), 1190–1195. https://doi.org/10.1016/j.renene.2010.10.012

Xie, W., Ding, J., Wei, X., Wang, W., Xia, G., & Xing, J. (2019). Corrosion resistance of stainless steel and pure metal in ternary molten nitrate for thermal energy storage. *Energy Procedia*, *158*, 4897–4902. https://doi.org/10.1016/j.egypro.2019.01.703

Ying-Zhang, X., Hui-Wang, G., Dan-Liu, & Ying-Wang. (2013). Section 2 Insulation Materials and Properties Mp-0 Section 2: Insulation Materials and Properties. *Advanced Materials Research*, *608–609*, 1783–1785.

Zhang, H. L., Baeyens, J., Degrève, J., Cáceres, G., Segal, R., & Pitié, F. (2014). Latent heat storage with tubular-encapsulated phase change materials (PCMs). *Energy*, *76*, 66–72. https://doi.org/10.1016/j.energy.2014.03.067

Zhao, W., Elmozughi, A. F., Oztekin, A., & Neti, S. (2013). Heat transfer analysis of encapsulated phase change material for thermal energy storage. *International Journal of Heat and Mass Transfer*, *63*, 323–335. https://doi.org/10.1016/j.ijheatmasstransfer.2013.03.061

Zheng, Y., Zhao, W., Sabol, J. C., Tuzla, K., Neti, S., Oztekin, A., & Chen, J. C. (2013). Encapsulated phase change materials for energy storage - Characterization by calorimetry. *Solar Energy*, *87*(1), 117–126. https://doi.org/10.1016/j.solener.2012.10.003

Zhong, J. Q., Fragoso, A. T., Wells, A. J., & Wettlaufer, J. S. (2012). Finite-sample-size effects on convection in mushy layers. In *Journal of Fluid Mechanics* (Vol. 704). https://doi.org/10.1017/jfm.2012.219

Zhou, D., Zhao, C. Y., & Tian, Y. (2012). Review on thermal energy storage with phase change materials (PCMs) in building applications. *Applied Energy*, *92*, 593–605. https://doi.org/10.1016/j.apenergy.2011.08.025

Appendix

Table A: Monocrystalline cell for the system design with the following specification from Hi-Tech 8

Specification	
Cell Type	Grade A Mono-crystalline
Number of cells	60
Maximum Power at STC (PMAX)	300Wp
Maximum Power Voltage (Vmp)	32.53V
Maximum Power Current (Imp)	9.21A
Open-circuit Voltage (Voc)	40.10V
Short-circuit Current (Isc)	9.60A
Cell Efficiency	21+%
Module Efficiency	18.4%
Operating Temperature (c)	-40C~+85c
Power tolerance Temperature	-1%/+3%
Temperature coefficients of Pmax	-0.43%/-
Temperature coefficients of Voc	0.3%
Temperature coefficients of Isc	0.040%
Nominal Operating cell temperature (NOCT)	45+2

Table B: Typical design data for shell thermia oil B heat transfer oil (Q, 2009)

Properties	Shell Thermia oil B heat transfer oil								
$Temp$ [℃]	0	20	40	100	150	200	250	300	340
$Density$ [kg/l]	0.876	0.863	0.850	0.811	0.778	0.746	0.713	0.681	0.655
$Specfic\ heat\ capacity, c$ [kJ/kg. k]	1.809	1.882	1.954	2.173	2.355	2.538	2.72	2.902	3.048

Thermal conducativity, k [w/m.k]	0.136	0.134	0.133	0.128	0.125	0.121	0.118	0.114	0.111
Prandtl no	3375	919	375	69	32	20	14	11	9
Coefficient of thermal expansion, β[1/℃]	0.0008								

Table C: Inverter Specifications

Model	LS-624	LS-1224	LS-1824	LS-2324	LS-3024	LS-4024
Continuous power	600W	1200W	1800W	2300W	3000W	4000W
Surge rating (5 sec)	1800W	3600W	5400W	6900W	9000W	12000W
½ hour rating	750W	1600W	2200W	2800W	3700W	4500W
DC voltage range	21-34V	21-34V	21-34V	21-34V	21-34V	21-34V
Standby current	22mA	28mA	30mA	45mA	50mA	60mA
Peak efficiency	92%	92%	94%	94%	93%	94%
Weight	5.5kg	11kg	14kg	22kg	24kg	30kg
Dimension (cm)	26*16*10	33*30*15	33*30*15	37*39*18	37*39*18	47*46*19

Part Drawing of the System

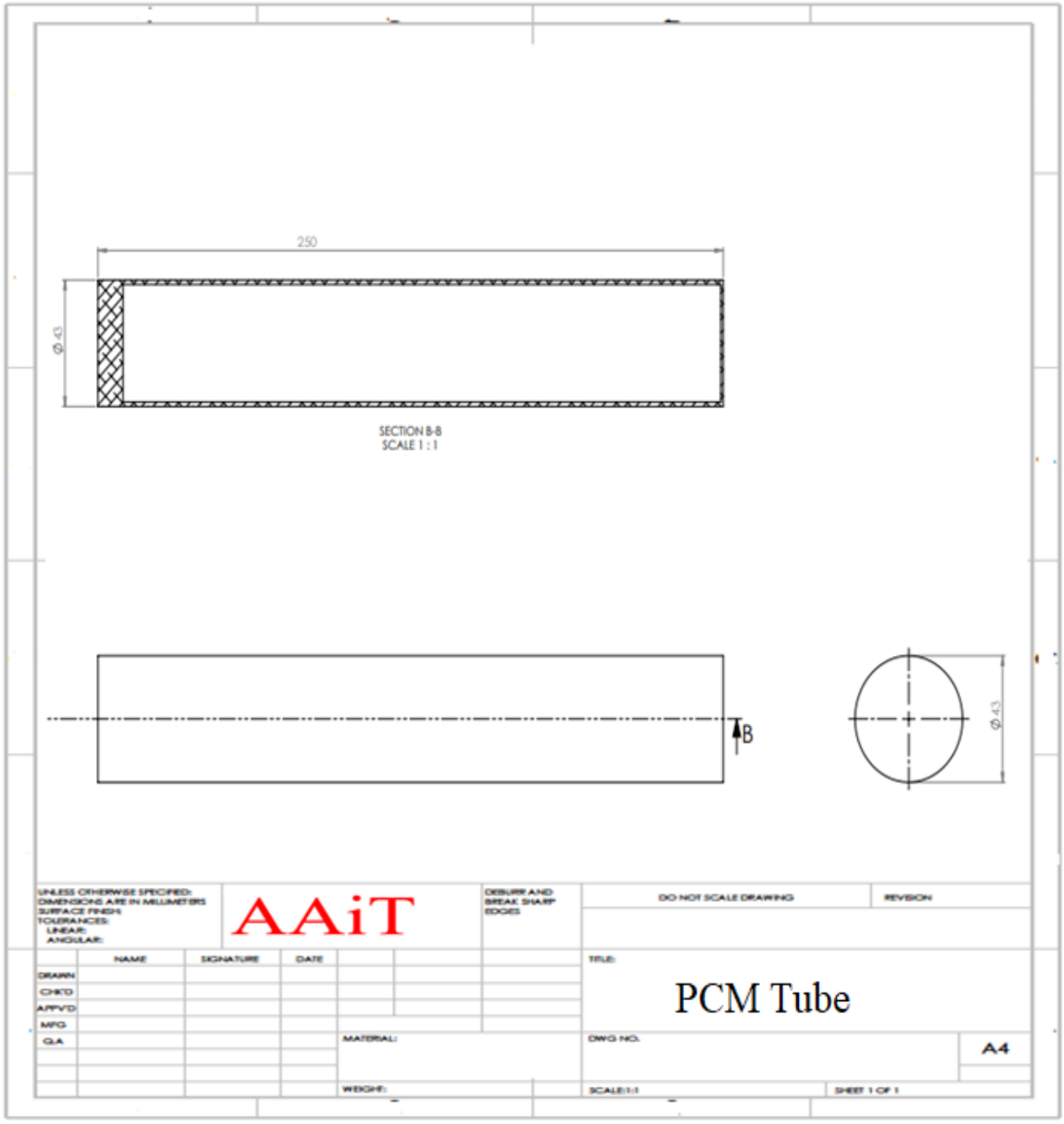

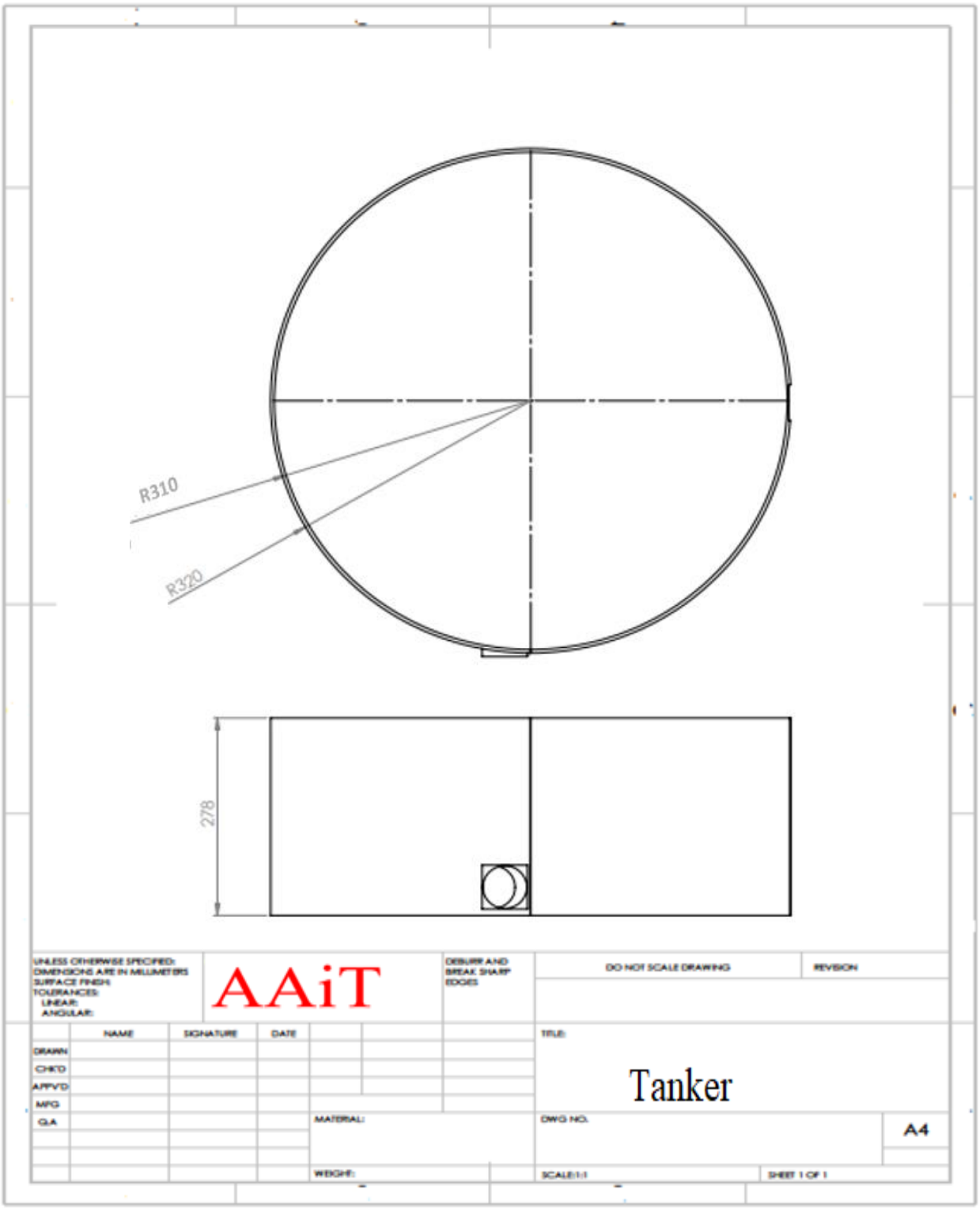
R310
R320
278
UNLESS OTHERWISE SPECIFIED:
DIMENSIONS ARE IN MILLIMETERS
SURFACE FINISH:
TOLERANCES:
LINEAR:
ANGULAR:
AAiT
DEBURR AND BREAK SHARP EDGES
DO NOT SCALE DRAWING
REVISION
NAME
SIGNATURE
DATE
DRAWN
CHK'D
APPV'D
MFG
Q.A
MATERIAL:
WEIGHT:
TITLE:
Tanker
DWG NO.
A4
SCALE:1:1
SHEET 1 OF 1

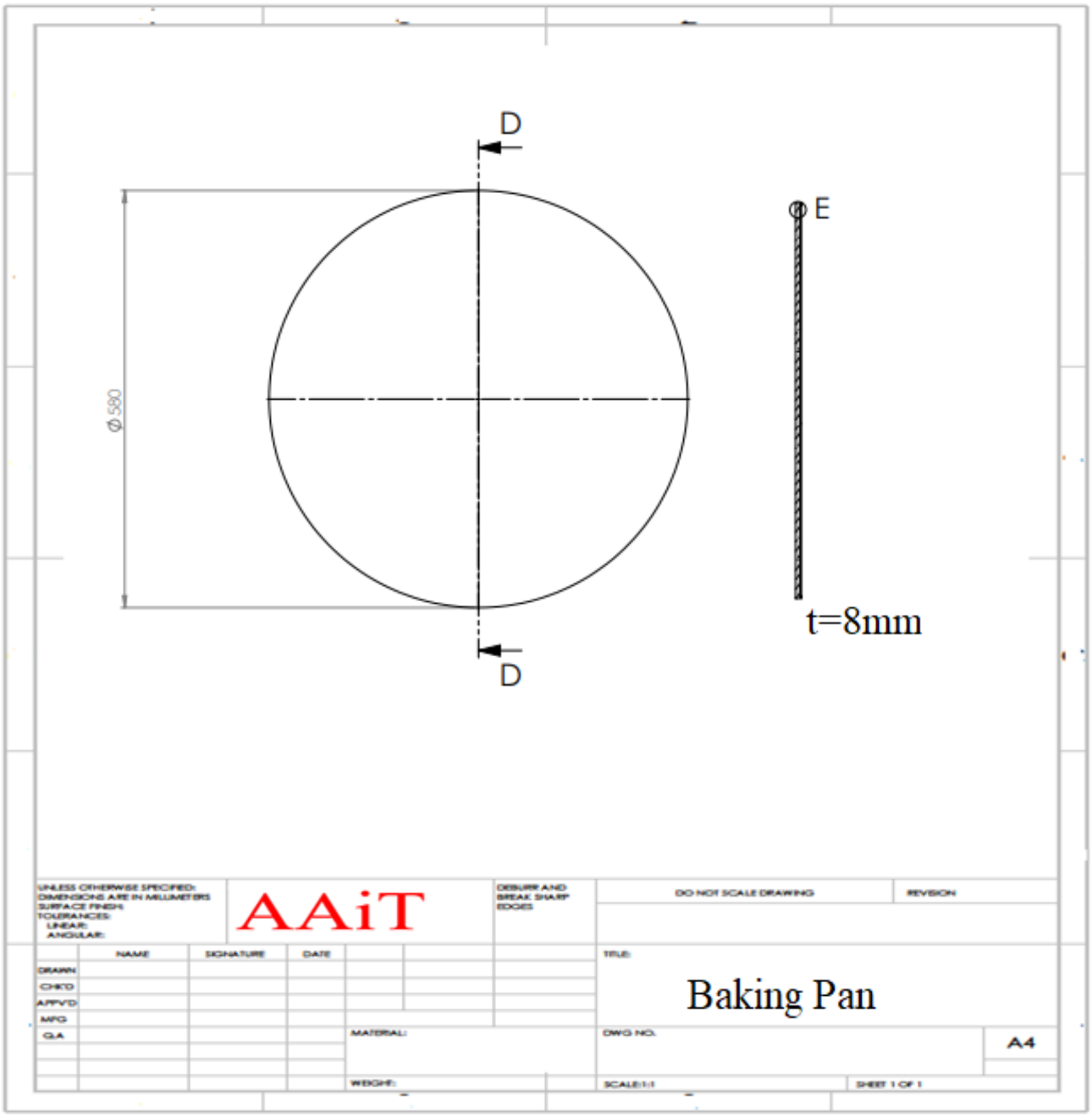
D
E
Ø 580
t=8mm
D
AAiT
Baking Pan
A4

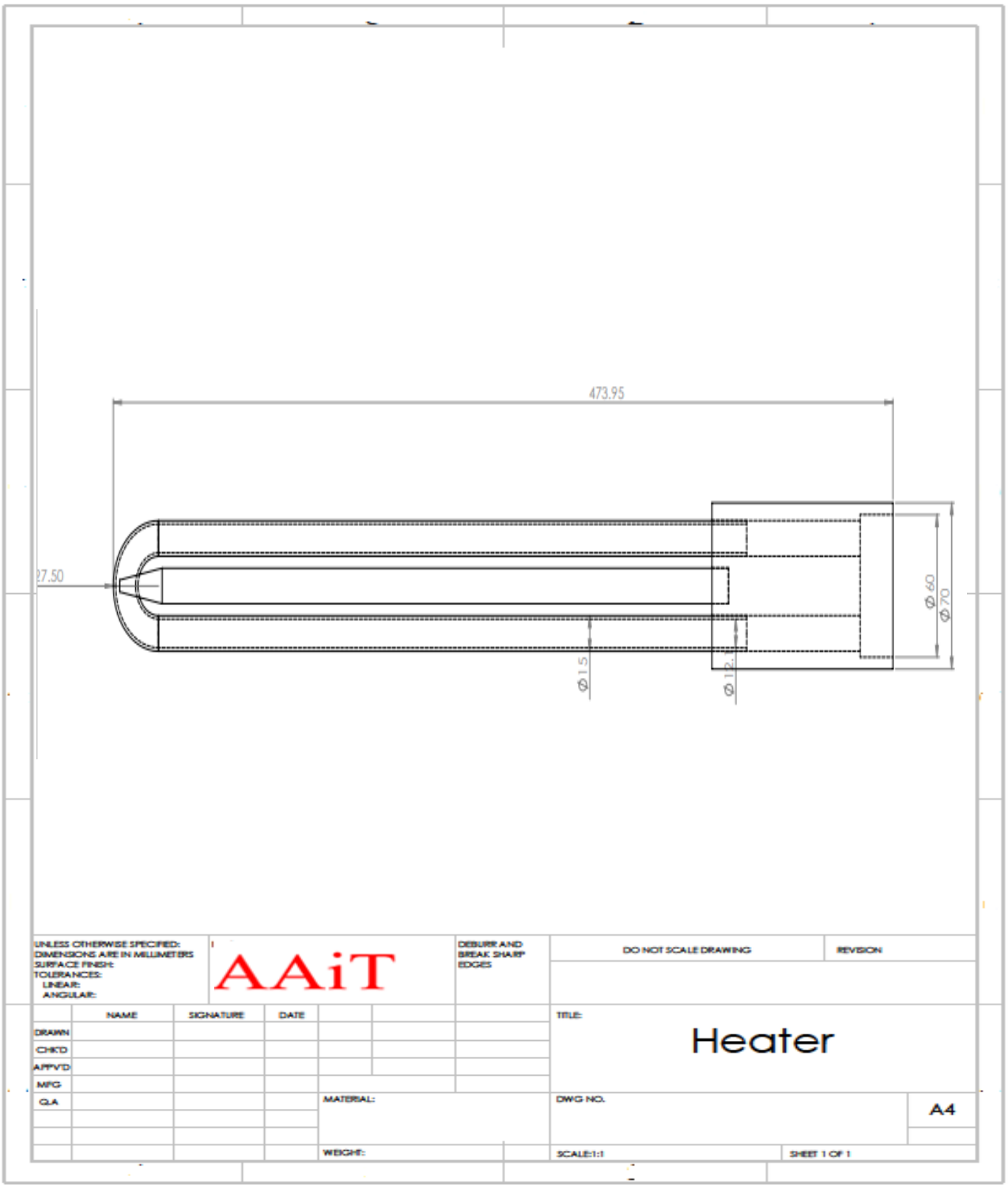
473.95
27.50
Ø60
Ø70
Ø15
Ø12
UNLESS OTHERWISE SPECIFIED:
DIMENSIONS ARE IN MILLIMETERS
SURFACE FINISH:
TOLERANCES:
LINEAR:
ANGULAR:
AAiT
DEBURR AND BREAK SHARP EDGES
DO NOT SCALE DRAWING
REVISION
NAME
SIGNATURE
DATE
DRAWN
CHK'D
APPV'D
MFG
Q.A
TITLE:
Heater
MATERIAL:
DWG NO.
A4
WEIGHT:
SCALE:1:1
SHEET 1 OF 1

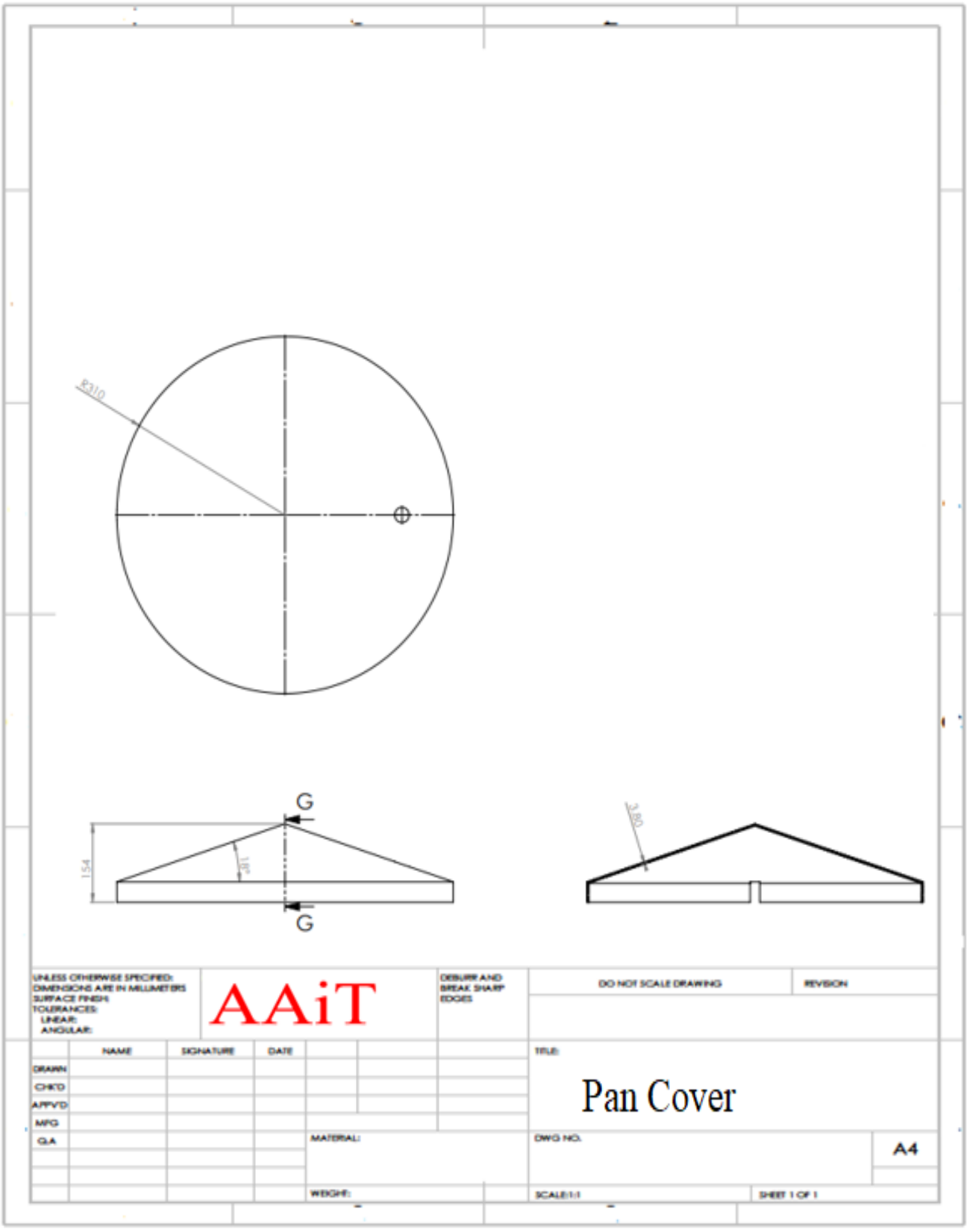
R310
G
154
185
G
380
UNLESS OTHERWISE SPECIFIED:
DIMENSIONS ARE IN MILLIMETERS
SURFACE FINISH:
TOLERANCES:
LINEAR:
ANGULAR:
AAiT
DEBURR AND BREAK SHARP EDGES
DO NOT SCALE DRAWING
REVISION
NAME
SIGNATURE
DATE
DRAWN
CHK'D
APPV'D
MFG
Q.A
MATERIAL:
WEIGHT:
TITLE:
Pan Cover
DWG NO.
A4
SCALE:1:1
SHEET 1 OF 1

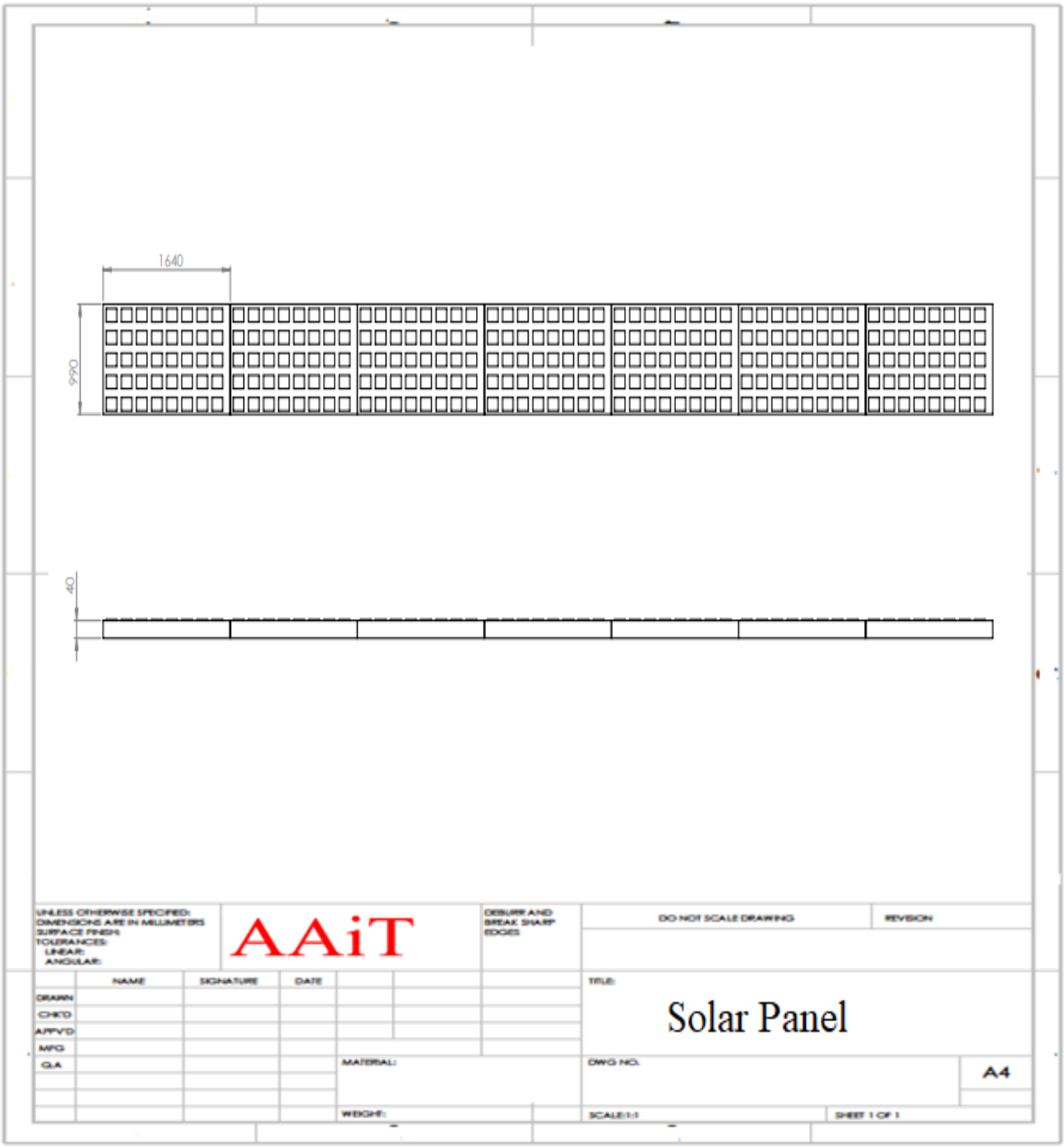
1640
990
40
AAiT
Solar Panel
A4

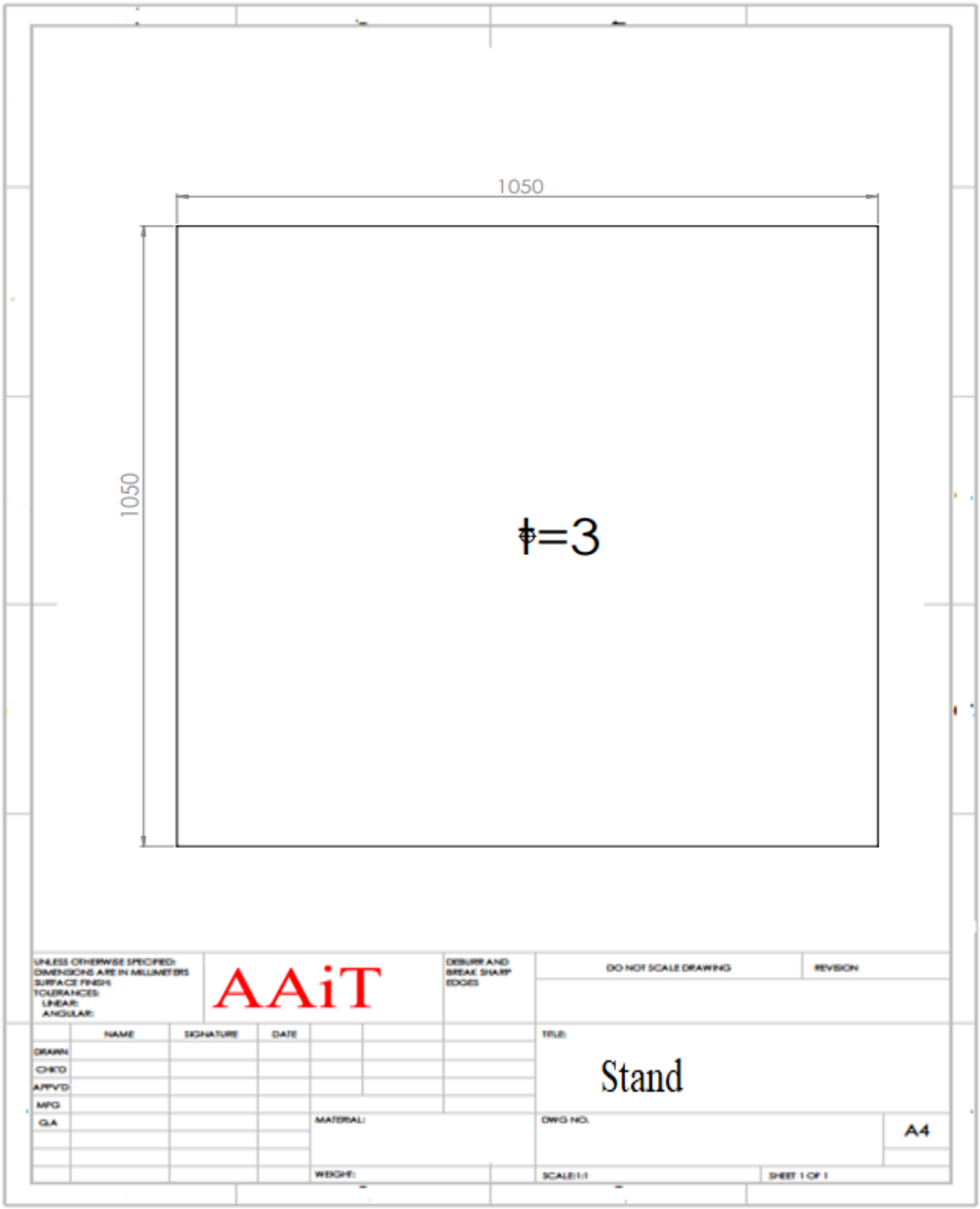
1050
1050
t=3
UNLESS OTHERWISE SPECIFIED:
DIMENSIONS ARE IN MILLIMETERS
SURFACE FINISH:
TOLERANCES:
LINEAR:
ANGULAR:
AAiT
DEBURR AND BREAK SHARP EDGES
DO NOT SCALE DRAWING
REVISION
NAME
SIGNATURE
DATE
DRAWN
CHK'D
APPV'D
MFG
QA
MATERIAL:
WEIGHT:
TITLE:
Stand
DWG NO.
A4
SCALE:1:1
SHEET 1 OF 1

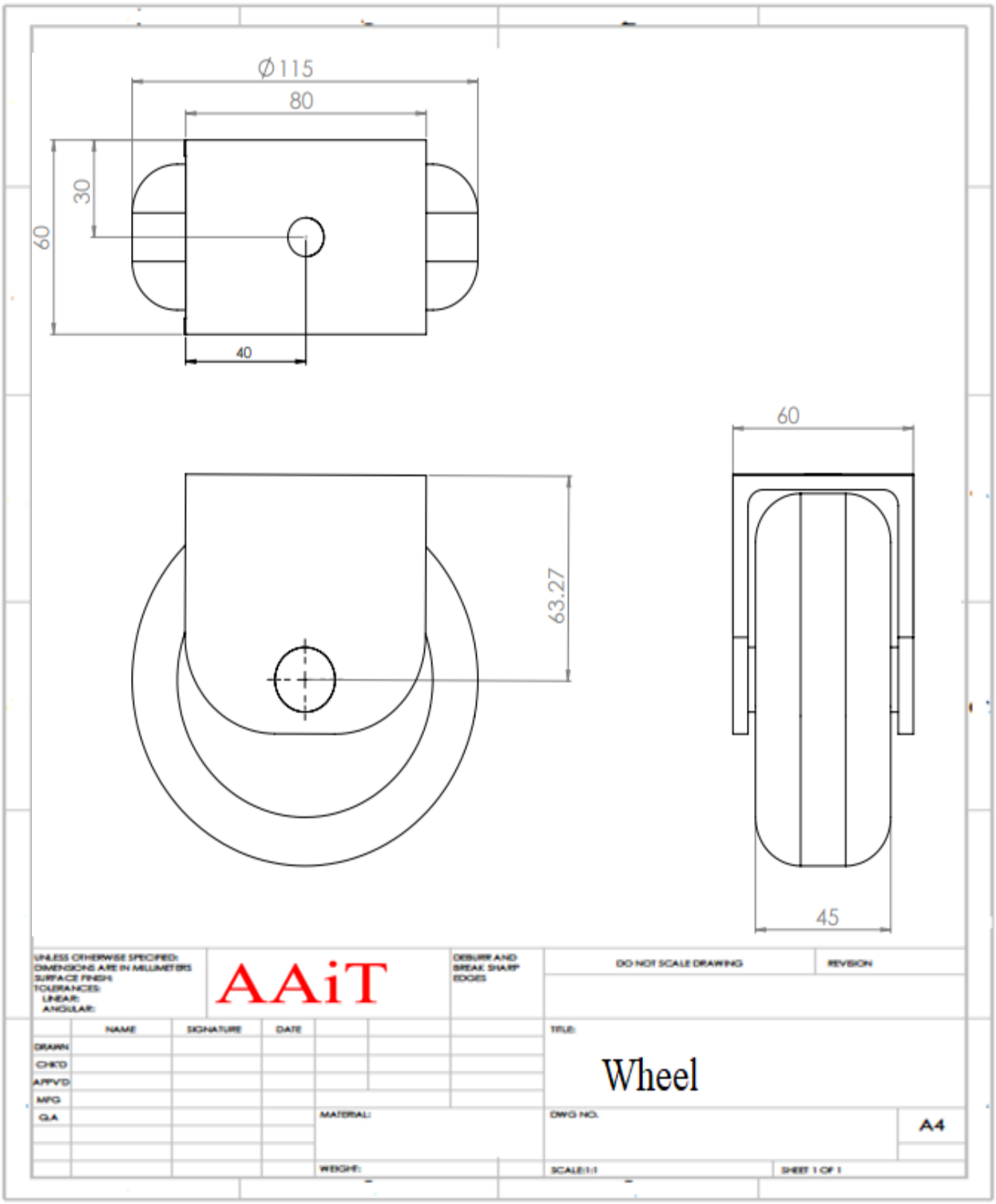
Ø115
80
30
60
40
63.27
60
45
AAiT
Wheel
A4

MATLAB CODE

```
% ANALYSIS OF CHARGING FOR PCM AND OIL STORAGE SYSTEM
% % % % % % % % % % % % % % % % % % % % % % % % % % % % % % % % % % %
% Parameters and values of the storage tank
clear
clc
dp=0.043;              %Diameter of PCM cylinder (capsules) in 'm'
Di=0.62;               %Inner diameter of the storage tank in 'm'
Do=0.64;               %Inner diameter of the storage tank in 'm'
r1=0.31;               %Inside radius of the cylinder (m)
r2=0.32;               %Outside radius of the cylinder (m)
r3=0.395;              %Outside radius of the cylinder + insulation layer
H=0.25;                %Storage height
It=0.075;              %Insulation thichkness in 'm'
Ht=0.26;               %Height of tank
Lh=1.54;               %length of heater 'm'
Dh=0.015;              %Diamter of heater 'm'
Ah=pi*Dh*Lh;           %Area of heater 'm'
L=0.25;                %Characterstic length (length of the storage) 'm'
Aw=(Ht*It);            %Area of wall (m^2)
g=9.81;                %Gravitational acceleration m/s^2
n=115;                 %Number of PCM cylnders
P=2100;                %Power input to the storage 'W'
qo=P/Ah;               %The inward heat flux in Watt per unit area normal to the boundary
Tinf=23;               %Average atmospheric temperature of Addis Ababa in dgree celcuis
V_st=(V_o+V_p);        %Volume of the storage in 'm^3
V_stt=pi*(r1^2)*Ht;                  %Volume of the total storage cylinder in 'm^3
```

```
V_INSU=(pi*It*L*(2*r2+It));            %Volume of the insulation in 'm^3
eps=(V_o/V_stt);                        %Porosity
Asp=((pi*dp^2)/4+2*(pi*dp/2)*H);       %Surface area of the PCM cylinder 'm^2
As=((2*pi*Do^2)/4+2*(pi*Do/2)*Ht);    %Surface area of the storage cylinder 'm^2)
% % % % % % % % % % % % % % % % % % % % % % % % % % % % % % % % % % % % % %
%properties of thermia oil at its film temperature
rho_o=750.64;                  %Density of oil in kg/m^3
Cp_o=2397;                     %Cp of oil in J/kg.k
K_o=0.124;                     %Thermal conductivity of oil in w/(m.k)
m=0.000002788;                 %Kenematic viscosity of oil m^2/s
Pr=29.24;                      %Prandetl number of oil
Bo=0.0008;                     %Coefficient  of thermal expansion
deltrho_o=15;                  %Change density of oil in kg/m^3
 % % % % % % % % % % % % % % % % % % % % % % % % % % % % % % % % % % % % %
%properties of the PCM
k_pcm=0.8;           %Thermal coductivity of PCM in W/(m.k)
rho_pcm=1800;        %Density of solid PCM in kg/m^3
rho_pcml=1700;       %Density of liquid PCM in kg/m^3
h_Lpcm=108670;       %Latent heat of fusion in J/kg
C_ppcm=1250;         %Specific heat capacity of PCM of solid state in J/kgk
C_ppcml=1600;        %Specific heat capacity of PCM of liquid state in J/kgk
Tm=220;              %Melting temperature of PCM
mupcm=0.0063;        %Kinematic viscosity of PCM in kg/ms%
B=0.0015;            %Thermal expansion of PCM in 1/k
% % % % % % % % % % % % % % % % % % % % % % % % % % % % % % % % % % % % % %
%correlation parameters
G=((g*Bo*L^3*detT)/(m^2));             %Grashof number
```

```
Ra=G*Pr;                              %Rayleigh number
Nuu1=(0.057*Ra^(1/3));                %Nusselet number
ho=(Nuu1*K_o)/(L);                    %The heat transfer coefficient for thermal storage
hv=(ho*n*Asp)/(V_stt);                %The volumetric heat transfer for thermal storage
% % % % % % % % % % % % % % % % % % % % % % % % % % % % % % % % % % %
T=4.7*3600;          %Final time given in seconds
dt=15;               %Time step in second
dx=0.025;            %Space step in meter
i_l=H/dx;            %Number of space element/sections/
i_lmax=i_l+1;        %Max number of space nodes
n_t=T/dt;            %Number of time step
n_tmax=n_t+1;        %Maximum number of time nodes
% % % % % % % % % % % % % % % % % % % % % % % % % % % % % % % % % % %
%loss analysis for the system
%properties of air at its film temperature betweeen oil and air
ma=0.000026;            %Kenematic viscosity of air m^2/s
rhoa=0.882475;          %Density of air in kg/m^3
Cpa=1011.7;             %Cp of air in J/kg.k
Ka=0.0328365;           %Thermal conductivity of air in w/(m.k)
dy=0.0000229235;        %Dynamic viscosity of air
Ba=0.0025;              %Thermal expansion of air in 1/k
Pra=0.70618;            %Prandetl number of air
Kss=15;                 %Thermal conductivity of stainless steel in W/m.k
Kins=0.0372;              %Thermal conductivity of fiberglass in W/m.k
% % % % % % % % % % % % % % % % % % % % % % % % % % % % % % % % % % %
detT=Ts-Tinf;
Ga=((g*Ba*L^3*detT)/(ma^2));          %Grashof number
```

```
Raa=Ga*Pra;                                %Rayleigh number
Nua=0.1*Raa^(1/3);                         %Nusselt number
hca=(Nua*Ka)/(L);                          %The heat transfer coefficient for air and storage
dd=5.67*10^(-8);                           %Stefan boltzman constant in w/(m^2K^4)
eglass=0.89;                               %Emmisivity of fiberglass
hra=dd*eglass*(Ts^2+Tinf^2)*(Ts-Tinf);     %Heat loss due to radiation in W/m^2k
hos=hca+hra;
 U=1/((1/ho)+(It/Kins)+(1/hos));       % Overall heat loss coefficient  through the wall
 Uw=U*Aw/V_INSU;                       % The volumetric heat loss coefficient  through the wall
%%%%%%%%%%%%%%%%%%%%%%%%%%%%%%%%%%%
RP=k_pcm*dt/((1-eps)*rho_pcm*C_ppcm*dx^2);
RPl=k_pcm*dt/((1-eps)*rho_pcml*C_ppcml*dx^2);
FP=hv*dt/((1-eps)*rho_pcm*C_ppcm);
FPl=hv*dt/((1-eps)*rho_pcml*C_ppcml);
R=hv*dt/(eps*rho_o*Cp_o);
F=(Uw*dt)/(eps*Cp_o*rho_o);
k=hv*dt/((1-eps)*rho_pcml*C_ppcml);
%%%%%%%%%%%%%%%%%%%%%%%%%%%%%%%%%%%
 % initial and boundary conditions
for i=1:i_lmax+1
   Tpcm(i,1)=23;
   To(i,1)=23;
   end
%%%%%%%%%%%%%%%%%%%%%%%%%%%%%%%%%%%
for n=2:n_t
   for i=2:i_lmax
       Tpcm(1,n)=Tpcm(2,n);
```

```
        To(2,n+1)=(qo/hv)+Tpcm(2,n+1);
        To(i+1,n)=To(i,n)+R*(Tpcm(i,n)-To(i,n))+F*(Tinf-To(i,n));
        Tpcm(i,n+1)=Tpcm(i,n)*(1-FP-2*RP)+FP*(To(i,n))+RP*(Tpcm(i+1,n)+Tpcm(i-1,n));
        To(1,n)=To(2,n);
          if Tpcm(i,n)>=220
           Tpcm(i,n)=220;
          end
       if Tpcm(i,n)<Tinf
           Tpcm(i,n)=Tinf;
       end
        if To(i,n)<Tinf
           To(i,n)=Tinf;
        end
       Tpcm(i_lmax+1,n)=Tpcm(i_lmax,n);
        To(i_lmax+1,n)=To(i_lmax,n);
    end
end
% % % % % % % % % % % % % % % % % % % % % % % % % % % % % % % % % %
%Molten fraction analysis
V=(1-eps)*(1-eps);
for n=nx1:n_tmax
    i=1;
    hold on
     X(i,n+1)=X(i,n)+dt*hv*(To(i,n)-Tpcm(i,n))/(rho_pcm*h_Lpcm*V);
    if X(i,n)>=1
        X(i,n)=1;
    end
```

```
end
hold on
for n=nx2:n_tmax
   i=2;
   hold on
     X(i,n+1)=X(i,n)+dt*hv*(To(i,n)-Tpcm(i,n))/(rho_pcm*h_Lpcm*V);
   if X(i,n)>=1
      X(i,n)=1;
   end
end
hold on
for n=nx3:n_t
   i=3;
   hold on
    X(i,n+1)=X(i,n)+dt*hv*(To(i,n)-Tpcm(i,n))/(rho_pcm*h_Lpcm*V);
   if X(i,n)>=1
      X(i,n)=1;
   end
end
hold on
for n=nx4:n_t
   i=4;
   hold on
     X(i,n+1)=X(i,n)+dt*hv*(To(i,n)-Tpcm(i,n))/(rho_pcm*h_Lpcm*V);
   if X(i,n)>=1
      X(i,n)=1;
   end
```

```
end
hold on
for n=nx5:n_t
    i=5;
   hold on
   X(i,n+1)=X(i,n)+dt*hv*(To(i,n)-Tpcm(i,n))/(rho_pcm*h_Lpcm*V);
   if X(i,n)>=1
      X(i,n)=1;
   end
end
hold on
for n=nx6:n_t
    i=6;
   hold on
    X(i,n+1)=X(i,n)+dt*hv*(To(i,n)-Tpcm(i,n))/(rho_pcm*h_Lpcm*V);
   if X(i,n)>=1
      X(i,n)=1;
   end
end
hold on
for n=nx7:n_t
   i=7;
   hold on
    X(i,n+1)=X(i,n)+dt*hv*(To(i,n)-Tpcm(i,n))/(rho_pcm*h_Lpcm*V);
   if X(i,n)>=1
      X(i,n)=1;
   end
```

```
end
hold on
for n=nx8:n_t
   i=8;
   hold on
    X(i,n+1)=X(i,n)+dt*hv*(To(i,n)-Tpcm(i,n))/(rho_pcm*h_Lpcm*V);
   if X(i,n)>=1
      X(i,n)=1;
   end
end
hold on
for n=nx9:n_t
   i=9;
   hold on
    X(i,n+1)=X(i,n)+dt*hv*(To(i,n)-Tpcm(i,n))/(rho_pcm*h_Lpcm*V);
   if X(i,n)>=1
      X(i,n)=1;
   end
end
hold on
for n=nx10:n_t
   i=10;
   hold on
    X(i,n+1)=X(i,n)+dt*hv*(To(i,n)-Tpcm(i,n))/(rho_pcm*h_Lpcm*V);
   if X(i,n)>=1
      X(i,n)=1;
   end
```

```
end
hold on
for n=nx11:n_t
    i=11;
    hold on
     X(i,n+1)=X(i,n)+dt*hv*(To(i,n)-Tpcm(i,n))/(rho_pcm*h_Lpcm*V);
    if X(i,n)>=1
        X(i,n)=1;
    end
end
%%%%%%%%%%%%%%%%%%%%%%%%%%%%%%%%%%%
% PCM liquid region
for n=nl1:n_tmax
     i=1;
    hold on
    Tpcml(i,n+1)=Tpcml(i,n)+k*(To(i,n)-Tpcml(i,n));
end
for n=nl2:n_tmax
    i=2;
     Tpcml(2,n)=Tpcml(1,n);
     To(2,n)=To(1,n);
      hold on
  Tpcml(i,n+1)=Tpcml(i,n)+k*(To(i,n)-Tpcml(i,n));
end
for n=nl3:n_tmax
     i=3;
    hold on
```

```
 Tpcml(i,n+1)=Tpcml(i,n)+k*(To(i,n)-Tpcml(i,n));
end
for n=nl4:n_tmax
    i=4;
    hold on
 Tpcml(i,n+1)=Tpcml(i,n)+k*(To(i,n)-Tpcml(i,n));
end
for n=nl5:n_tmax
     i=5;
    hold on
 Tpcml(i,n+1)=Tpcml(i,n)+k*(To(i,n)-Tpcml(i,n));
end
for n=nl6:n_tmax
    i=6;
    hold on
  Tpcml(i,n+1)=Tpcml(i,n)+k*(To(i,n)-Tpcml(i,n));
end
for n=nl7:n_tmax
    i=7;
    hold on
 Tpcml(i,n+1)=Tpcml(i,n)+k*(To(i,n)-Tpcml(i,n));
end
for n=nl8:n_tmax
    i=8;
    hold on
Tpcml(i,n+1)=Tpcml(i,n)+k*(To(i,n)-Tpcml(i,n));
end
```

```
for n=nl9:n_tmax
   i=9;
   hold on
Tpcml(i,n+1)=Tpcml(i,n)+k*(To(i,n)-Tpcml(i,n));
end
for n=nl10:n_tmax
   i=10;
   hold on
Tpcml(i,n+1)=Tpcml(i,n)+k*(To(i,n)-Tpcml(i,n));
end
for n=nl11:n_tmax
   i=11;
   hold on
Tpcml(i,n+1)=Tpcml(i,n)+k*(To(i,n)-Tpcml(i,n));
Tpcml(12,n)=Tpcml(10,n);
end
% % % % % % % % % % % % % % % % % % % % % % % % % % % % % % % % % % %
%Effecency of the storage or charging efficency
i=1:i_lmax;
av_p=mean(Tpcmf,1);       %Average final temperature for each columen for PCM matrixs
av_o=mean(To,1);          %Average final temperature for each columen for oil matrixs
zp=av_p(1,n_t);           %The average final temperature of PCM storage
zo=av_o(1,n_t);           %The average final temperature of oil
% % % % % % % % % % % % % % % % % % % % % % % % % % % % % % % % % % %
Est=Qpcm+Qoil;                        %Total energy stored in a system (output)
Eff_s=Est/Esolar;                     %Effecency of the storage or charging efficency
% % % % % % % % % % % % % % % % % % % % % % % % % % % % % % % % % % %
```

```
%ANALYSIS OF DISCHARGING
%%%%%%%%%%%%%%%%%%%%%%%%%%%%%%%%%%%%%%%%
%correlation parameters
G=((g*Bo*L^3*detT)/(m^2));          %Grashof number
Ra=G*Pr;                            %Rayleigh number
Nuu1=(0.057*Ra^(1/3));              %Nusselt number
ho=(Nuu1*K_o)/(L);                  %The heat transfer coefficient for thermal storage
hv=(ho*n*Asp)/(V_stt);              %The volumetric heat transfer for thermal storage
%%%%%%%%%%%%%%%%%%%%%%%%%%%%%%%%%%%%%%%%
T=3600*3;                   %Final time given in hours
H=0.25;                     %Hight of storage in m
Hp=0.008;                   %Hight of baking pan in m
dt=0.1;                     %Time step in second
dx=0.05;                    %Space step on storage in meter
dxp=0.0016;                 %Space step on baking pan in meter
x_d=(H/dx)+1;               %Max number of space nodes
%%%%%%%%%%%%%%%%%%%%%%%%%%%%%%%%%%%%%%%%
m=T/dt;% maximum time step number
m_1=m+1;
Gdd=((g*Bo*L2^3*detT)/(mdd^2));     %Grashof number
Radd=Gdd*Prdd;                      %Rayleigh number
Nuu11=(0.825+(0.387*Radd^(1/6))/(1+(0.492/Prdd)^(9/16))^(8/27))^(2);  % NUsslet number
ho08=(Nuu11*K_od)/(L2);
hod=(ho08*n*Asp)/(V_stt);
%%%%%%%%%%%%%%%%%%%%%%%%%%%%%%%%%%%%%%%%
%property of baking pan
dpan=0.58;                  %Diameter of Baking pan in 'm'
```

```
Lpan=0.008;              %Thickness of baking pan in 'm'
kp=0.8;                  %Thermal conductivity of Baking Pan in 'w/(m.k)'
rho_p=2400;              %Density of bakong pan in 'kg/m^3'
Cp_p=960;                %Spacific heat capacity of of pan in J/kg.K
d=2.5;                   %The assumed temperature differfce where the Pcm start to discharge
heat to the oil
% % % % % % % % % % % % % % % % % % % % % % % % % % % % % % % % % % % % % % % % % % % % % % %
Gab=((g*Bab*L^3*detT)/(mab^2));          %Grashof number
Rab=Gab*Prb;                             %Rayleigh number
Nub=0.15*Rab^(1/3);                      %Nusselt number
hcab=(Nub*Kab)/(L);                      %The heat transfer coefficient for air and baking
pan
hcabp=(Nub*Kab)/(L);
dd=5.67*10^(-8);                         %Stefan boltzman constant in w/(m^2K^4)
epan=0.95;                               %Emmisivity of fiber glass
hrab=dd*epan*(Ts^2+Tinf^2)*(Ts-Tinf);    %Heat loss due to radiation in W/m^2k
hca=hcab+hrab;
% % % % % % % % % % % % % % % % % % % % % % % % % % % % % % % % % % % % % % % % % % % % % % %
   Fd=(kp*dt)/(rho_p*Cp_p*(dxp)^2);
   Rbc=(hod*dt)/(eps*Cp_ol*rho_ol);
   Fbr=(epan*dd*dt)/(Cp_p*rho_p);
   Rbcl=(hca*dt)/(Cp_p*rho_p);
   Rp=hod*dt/(eps*rho_ol*Cp_ol);
   FPd=(hod*dt)/((1-eps)*rho_pcm*C_ppcm);
   FPld=(hod*dt)/((1-eps)*rho_pcml*C_ppcml);
   RPd=(k_pcm*dt)/((1-eps)*rho_pcm*C_ppcm*dx^2);
   F=(Uw*dt)/(eps*Cp_o*rho_o);
   % % % % % % % % % % % % % % % % % % % % % % % % % % % % % % % % % % % % % % % % % % % % % % %
```

```
for t=2:m
    for i=2:x_d
        Tpcmd(i,1)=Tf;
          Tod(i,1)=Tf;
         Tpan(i,1)=Tf;
   Tpcmd(i,t+1)=Tpcmd(i,t)*(1-FPld)+FPld*(Tod(i,t));
    Tod(i+1,t)=Tod(i,t)-Rp*(Tpcmd(i,t)-Tod(i,t))+F*(Tinf-Tod(i,t))-Rbc*(Tod(i,t)-Tpan(i,t));
    Tpan(i,t+1)=Tpan(i,t)*(1-2*Fd)+Fd*(Tpan(i+1,t)+Tpan(i-1,t))+Rbcl*(Tinf-Tpan(i,t));
       if Tpcmd(i,t)>220
          Xd(i,t)=1;
      else
           Xd(i,t)=0;
      end
%%%%%%%%%%%%%%%%%%%%%%%%%%%%%%%%%%%
%Molten fraction analysis
V=((1-eps)*(1-eps));
for t=nxd1:m_1
    i=1;
    hold on
   Xd(i,t+1)=Xd(i,t)+((dt*hod*(Tod(i,t)-Tpcmd(i,t)))/(rho_pcm*h_Lpcm*V));
     if Xd(i,t)<=0
         Xd(i,t)=0;
     end
end
hold on
for t=nxd2:m_1
    i=2;
```

```
    hold on
     Xd(i,t+1)=Xd(i,t)+((dt*hod*(Tod(i,t)-Tpcmd(i,t)))/(rho_pcm*h_Lpcm*V));
     if Xd(i,t)<=0
        Xd(i,t)=0;
     end
end
hold on
for t=nxd3:m_1
    i=3;
    hold on
    Xd(i,t+1)=Xd(i,t)+((dt*hod*(Tod(i,t)-Tpcmd(i,t)))/(rho_pcm*h_Lpcm*V));
     if Xd(i,t)<=0
        Xd(i,t)=0;
     end
end
hold on
for t=nxd4:m_1
    i=4;
    hold on
     Xd(i,t+1)=Xd(i,t)+((dt*hod*(Tod(i,t)-Tpcmd(i,t)))/(rho_pcm*h_Lpcm*V));
     if Xd(i,t)<=0
        Xd(i,t)=0;
     end
end
hold on
for t=nxd5:m_1
    i=5;
```

```
    hold on
   Xd(i,t+1)=Xd(i,t)+((dt*hod*(Tod(i,t)-Tpcmd(i,t)))/(rho_pcm*h_Lpcm*V));
     if Xd(i,t)<=0
         Xd(i,t)=0;
     end
end
hold on
for t=nxd6:m_1
     i=6;
    hold on
      Xd(i,t+1)=Xd(i,t)+((dt*hod*(Tod(i,t)-Tpcmd(i,t)))/(rho_pcm*h_Lpcm*V));
     if Xd(i,t)<=0
         Xd(i,t)=0;
     end
end
% % % % % % % % % % % % % % % % % % % % % % % % % % % % % % % % % % %
for t=2:nxd2
    i=2;
    Tpcmds(1,t)=Tpcmds(2,t);
     Tod(1,t)=(Tpcmds(1,t)-(d));
     Tpan(1,t)=(Tod(2,t)-(p));
      Tod(i+1,t)=Tod(i,t)-Rp*(Tpcmds(i,t)-Tod(i,t))+F*(Tinf-Tod(i,t));
    Tpan(i,t+1)=Tpan(i,t)*(1-2*Fd)+Fd*(Tpan(i+1,t)+Tpan(i-1,t));
      hold on
end
for t=nxd2:nd2
    i=2;
```

```
    Tpcmds(i,t)=220;
     Tod(1,t)=(Tpcmds(1,t)-(d));
     Tpan(1,t)=(Tod(2,t)-(p));
     Tod(1,t)=Tod(2,t);
   Tod(i+1,t)=Tod(i,t)-Rp*(Tpcmds(i,t)-Tod(i,t))+F*(Tinf-Tod(i,t));
   Tpan(i,t+1)=Tpan(i,t)*(1-2*Fd)+Fd*(Tpan(i+1,t)+Tpan(i-1,t));
      hold on
end
for t=nd2:m_1
    i=2;
    Tpcmds(1,t)=Tpcmds(2,t);
     Tod(1,t)=(Tpcmds(1,t)-(d));
     Tpan(1,t)=(Tod(2,t)-(p));
     Tod(1,t)=Tod(2,t);
     Tod(i,1)=Tf;
     Tod(i,2)=Tf;
   Tpcmds(i,t+1)=Tpcmds(i,t)*(1-FPd)+FPd*(Tod(i,t));
  Tod(i+1,t)=Tod(i,t)-Rp*(Tpcmds(i,t)-Tod(i,t))+F*(Tinf-Tod(i,t));
  Tpan(i,t+1)=Tpan(i,t)*(1-2*Fd)+Fd*(Tpan(i+1,t)+Tpan(i-1,t));
   hold on
end
for t=2:nxd3
    i=3;
     Tpcmds(1,t)=Tpcmds(2,t);
     Tod(2,t)=(Tpcmds(1,t)-(d));
     Tpan(1,t)=(Tod(2,t)-(p));
    Tod(i+1,t)=Tod(i,t)-Rp*(Tpcmds(i,t)-Tod(i,t))+F*(Tinf-Tod(i,t));
```

```
    Tpan(i,t+1)=Tpan(i,t)*(1-2*Fd)+Fd*(Tpan(i+1,t)+Tpan(i-1,t));
      hold on
end
for t=nxd3:nd3
    i=3;
    Tpcmds(i,t)=220;
     Tod(i+1,t)=Tod(i,t)-Rp*(Tpcmds(i,t)-Tod(i,t))+F*(Tinf-Tod(i,t));
   Tpan(i,t+1)=Tpan(i,t)*(1-2*Fd)+Fd*(Tpan(i+1,t)+Tpan(i-1,t));
    hold on
end
for t=nd3:m_1
    i=3;
  Tpcmds(i,t+1)=Tpcmds(i,t)*(1-FPd)+FPd*(Tod(i,t));
 Tod(i+1,t)=Tod(i,t)-Rp*(Tpcmd(i,t)-Tod(i,t))+F*(Tinf-Tod(i,t));
 Tpan(i,t+1)=Tpan(i,t)*(1-2*Fd)+Fd*(Tpan(i+1,t)+Tpan(i-1,t));
   hold on
 end
for t=2:nxd4
    i=4;
  Tod(i+1,t)=Tod(i,t)-Rp*(Tpcmds(i,t)-Tod(i,t))+F*(Tinf-Tod(i,t));
    Tpan(i,t+1)=Tpan(i,t)*(1-2*Fd)+Fd*(Tpan(i+1,t)+Tpan(i-1,t));
      hold on
end
for t=nxd4:nd4
    i=4;
   Tpcmds(i,t)=220;
   Tod(i+1,t)=Tod(i,t)-Rp*(Tpcmds(i,t)-Tod(i,t))+F*(Tinf-Tod(i,t));
```

```
   Tpan(i,t+1)=Tpan(i,t)*(1-2*Fd)+Fd*(Tpan(i+1,t)+Tpan(i-1,t));
    hold on
end
for t=nd4:m_1
    i=4;
 Tpcmds(i,t+1)=Tpcmds(i,t)*(1-FPd)+FPd*(Tod(i,t));
 Tod(i+1,t)=Tod(i,t)-Rp*(Tpcmds(i,t)-Tod(i,t))+F*(Tinf-Tod(i,t));
 Tpan(i,t+1)=Tpan(i,t)*(1-2*Fd)+Fd*(Tpan(i+1,t)+Tpan(i-1,t));
  hold on
  end
for t=2:nxd5
    i=5;
    Tod(i+1,t)=Tod(i,t)-Rp*(Tpcmds(i,t)-Tod(i,t))+F*(Tinf-Tod(i,t));
    Tpcmds(i,t+1)=Tpcmds(i,t)*(1-FPld)+FPld*(Tod(i,t));
    Tpan(i,t+1)=Tpan(i,t)*(1-2*Fd)+Fd*(Tpan(i+1,t)+Tpan(i-1,t));
      hold on
end
for t=nxd5:nd5
    i=5;
   Tpcmds(i,t)=220;
  Tod(i+1,t)=Tod(i,t)-Rp*(Tpcmds(i,t)-Tod(i,t))+F*(Tinf-Tod(i,t));
   Tpan(i,t+1)=Tpan(i,t)*(1-2*Fd)+Fd*(Tpan(i+1,t)+Tpan(i-1,t));
    hold on
end
for t=nd5:m_1
    i=5;
   Tpcmds(i,t+1)=Tpcmds(i,t)*(1-FPd)+FPd*(Tod(i,t));
```

```
  Tod(i+1,t)=Tod(i,t)-Rp*(Tpcmds(i,t)-Tod(i,t))+F*(Tinf-Tod(i,t));
  Tpan(i,t+1)=Tpan(i,t)*(1-2*Fd)+Fd*(Tpan(i+1,t)+Tpan(i-1,t));
   end
  hold on
 end
for t=2:nxd6
   i=6;
     Tpcmds(x_d+1,t)=Tpcmds(x_d,t);
   Tod(i+1,t)=Tod(i,t)-Rp*(Tpcmds(i,t)-Tod(i,t))+F*(Tinf-Tod(i,t))-Rbc*(Tod(i,t)-Tpan(1,t));
   Tpan(i,t+1)=Tpan(i,t)*(1-2*Fd)+Fd*(Tpan(i+1,t)+Tpan(i-1,t))+Rbcl*(Tinf-Tpan(i,t));
     hold on
end
for t=nxd6:nd6
   i=6;
  Tpcmds(x_d+1,t)=Tpcmds(x_d,t);
  Tod(x_d+1,t)=Tod(x_d,t);
  Tpan(x_d+1,t)=Tpan(x_d,t);
  Tod(i+1,t)=Tod(i,t)-Rp*(Tpcmds(i,t)-Tod(i,t))+F*(Tinf-Tod(i,t))-Rbc*(Tod(i,t)-Tpan(1,t));
  Tpan(i,t+1)=Tpan(i,t)*(1-2*Fd)+Fd*(Tpan(i+1,t)+Tpan(i-1,t))+Rbcl*(Tinf-Tpan(i,t));
  hold on
end
for t=nd6:m_1
   i=6;
      Tpcmds(x_d+1,t)=Tpcmds(x_d,t);
     Tod(x_d+1,t)=Tod(x_d,t);
      Tpan(x_d+1,t)=Tpan(x_d,t);
 Tpcmds(i,t+1)=Tpcmds(i,t)*(1-FPd)+FPd*(Tod(i,t));
```

```
 Tod(i+1,t)=Tod(i,t)-Rp*(Tpcmds(i,t)-Tod(i,t))+F*(Tinf-Tod(i,t))-Rbc*(Tod(i,t)-Tpan(1,t));
 Tpan(i,t+1)=Tpan(i,t)*(1-2*Fd)+Fd*(Tpan(i+1,t)+Tpan(i-1,t))+Rbcl*(Tinf-Tpan(i,t));
  end
% % % % % % % % % % % % % % % % % % % % % % % % % % % % % % % % % % %
%Thermal Efficiency of the storage or discharging efficiency
av_pd=mean(Tpcmds,1);        %Average final temperature for each column for PCM matrix
av_od=mean(Tod,1);           %Average final temperature for each column for oil matrix
zpd=av_pd(1,m_1);            %The average final temperature of PCM storage
zod=av_od(1,m_1);            %The average final temperature of oil
% % % % % % % % % % % % % % % % % % % % % % % % % % % % % % % % % % %
E_used=Qpcmd+Qoild;                       %Total energy used from a system
Eff_thermal=(E_used/Est);                 %Discharging efficiency
Eff_overal=(E_used/E_solar);              %Overall effecency of the system
% % % % % % % % % % % % % % % % % % % % % % % % % % % % % % % % % % %
```